General Disclaimer

One or more of the Following Statements may affect this Document

- This document has been reproduced from the best copy furnished by the organizational source. It is being released in the interest of making available as much information as possible.

- This document may contain data, which exceeds the sheet parameters. It was furnished in this condition by the organizational source and is the best copy available.

- This document may contain tone-on-tone or color graphs, charts and/or pictures, which have been reproduced in black and white.

- This document is paginated as submitted by the original source.

- Portions of this document are not fully legible due to the historical nature of some of the material. However, it is the best reproduction available from the original submission.

NASA CR-135263
TE 4233-152-77

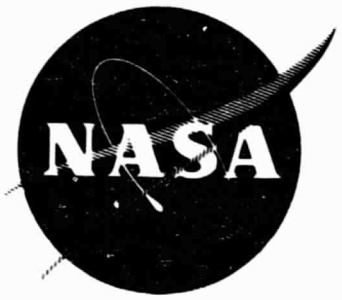

HIGH EFFICIENCY THERMIONIC CONVERTER STUDIES

by F. N. Huffman, A.H. Sommer, C.L. Balestra
T.R. Briere, D.P. Lieb, P.E. Oettinger, and D.B. Goodale

THERMO ELECTRON CORPORATION

prepared for

NATIONAL AERONAUTICS AND SPACE ADMINISTRATION

NASA Lewis Research Center
Contract NAS 3-20302

Page intentionally left blank

1. Report No.	2. Government Accession No.	3. Recipient's Catalog No.
NASA CR-135263		

4. Title and Subtitle	5. Report Date
HIGH EFFICIENCY THERMIONIC CONVERTER STUDIES	July 1977
	6. Performing Organization Code

7. Author(s)	8. Performing Organization Report No.
F.N. Huffman, A.H. Sommer, C.L. Balestra, T.R. Briere, D.P. Lieb, P.E. Oettinger, D.B. Goodale	TE 4233-152-77
	10. Work Unit No.

9. Performing Organization Name and Address	11. Contract or Grant No.
Thermo Electron Corporation 85 First Avenue Waltham, Mass. 02154	NAS 3-20302
	13. Type of Report and Period Covered
12. Sponsoring Agency Name and Address	7/1/76 - 4/30/77
National Aeronautics and Space Administration Washington, DC 20546	14. Sponsoring Agency Code

15. Supplementary Notes

Project Manager, James Morris, Thermionics and Heat Pipe Section,
NASA Lewis Research Center, Cleveland, Ohio

16. Abstract

This report summarizes NASA-sponsored research in thermionic energy conversion technology conducted at Thermo Electron Corporation from July 1976 through April 1977. The objectives of this study were to produce converters suitable for use in out-of-core space reactors, radioisotope generators, and solar satellites. Such applications require higher converter efficiency. Improved thermionic converter performance requires the development of emitter electrodes that operate at low cesium pressure, stable low work function collector electrodes, and more efficient means of space charge neutralization. All of these avenues to improved performance are being explored. Potential improvements in collector properties were noted with evaporated thin film barium oxide coatings, which were measured to have nearly temperature-independent bare work functions of 1.4 eV. Experiments with cesium carbonate suggest that this substance may provide optimum combinations of cesium and oxygen for thermionic conversion. Diodes constructed with lanthanum hexaboride collectors were observed to have barrier indices below 2.0 eV at low cesium pressures. A pulsed ring triode substantially reduced the interelectrode plasma arc drop at current densities less than 2 A/cm^2 in cesium-xenon mixtures, and could be operated at 0.5-mm electrode spacings and 0.5 torr cesium pressure. In particulate-spaced diode experiments, significant power was produced in devices spaced (0.012 mm) with magnesium oxide and barium oxide.

17. Key Words (Suggested by Author(s))	18. Distribution Statement
Thermionic converter Emitter Collector Plasma arc drop Barrier index	Unclassified - unlimited

19. Security Classif. (of this report)	20. Security Classif. (of this page)	21. No. of Pages	22. Price*
Unclassified	Unclassified	94	

* For sale by the National Technical Information Service, Springfield, Virginia 22151

TABLE OF CONTENTS

TABLE OF CONTENTS (Continued)

SUMMARY

Efficient thermionic energy converters operating as critical components in space vehicles require improvements in emitter and collector properties, as well as decreased potential losses in the plasma as the electrons flow across the interelectrode space. This report details the results from a ten-month effort aimed at these objectives.

Experiments with evaporated thin films (less than 100 Å) of BaO have yielded bare work functions approximating 1.4 eV, which are lower than those observed for the thicker, sprayed material. In addition, this work function is almost independent of temperature in the range from 400 to 750 K.

Heated cesium carbonate dispenses optimum amounts of cesium and oxygen for low work function surfaces. Measurements made on several substrates exposed to a heated cesium carbonate source yielded work functions between 1.05 and 1.15 eV.

Thermionic converter performance is substantially enhanced by the addition of oxygen, which normally lowers the collector work function and reduces the cesium pressures required for practical current densities from the emitter. Oxygen is either introduced directly into a converter through a silver leak tube or dispensed from a metallic oxide coating on the collector. A thermionic converter with a leak tube and a LaB_6 collector gave a work function measured by back emission of 1.28 eV. A converter constructed with a double layer of tungsten oxide on a columbium-1% zirconium collector operated for 2200 hours at power levels near 3 W/cm^2 and a barrier index of 2.06 eV.

An auxiliary ring electrode replaced the grid formerly used in triode experiments. This design allowed closer interelectrode spacings to minimize coulombic resistance. Uniform pulsed discharges were visually observed through a sapphire window in the converter at electrode spacings as low as 0.5 mm, and cesium pressures up to 0.5 torr. In comparison to the grid configuration, the ring triode exhibited improved performance.

A noncesiated particulate-spaced diode with molybdenum electrodes has given short-circuit currents greater than one ampere at an emitter temperature of 1450 K. The spacing of 13 μm was maintained with a

porous BaO coating. No shorting was observed for over 100 hours. Spacings as low as 3.3 μm have been achieved with molybdenum laser mirrors with an area of 5 cm^2 at room temperature. Practical electrical resistance was maintained in a MgO spaced diode with a flexible foil collector at a cesium pressure of 0.1 torr.

I. INTRODUCTION

Space missions require reliable power systems with a high power-to-weight ratio. These requirements are fulfilled by thermionic converters, which contain no moving parts, and which operate with relatively small radiators because of the high heat rejection temperatures. Because such converters lend themselves to modular construction, an added benefit of these systems is the elimination of single-point failures. A variety of reactor and radioisotope systems have demonstrated the potential of thermionic conversion for space applications.

Although most of the U.S. thermionic reactors in the sixties, as well as U.S.S.R. TOPAZ thermionic reactors, were based on in-core thermionic converters, out-of-core systems have the advantages of reduced shield weight and increased design flexibility. However, out-of-core reactor designs necessitate reduced emitter temperatures. Consequently, it is important to improve thermionic converter performance with better electrodes and reduced plasma losses in the inter-electrode spacing.

This report describes the NASA-sponsored thermionic energy conversion research and technology program conducted between July 1976 and April 1977 at Thermo Electron Corporation. This program was aimed at providing efficient thermionic converters for space missions by developing high-current emitters operating at temperatures from 1400 to 1800 K with stable low work function collectors and inter-electrode voltage drops of a few tenths of a volt. This effort compliments an ERDA-sponsored program to produce efficient and economical thermionic conversion systems for use in topping fossil-fueled steam powerplants.

Basic surface experiments are described in Section II, high-efficiency diode tests are detailed in Section III, pulsed triode converter investigations are discussed in Section IV, and particulate-spaced diode studies are summarized in Section V. The major results of these sections are discussed in Section VI, with the important conclusions listed in Section VII.

II. BASIC SURFACE EXPERIMENTS

A. ACTIVATION CHAMBER STUDIES

1. Experiments with Evaporated Barium Oxide Films

A conventionally sprayed thermionic cathode consists of an approximately 100-um thick barium oxide (more accurately, barium-strontium-calcium oxide) layer deposited on a metallic substrate. This electrode has a work function of approximately 1.5 eV. Earlier experiments in the Activation Chamber showed that this work function could be further reduced by exposure to cesium vapor. On the basis of these results, several thermionic diodes were constructed with sprayed barium oxide collectors. The collector work functions (as determined from back-emission measurements) looked promising, but the current-voltage characteristics indicated that the barium oxide layer had an excessive resistance.

Because of the difficulty of appreciably reducing the thickness of the sprayed layer, a project was initiated to produce much thinner barium oxide films by evaporation. From earlier work on such films produced at the Naval Research Laboratories (private communication with R. Thomas), it was known that low work functions could be obtained with evaporated layers. A total of 15 evaporation experiments were performed in the Activation Chamber. The following is a brief summary of the results.

All evaporated films were produced by spraying a thick layer of either barium carbonate or the conventional (Ba, Sr, Ca) carbonate onto a platinum ribbon filament. On heating this filament, the organic binder evaporated at around 675 K, then the carbonates decomposed into oxide and carbon dioxide at about 1075 K, and finally the barium oxide evaporated above approximately 1475 K. Strontium oxide and calcium oxide evaporated at much higher temperatures. Auger analysis confirmed that the deposit obtained by heating the oxide mixture to the evaporation temperature of barium oxide contained no strontium or calcium. Thus, it is immaterial whether barium oxide was evaporated from the mixed carbonate or from pure barium carbonate; however, most experiments were performed with barium carbonate.

The experimental arrangement for the investigation of evaporated barium oxide is shown in Figure 1. The carbonate was sprayed to approximately the same thickness on both sides of the platinum strip. On heating the strip, barium oxide was deposited from one side of the strip onto the nickel substrate, and from the other side onto the Sloan Digital Thickness Monitor 200. This monitor was mounted at approximately the same distance from the strip as the sample, and the geometry of the apparatus was such that the accuracy of the thickness measurement was within $\pm$20 percent, which was sufficient for the immediate purpose. The cesium channel was provided for studying the effect of cesium on the work function of barium oxide.

During the evaporation process, the following properties of the deposited layer were studied: 1) change of work function with thickness, 2) change of photoemission with thickness, and 3) change of work function with temperature. Typical results for the changes with increasing thickness are shown in Figure 2. The change of work function with thickness is in good agreement with the findings of Thomas (private communication with R. Thomas of the Naval Research Laboratories); i.e., the work function decreases with increasing thickness, reaching a minimum in the 1.4 eV region at a thickness below 100 Å. It is apparent from the figure that the photoemission continues to rise when the thickness is increased beyond the value at which the work function becomes constant. Qualitatively, these effects can be explained as follows: At the layer thickness at which the work function reaches its minimum, only a small fraction of the incident light is absorbed; hence, with increasing thickness, more photons are absorbed and converted into photoelectrons.

As shown in Figure 3, the work function of evaporated barium oxide is inexplicably much less temperature-dependent than that of sprayed material; thus, the evaporated material is more suitable for use as diode collectors operating above 400 K.

Contrary to the earlier results with sprayed barium oxide films, exposure to low-pressure cesium vapor did not improve the work function. However, there is a possibility that the higher cesium vapor pressures available in a diode may have a beneficial effect.

The evaporation from the platinum strip was convenient for preliminary experiments, but it is impractical for producing an evaporated barium oxide deposit on the collector after assembly of the diode because

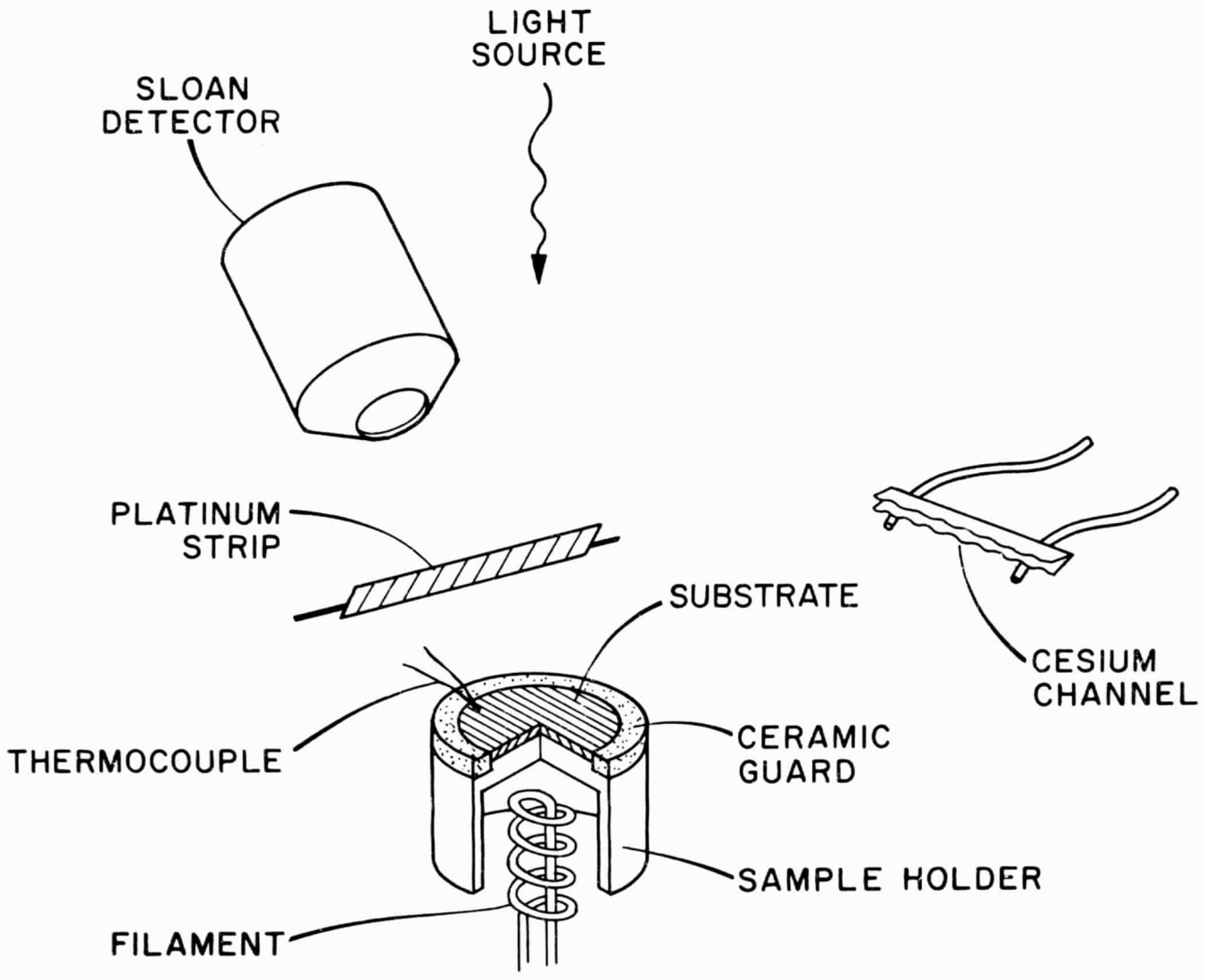

Figure 1. Experimental Arrangement for Barium Oxide Studies.

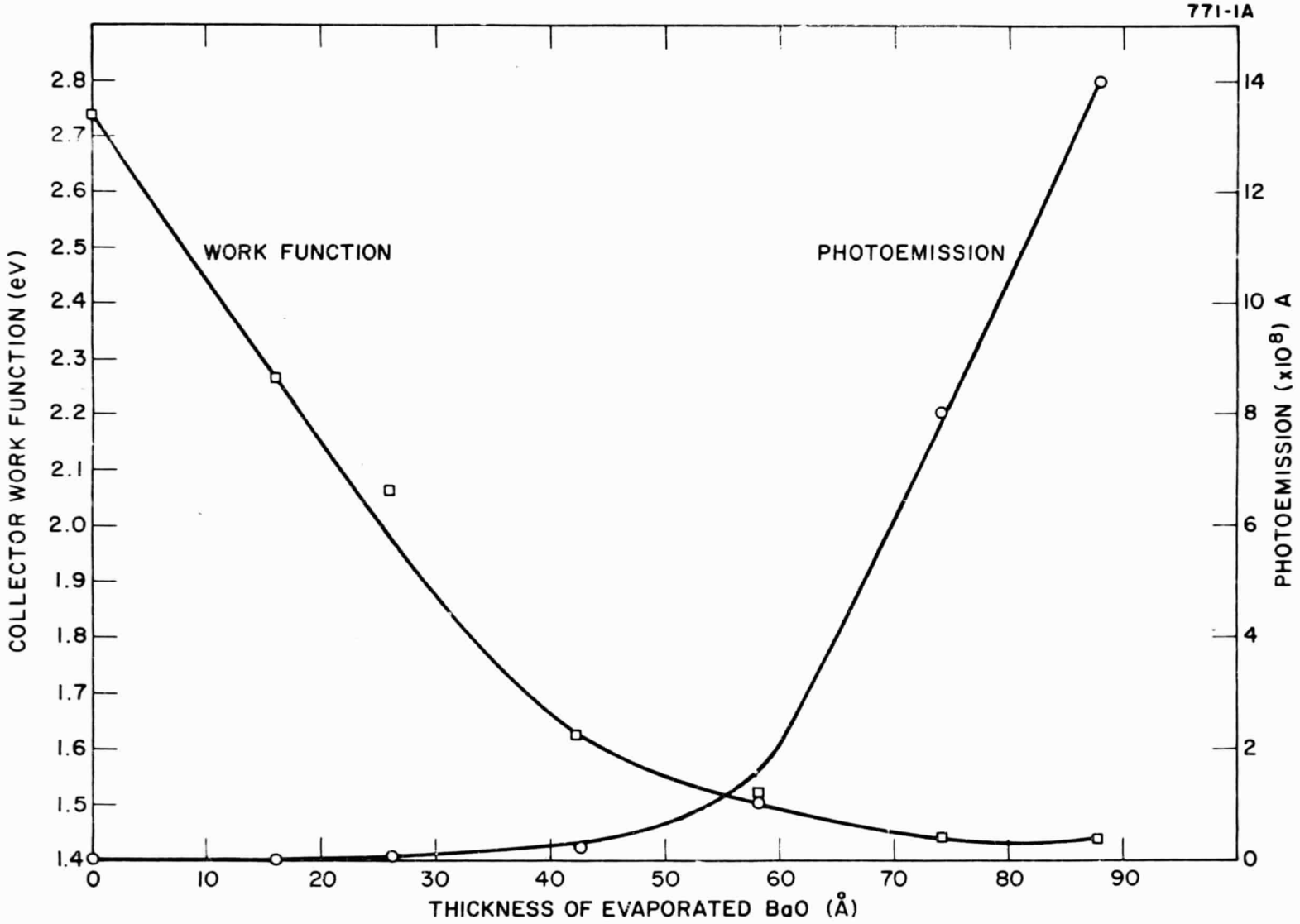

Figure 2. Change of Work Function and Photoemission With Increasing Thickness of BaO Film.

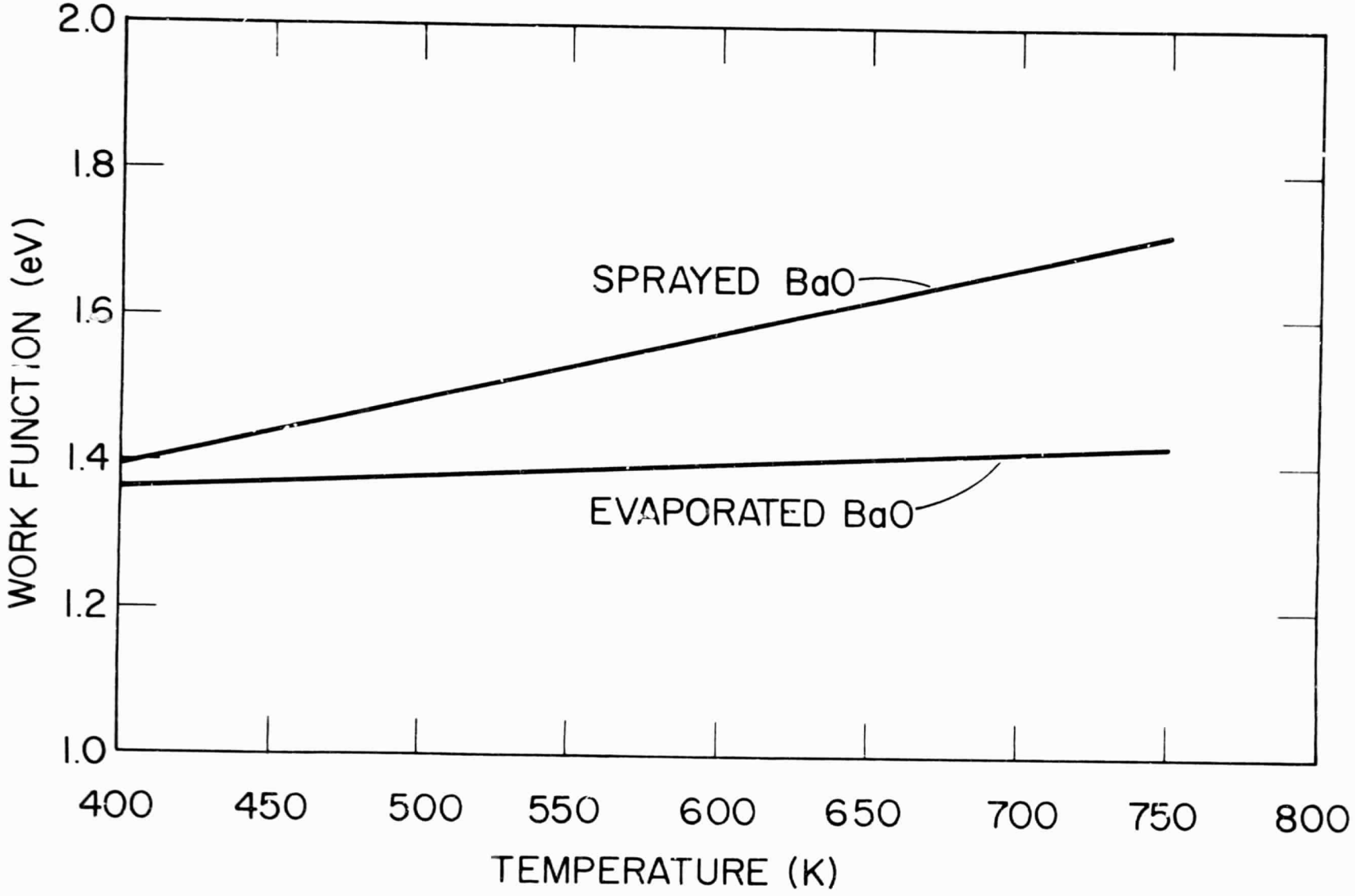

Figure 3. Barium Oxide Work Function Versus Temperature.

there is no room for the strip in the diode geometry. Therefore, experiments were made to explore the possibility of evaporating barium oxide onto the collector substrate before assembling the diode. This procedure necessitated that the evaporated film be exposed to air before final evacuation of the diode.

It is a common experience with standard sprayed barium oxide cathodes that exposure of an activated cathode to air destroys the emission, but that the emission recovers on heating the cathode in a vacuum to the original activation temperature. Assuming similar behavior, an evaporated barium oxide film was exposed to air and then remounted in the vacuum chamber. Heat treatment did, in fact, reduce the work function considerably, but it was never restored to the original value. The lowest work functions obtained by this method were in the 1.8 eV region, about 0.4 eV higher than before exposure to air, and 0.2 eV higher than the work functions of standard sprayed material. At present there is no explanation for this irreversible deterioration of the evaporated barium oxide films.

An alternative method was tried in order to avoid the detrimental effect of air exposure. Barium oxide was evaporated from a platinum strip onto a second platinum strip to a thickness of about 3000 Å. The second strip was then exposed to air and mounted in the vacuum chamber in such a way that the barium oxide could be evaporated onto the nickel substrate. This reevaporated film showed the low work function and other properties of the barium oxide films that were evaporated directly from a platinum strip in the vacuum chamber. The success of this double evaporation is probably due to the fact that the portion of the surface film exposed to air was reevaporated first, and then covered by the subsequently evaporated clean material.

For use as collector material, the double evaporation technique has an additional advantage. The first deposit can be evaporated onto a well-degassed emitter for later reevaporation onto the collector. In this way, the collector and the whole system can be outgassed before the final evaporation of barium oxide from the emitter onto the collector. This procedure was followed in preparing evaporated barium oxide as a collector material. Because barium oxide is known to react chemically with tungsten to form tungsten oxide and elemental barium (ref. 1), a platinum emitter was used in the first diode experiment.

2. Experiments with Cesium Carbonate

a. Introduction

The lowest effective work functions are obtained on surfaces containing both cesium and oxygen. (Effective work function is defined as that value derived from the Richardson equation, with A = 120 A/cm^2K^2 (ref. 2).) Effective work functions as low as 1.0 to 1.1 eV have been observed with compositions of W-O-Cs (ref. 3), Ag-O-Cs (S-1 photocathode) (ref. 4), and Si-O-Cs (negative electron affinity emitter) (ref. 5).

The exact chemical and physical structure of the cesium-oxygen layer that produces the lowest work function is unknown. Indeed, there appear to be two types of cesium-oxygen surfaces. The first, represented by W-O-Cs and Si-O-Cs, contains the two elements in quantities of monatomic dimension. The second type, represented by Ag-O-Cs, contains tens of monolayers of the two elements. (This second, bulk, effect is probably responsible for thermionic emission from BaO cathodes, whereas the first type resembles the monolayer barium-oxygen surface of the dispenser cathode (ref. 6).)

Characterization of the low work function cesium-oxygen combination is difficult because:

(1) The material is unstable in air and must, therefore, be studied in the vacuum environment in which it is formed.

(2) The absolute amounts of cesium and oxygen involved are exceedingly small, especially in the monolayer surfaces.

(3) Cesium and oxygen form many compounds of varying Cs:O ratios (ref. 7). Hence, even an accurate determination of the Cs:O ratio in the surface film does not define unambiguously whether the optimum (lowest work function) combination consists of one specific oxide or of a mixture of different oxides. Moreover, it is likely that the surfaces contain some of the cesium in the form of adsorbed, rather than chemically bound, atoms, because extended exposure to oxygen always reduces the electron emission.

Cesium-oxygen surfaces are usually produced by exposing the substrate material to separate sources of cesium vapor and oxygen, or by exposing a metal oxide to cesium vapor. The thermionic emission can then be measured from a well-defined cesium oxide vapor deposited onto a metal substrate during exposure to elemental cesium. A convenient way of producing such a cesium oxide deposit seemed to be a method analogous to that conventionally used for the formation of (Ba, Sr, Ca)O thermionic cathodes; i.e., the thermal decomposition of the carbonate according to

$$Cs_2CO_3 \rightarrow Cs_2O + CO_2 \ . \qquad (1)$$

The relatively high vapor pressure of Cs_2O should then permit the evaporation of a Cs_2O film of controlled thickness. However, results found in earlier publications (refs. 8 and 9) made it doubtful whether Cs_2O could be produced in accordance with equation (1).

Lebeau (ref. 8) observed decomposition of Cs_2CO_3 occurring near 875 K in vacuum, but he did not identify the resulting cesium oxide. Klemm and Scharf (ref. 9) observed that Cs_2O evaporates in vacuum as Cs_2O up to about 675 K, but that above 775 K the compound decomposes into metallic cesium and cesium peroxide according to

$$2\ Cs_2O \rightarrow 2\ Cs + Cs_2O_2 \ . \qquad (2)$$

As one would expect, elemental cesium evaporates first; however, with increasing temperature, the peroxide evaporates as well. Both Cs and Cs_2O_2 were unambiguously identified in the condensate of the high-temperature Cs_2O decomposition by X-ray analysis (ref. 9). In accordance with references 8 and 9, at temperatures of 875 K and above, the decomposition of Cs_2CO_3 would be expected to produce Cs_2O_2 and Cs rather than Cs_2O.

b. Experimental Arrangement

All experiments were performed in the Activation Chamber. The apparatus was similar to that shown in Figure 1. A 30 x 3 x 0.025-mm platinum ribbon filament, spray-coated on both sides with a Cs_2CO_3 powder suspension, was mounted about 1 cm above the sample, with a Sloan monitor positioned at about the same distance below the sample.

c. Experimental Results with Cs_2CO_3

In the first experiment, the Cs_2CO_3-coated platinum ribbon was slowly heated to about 675 K to remove the organic binder. The nickel sample was then cleaned by heating to 1075 K. Thermionic emission from the sample corresponded to a work function much greater than 2 eV with no measureable photoemission. Increasing the temperature of the platinum ribbon to between 825 and 875 K, as measured with an Ircon (Model 300 LC) infrared pyrometer, produced a drop in work function and a photoemission of approximately 10^{-5} to 10^{-4} electrons per photon. On further heating of the platinum ribbon, the photosensitivity increased by approximately an order of magnitude, and the threshold wavelength moved into the infrared range, as indicated by response through a Corning 7-56 filter (cut-off near 8000 Å). Concurrently, the thermionic emission current, at a sample temperature of 450 K, increased rapidly to a value corresponding to a work function around 1.2 eV.

Heating the platinum ribbon for a longer time did not affect the photoemission appreciably; however, the work function decreased further, reaching a stable value in the 1.05 to 1.15 eV range at sample temperatures below 475 K. At higher sample temperatures, both thermionic emission and photoemission decreased, but reheating the platinum ribbon recovered the optimum values of photo- and thermionic emission.

This experiment was repeated several times with remarkably reproducible results. In later experiments, the thickness of the deposit was monitored with the Sloan instrument to measure the thickness required for minimum work function (Figure 4). These measurements are approximate because geometry problems make it uncertain whether equal amounts (per unit area) of material are deposited on both sample and monitor. Moreover, the chemical composition and, hence, the density of the deposit are not known. The deposit thickness is estimated to be between 70 and 140 Å, corresponding to 25 to 50 monolayers.

Attempts were made to lower the work function below the 1.05 to 1.15 eV range by exposing the sample to small amounts of cesium vapor released from the cesium channel. In all cases, both thermionic and photoelectric emission decreased, but recovered on heating the sample to between 400 and 450 K.

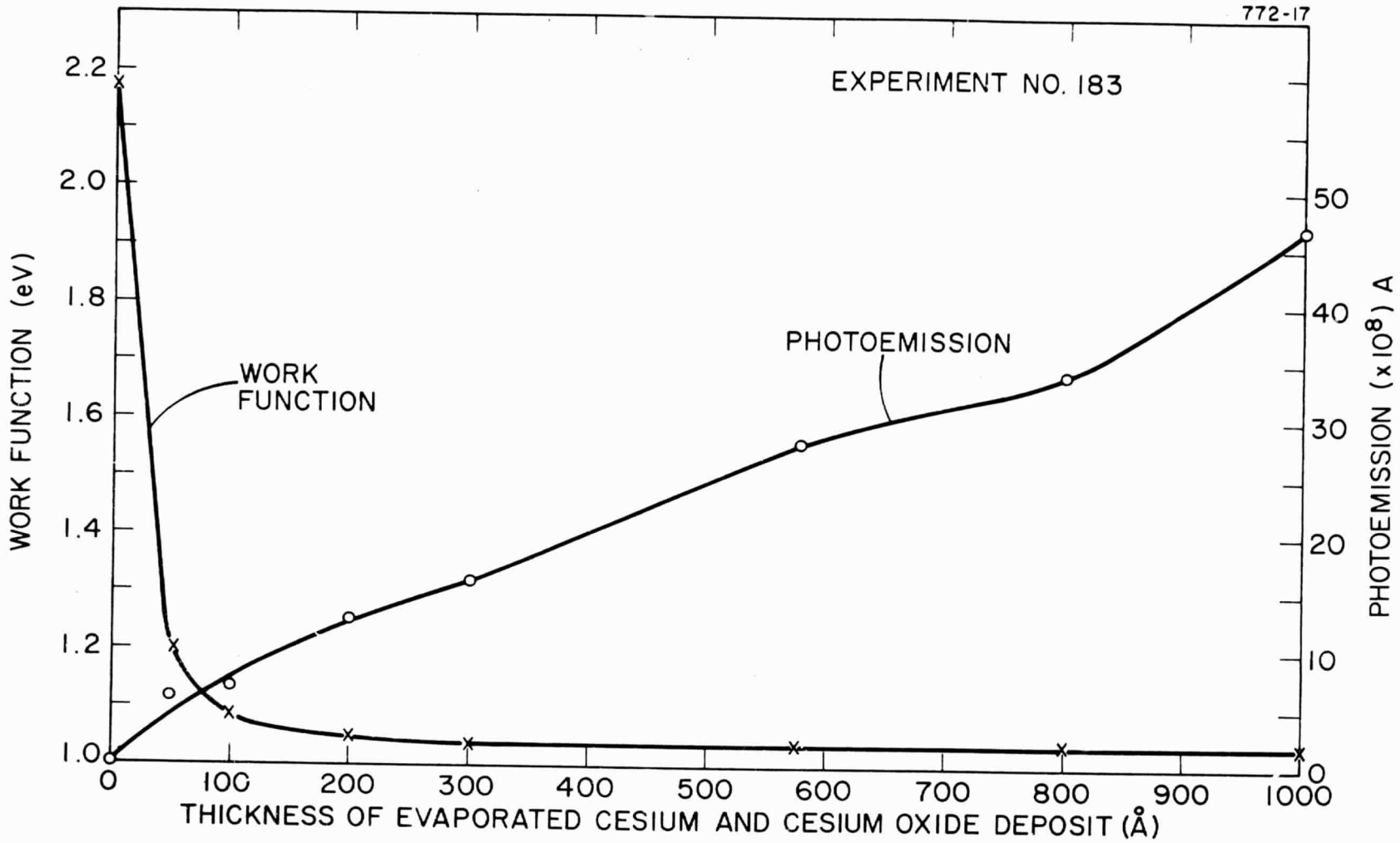

Figure 4. Change of Work Function and Photoemission with Increasing Thickness of Cesium and Cesium Oxide Deposit.

Experiments were also performed to determine the effect of the substrate material on the emission properties of the deposited material. In addition to nickel, substrates of silver and sprayed (Ba, Sr, Ca)O cathode material (RCA 33C-175A) were used. The results were indistinguishable from those produced on the nickel substrate.

d. Discussion of Cs_2CO_3 Experiments

The chemical composition of the low work function surface produced by evaporating Cs_2CO_3 is not known. Although a direct analysis of the material is difficult, the experimental results suggest the following:

(1) A minimum layer of thickness of tens of monolayers is required to obtain a work function below 1.15 eV. This "thick" coating suggests that the emission is due to a bulk, rather than to a purely surface, effect. Thus, the material resembles the BaO-cathode rather than the barium dispenser cathode. Additional evidence for a bulk effect is the independence of the work function from the substrate material.

(2) It is usually assumed (ref. 4) that surfaces having work functions in the 1 eV range consist of Cs_2O and adsorbed Cs. However, if the deposit produced by the decomposition of Cs_2CO_3 consists of Cs_2O_2 and Cs in accordance with reference 8, the following possibilities must be considered:

(a) The material is and remains a mixture of Cs_2O_2 and Cs.

(b) The reaction shown in equation (2) is partially reversible, and reformed Cs_2O is responsible for the low work function in agreement with the usual assumption.

(c) Some of the evaporating cesium may react with the simultaneously released CO_2 according to

$$2\,Cs + CO_2 \rightarrow Cs_2O + CO\,. \qquad (3)$$

Although this reaction could explain the presence of Cs_2O, it would not reduce the amount of Cs_2O_2 in the deposit.

The following arguments can be made favoring possibility (b) above:

- If (a) occurred, considerable amounts of elementary cesium should be deposited on the substrate. However, two experimental facts indicate that the amount of elemental cesium in the deposit is small. First, appreciable amounts of free cesium deposited on the Sloan monitor gradually evaporated in the high vacuum system. In fact, the reading on the monitor remained stable, even after pumping for over 18 hours. Second, additional exposure to cesium vapor was always detrimental, but the low work function was restored by a brief heating above 400 K. This suggests that the minimum work function is associated with an adsorbed monolayer, or fractional monolayer, of elemental cesium.

- It is doubtful that cesium reacts with CO_2 because of the low probability of collisions of this element with CO_2.

- Although Klemm and Scharf (ref. 9) produced convincing evidence for the decomposition of Cs_2O_2 and Cs from a Cs_2O source, conditions in our experiments differed in three important respects. First, the quantities involved in their studies were orders of magnitude larger than those in our experiments. Therefore, a surface film of Cs_2O corresponding to our approximately 100-Å thick deposit would not have been detected in their X-ray analysis. Second, their material was deposited on a water-cooled cold finger. By contrast, in our experiments both sample and Sloan monitor were close to the hot platinum ribbon and, therefore, usually above 375 K. At this temperature, the reverse reaction, $Cs_2O_2 + 2\ Cs \rightarrow 2\ Cs_2O$, may occur. Third, Klemm and Scharf used Cs_2O as a source of evaporation, whereas we used Cs_2CO_3. This difference does not necessitate the formation of Cs_2O, but it does not preclude depositions other than (Cs_2O_2 + Cs).

Summarizing, we suggest that our low work function material is essentially Cs_2O with adsorbed cesium atoms. In order to check this interpretation, an attempt was made to convert the deposit produced by heating Cs_2CO_3 into a silver-oxygen-cesium (Ag-O-Cs) photocathode by adding small amounts of silver. If the incorporation of silver into

the deposit produced the "normal" photoemissive and thermionic characteristics of an Ag-O-Cs cathode, the argument for the presence of the oxide Cs_2O would be strengthened, because there is good evidence that the Ag-O-Cs cathode contains the cesium oxide Cs_2O (ref. 10).

e. Experimental Results with Cs_2CO_3 and Silver

As in the earlier depositions, the Cs_2CO_3-coated platinum ribbon was heated until the work function of the deposit on the nickel substrate decreased to a minimum value, at 400 K, of 1.13 eV. Next, a silver bead attached to a tungsten wire was resistance-heated to evaporation temperature while the photoemission current from the sample was monitored. The sample was held at about 400 K. The evaporation was continued until the white-light sensitivity reached a peak value of approximately three times the initial value. The evaporation was accompanied by a slight decrease of the thermionic emission (increased work function). Additional evaporation from the Cs_2CO_3-coated platinum ribbon at this stage restored the low work function without appreciable change in photoemission.

Alternate heating of the silver bead and the platinum ribbon was continued until the photoemission finally peaked at 30 times the original value. During this process, the work function remained almost constant at 1.13 eV (Figure 5). Additional evaporation caused a slight discoloration of the photosensitivity without affecting the work function.

The absolute value of the white-light sensitivity was approximately 25 μA/lm (microamperes per lumen) with an infrared response (through the Corning 7-56 filter) of about 7 percent. This sensitivity, as well as the work function, is typical for an Ag-O-Cs photocathode.

Three interesting conclusions can be drawn from the silver evaporation experiment:

(1) The almost constant work function during the addition of silver is a clear indication that the thermionic emission of the Ag-O-Cs cathode is associated with the cesium-oxygen component of the cathode.

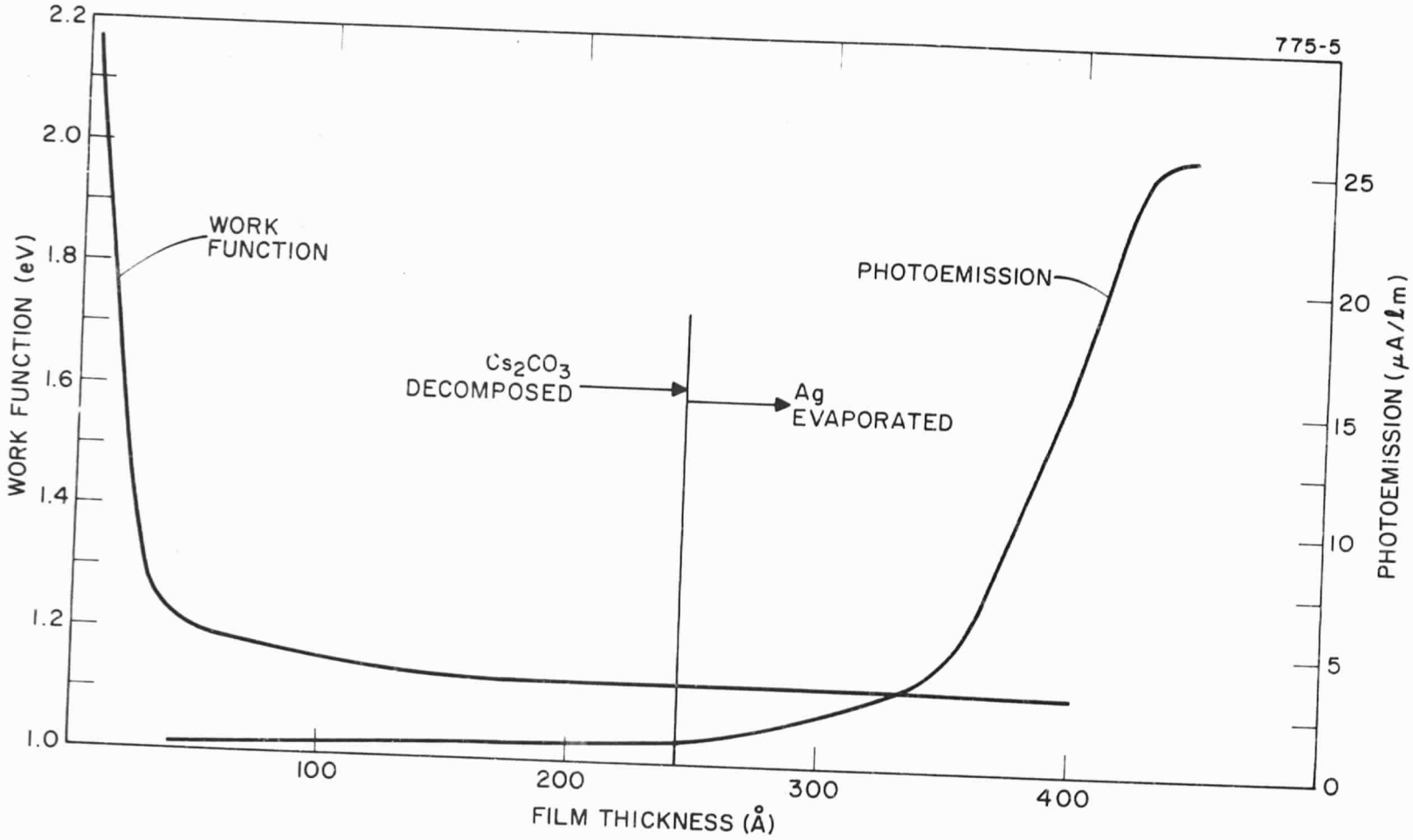

Figure 5. Change of Work Function and of Photoemission as a Function of Cs_2CO_3 Decomposition and of Subsequent Silver Deposition.

(2) Conversely, the dramatic increase of photoemission during the addition of silver confirms earlier results (refs. 10-14) that the response of the Ag-O-Cs cathode in the visible and infrared regions of the spectrum is associated with the silver, rather than the cesium, oxide.

(3) The typical thermionic and photoemissive Ag-O-Cs characteristics after silver evaporation provide additional, though still circumstantial, evidence that the predominant oxide in the material is Cs_2O rather than Cs_2O_2.

f. Use of Cesium Carbonate in Thermionic Converters

Previous attempts to produce low work function collectors by simultaneously introducing optimum amounts of cesium and oxygen into an operating diode have been only partially successful. The experiments with the decomposition products of Cs_2CO_3 suggest that the desired Cs:O ratio may be obtained by replacing the conventional Cs reservoir with a Cs_2CO_3 reservoir. Thus, the need for a separate oxygen source is eliminated. A diode with a Cs_2CO_3 reservoir is under construction.

B. SURFACE CHARACTERIZATION CHAMBER

1. Introduction

The Surface Characterization Chamber, shown in Figures 6 and 7, is used for analytical support of thermionic development and for the fundamental characterization of low work function surfaces. Samples can be introduced into the chamber by an interlock that permits ultrahigh vacuum to be maintained in the chamber while the interlock is open to the laboratory atmosphere for sample loading. Inside the chamber, a sample is transferred from the tray onto a rotatable manipulator by means of a hook or pneumatically activated jaws. The inboard jaw constitutes a hot/cold stage, inside of which hot or cold gases can flow to maintain sample temperatures from 77 to 575 K.

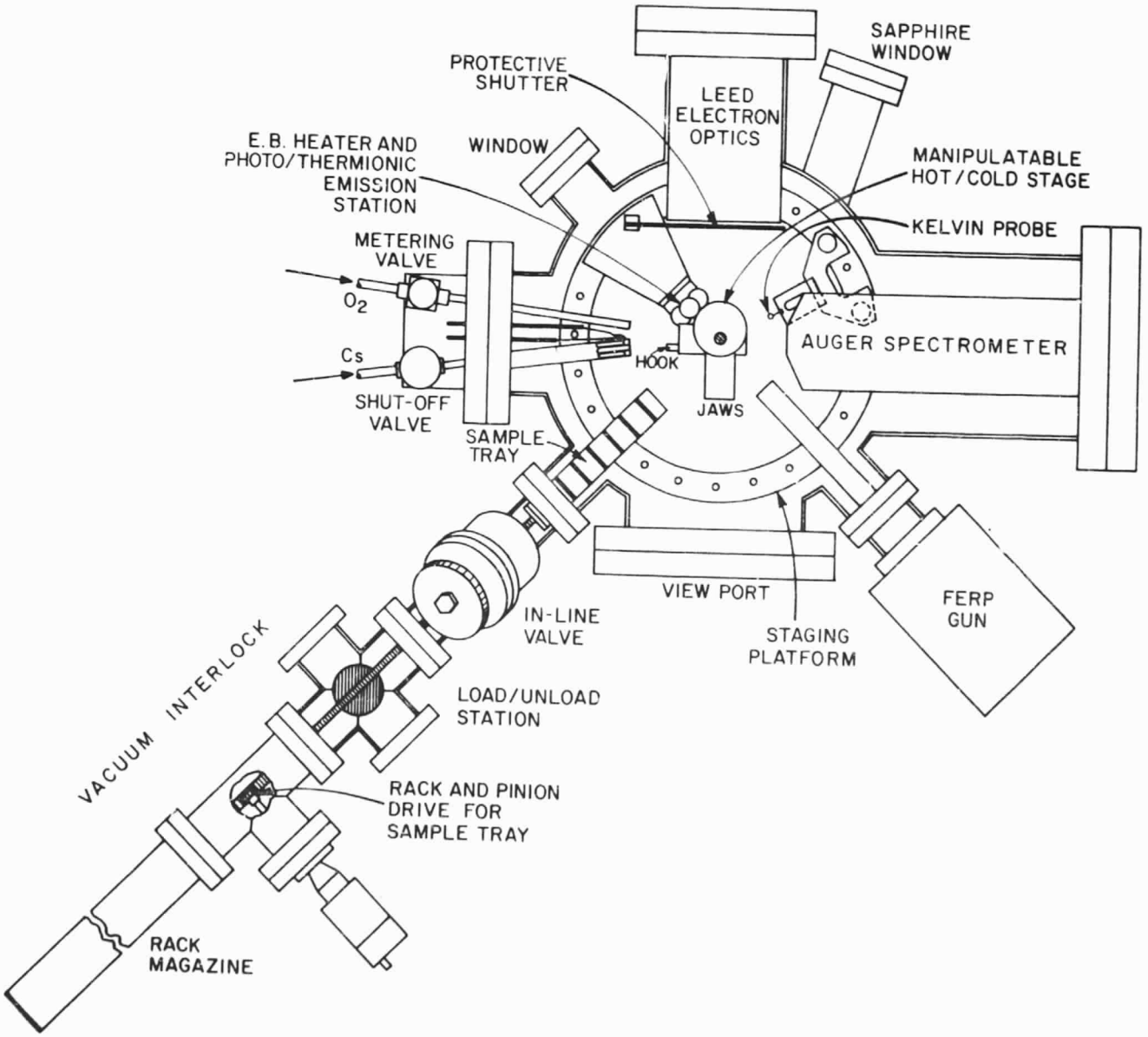

Figure 6. Surface Characterization Chamber.

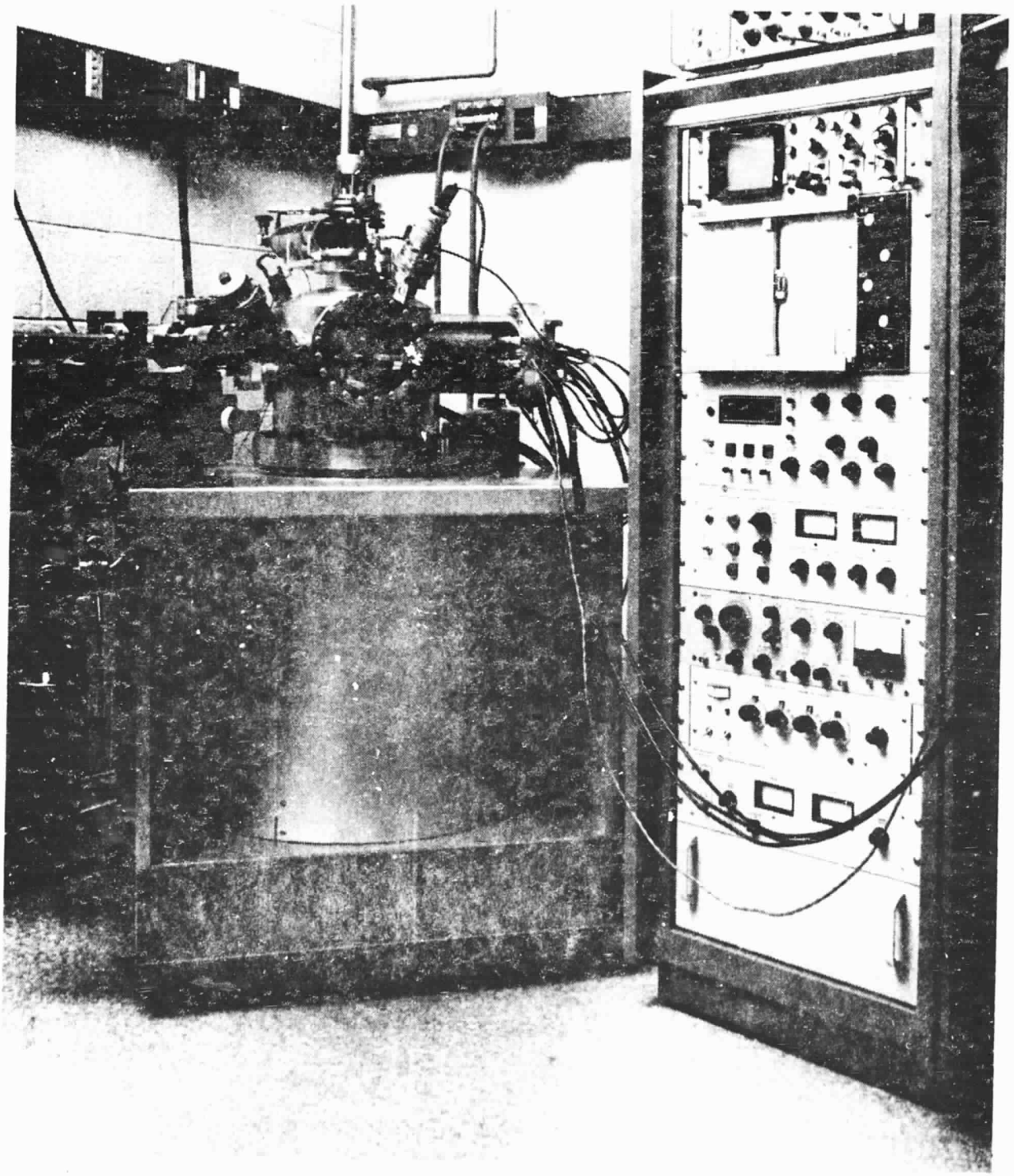

Figure 7. Surface Characterization Chamber and Support Electronics.

A sample admitted to the chamber can be cleaned thermally by electron bombardment from behind, or by sputter etching from above. A sample surface can be exposed to cesium vapor from heated elemental cesium, and to oxygen from a silver diffusion tube, when positioned in front of the station at the left.

Sample work functions can be measured by photoemission, thermionic emission, Kelvin probe, and field emission retarding potential (FERP) methods. The physical principle underlying the FERP technique is illustrated in Figure 8. This method is especially valuable in characterizing collector surfaces in that it provides not only an absolute measurement of work function, but also a measurement of the sample electron reflectivity spectrum. The field emitter electron source gives a fairly monoenergetic (~0.06 eV full-width-at-half-maximum (FWHM)) probe beam that is independent of contact potential. For semiconductor surfaces, the electronic structure of surface traps can be determined by the Kelvin probe by surface photovoltage spectroscopy. This method allows determination of the position of surface states in the band gap. Such states cause energy band-bending at the surface of a semiconductor, and therefore play a role in determining work function.

At practically any stage of sample processing, an ordered surface can be structurally characterized by means of low energy electron diffraction (LEED), and chemically characterized by means of Auger spectroscopy. Special holders are available for mounting simulated converter tests and reference surface samples, as well as for mounting entire emitter and collector assemblies from thermionic converters. Other holders can be made for almost any sample that can fit through the 3.6-cm opening of the interlock's in-line valve.

The sample support system, which is suspended from the top of the chamber, is made up of a series of three electrically isolated sections. The triaxial cable that electronically links the sample to laboratory instrumentation also permits guarded mode measurements to be made on the sample. This feature has proven essential to obtaining FERP data after a number of cesium exposures.

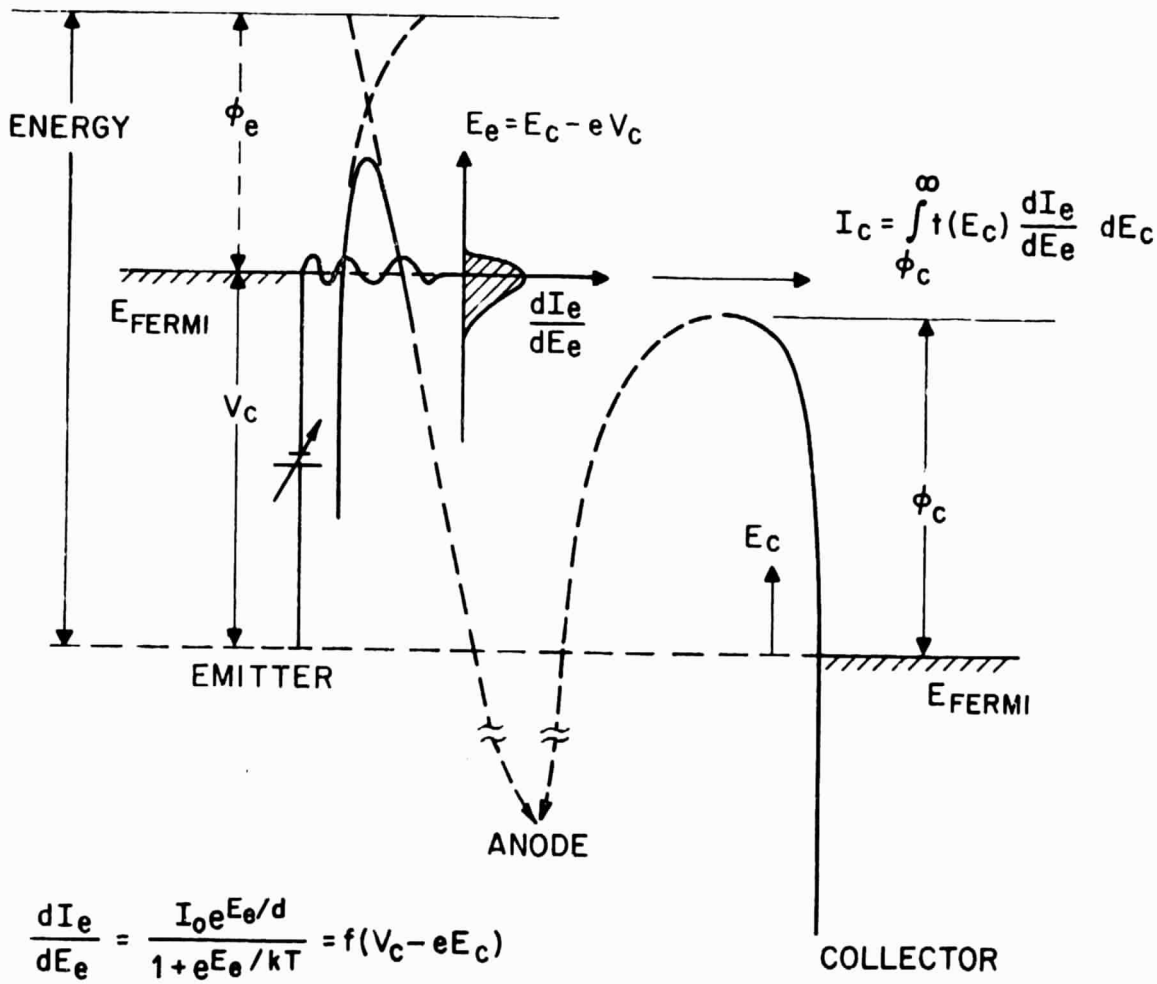

$$\frac{dI_e}{dE_e} = \frac{I_o e^{E_e/d}}{1+e^{E_e/kT}} = f(V_c - eE_c)$$

$$\frac{d^2 I_e}{dE_e^2} = 0,\ E_e = kT \ell n \frac{kT}{d-kT}$$

$$I_c(V_c) = \int_{-\infty}^{\infty} t(E_c)\, f(V_c - eE_c)\, dE_c$$

Figure 8. Field Emission Retarding Potential (FERP) Diagram.

2. Surface Analysis of Converter Electrodes

This section contains a few of the many Auger analyses performed on converter components.

A post-mortem analysis was made of Converter No. 142 (tungsten emitter, sprayed strontium-oxide-on-nickel collector). About one-third of the electropolished tungsten emitter surface had become a dull white. The corresponding position of the collector surface directly across from this dull white area was black. Microscopic inspection indicated that these areas were pitted.

The results of Auger analyses on the emitter and collector surfaces of Converter No. 142 are given in Table I. A considerable amount of strontium oxide was transferred from collector to emitter, most likely through physical contact of the electrodes, where changes in appearance occurred.

Table II summarizes the results of Auger analyses performed upon the emitter of Converter No. 149 and the collectors of Nos. 148 and 149. Both of these converters have platinum emitters. Converter No. 148 has a structured nickel collector, and Converter No. 149 has a central-plane nickel collector. Platinum was found to be present on both collectors. Converter No. 149 was apparently contaminated with phosphorus. The collectors of both converters had approximately 1-mm dark spots, one each, spaced about 2 mm from their perimeters. The spot on Converter No. 148 contained silicon in the form of SiO_2, whereas the spot on Converter No. 149 appeared to be, if anything, cleaner than the rest of the surface. Magnesium was not present on the emitter surface of Converter No. 149. This may indicate that the magnesium contamination, not usually seen in Auger analyses of converter components, was produced in preliminary collector processing. However, it must also be recognized that evaporation of magnesium from the hotter emitter is possible. The emitter of Collector No. 149 had a coarse grain-like structure, with particles about 2 mm across. An Auger scan analysis (the electron beam is about 0.25 mm in diameter) of this surface did not reveal any remarkable nonuniformities in surface chemical composition. A FERP scan of this surface did not reveal any substantial differences in work function among the grains.

TABLE I

CHEMICAL COMPOSITION OF ELECTRODE SURFACES OF CONVERTER NO. 142

Chemical Species	Emitter - %		Collector - %	
	Dull White Deposit	Reflective Area	White Deposit	Black Area
C	10	17		
O	30	19	57	64
Na	0.4			
S	3.2	4.9	0.2	
Ca			0.3	
Ni		1.6	0.4	
Cu	0.4	3.0		
Sr	40	17		
Cs	6.1	16		
W	9.7	21	42	36

TABLE II

AUGER ANALYSES OF ELECTRODE SURFACES
OF CONVERTER NOS. 148 AND 149

Chemical Species	Converter No. 148		Converter No. 149		
	Collector - %		Collector - %		
	Spot	Off-Spot	Spot	Off-Spot	Emitter - %
C	2.8	3.1	8.6	16	16
N				1.9	
O	45	19	15	23	5.5
Cl			0.7		
Mg		7.3	4.9	2.8	
Si	22				
P			2.9	3.1	3.2
S		2.1	1.9	1.2	
Ca	0.1	2.1	3.1		
Ni	11	11	25	4.7	
Cs	19	47	34	31	19
Pt		7.2	4	6.1	56

3. Surface Activation Chamber Analyses

Auger analyses were performed upon evaporated deposits and deposition sources that had been studied in the Activation Chamber. It was found that barium oxide, deposited from a barium carbonate spray-coated platinum strip, deposited as barium oxide with negligible traces of carbon (in some cases along with detectable amounts of platinum). Cesium oxide, deposited from a cesium carbonate spray-coated platinum strip, showed sodium impurities, but with negligible traces of carbon. Platinum was barely detectable in this deposit, which is understandable since the cesium oxide deposition occurred at a considerably lower source temperature than for barium oxide. Platinum was probably transported to the evaporated surface by means of vaporized platinum oxide, which is considerably more volatile than pure platinum.

4. Fundamental Materials Studies

Surface chemistry, work function, and electron reflectivity of a 0.025-mm thick sheet of platinum were studied. The foil was spot welded to a standard tungsten sample holder and given a standard degreasing treatment prior to insertion into the interlock of the Surface Characterization Chamber. The results are summarized in Table III. Copper was most likely introduced by the spot-welder's copper tweezers; calcium, probably a native impurity, was easily expelled; cesium was deposited onto the sample when it was inadvertently placed in front of the cesium gun over the weekend.

The most tenacious impurity was carbon. Its effect upon normally high bare work functions of platinum was substantial. In view of the increase of surface carbon with respect to heat treatment temperature, its presence was due to the bulk material and not hydrocarbons adsorbed during atmospheric exposure. Carbon is known to have negligible solubility in solid platinum (ref. 15). Heat treatment in ultrahigh vacuum alone cannot expel carbon from platinum since this procedure serves only to cause any graphite entrapped in the bulk to segregate out at the surface. Significantly long heat treatment in the presence of oxygen, to allow all the bulk carbon to diffuse to the surface and leave in the form of an oxide, did serve to clean the sample and to establish the known high platinum bare work function.

TABLE III

CHRONOLOGY OF CLEANING TREATMENT OF PLATINUM FOIL

771-16

Treatment Chemical Species	As Admitted	500 K 2 Min	670 K 5 Min	870 K 5 Min	1070 K 5 Min	1370 K 5 Min	1770 K 5 Min	10^{-6} TO_2 UV+300 K 15 Min	10^{-6} TO_2 0.5 Min 970 K	10^{-6} TO_2 1 Min 1270 K	10^{-6} TO_2 1 Min 1570 K	10^{-6} TO_2 2 Min 1570 K	16 Hr 300 K
	σ_0	σ_0	σ_0	σ_0	σ_0	σ_0	σ_0	σ_0	σ_0	σ_0	σ_0	σ_0	σ_0
C	37	44	47	46	42	54	59	32	62	60	36	0.5	2.2
O	1.1	0.9	0.8	0.6	0.1						0.4	0.6	0.8
Ca					5.3	3.6							
Cu	4.9	8.9	0.3	0.3									
Cs								46	1.8	1.6			
Pt	57	50	50	53	53	42	41	22	36	38	63	99	97
φ_e(eV) (FERP)	4.92	4.22	4.51	4.50	4.65			4.50			4.83	5.77	5.63
Reflectivity	Considerable	Substantial	Negligible	Low	Negligible	Substantial		Substantial			Substantial	Negligible	Negligible

When the sample was left overnight in the vacuum chamber ($P = 3 \times 10^{-10}$ torr), the surface carbon concentration increased slightly and, correspondingly, the work function decreased slightly. The presence of residual carbon monoxide is the most likely source of carbon supply.

A cesium carbonate vaporization study was conducted in the Surface Characterization Chamber. A 3.125-mm wide strip of 0.025-mm thick platinum was sprayed with a suspension of cesium carbonate in a nitrocellulose-butyl acetate solution. The 201-nickel substrate was heated in the vacuum chamber to 1000 K to clean the surface of oxygen. The efficacy of this treatment was demonstrated by Auger spectroscopy. Initial deposition from the platinum strip, at a temperature of about 700 K, produced approximately one monolayer of cesium on the substrate and a corresponding FERP work function of 1.90 eV. Further heating of the strip at this temperature resulted in a detectable amount of oxygen, but no improvement of work function.

Evaporation at 830 K increased the Cs:O ratio to 6.8 and reduced the FERP work function to 1.70 eV. During the remainder of the investigation, this ratio stayed between 4.7 and 8.4, whereas the work function varied between 1.35 eV and 3.00 eV. Heating the strip to 980 K (considered to be the "decomposition temperature" of cesium carbonate) gave the highest measured Cs:O ratio ($\sim$8.4) and a work function of 1.46 eV. At this stage, interference color bands were visible on the sample. Further evaporations at higher temperatures did not improve the work function until the sample-to-strip distance was increased. With a distance greater than 2.5 cm, the lowest work function of 1.35 eV was obtained for a region that was about 6 mm from the centerline of the deposition pattern; the highest work function (2.30 eV) occurred at the centerline. There was little variation of work function along any line parallel to the centerline. A corresponding Auger analysis showed that the Cs:O ratio of the sample surface increased monotonically with distance from the centerline of deposition.

Apparently, the wide range in work function of the heavy cesium oxide layer was a result of both bulk and surface phenomena. The lower Cs:O ratio along the deposit's centerline is indicative of re-evaporation of cesium due to radiative heating of the platinum strip.

Although there is no direct evidence of any bulk effects produced by this heating, the higher work function along the centerline is consistent with an upward bending of energy bands, which bulk depletion of cesium would be expected to produce.

5. New Support Facilities

Since the sample sputter ion gun configuration was too oblique, a hod-type carrier was designed and fabricated for improving the splutter-etching capability of the Surface Characterization Chamber. The hod, activated from outside the chamber by means of a linear motion feedthrough, removes the sample from its carrier hook and orients it perpendicular to the sputter ion gun axis for improved operation.

A revised Surface Characterization Amplifier, shown in Figure 9, was designed and fabricated in order to permit biasing of low-level collection current without batteries. Input bias can be swept manually by means of a ten-turn potentiometer, or automatically by means of a linear ramp generator. Sweep and amplified signal outputs permit X-Y recording for collection I-V curves. Bias voltage or signal strength is read out on a digital display. The amplifier processes ac as well as dc signals, thus permitting differentiation of currents collected from the FERP gun. The current detection range of the amplifier is from 100 μA to 0.01 nA.

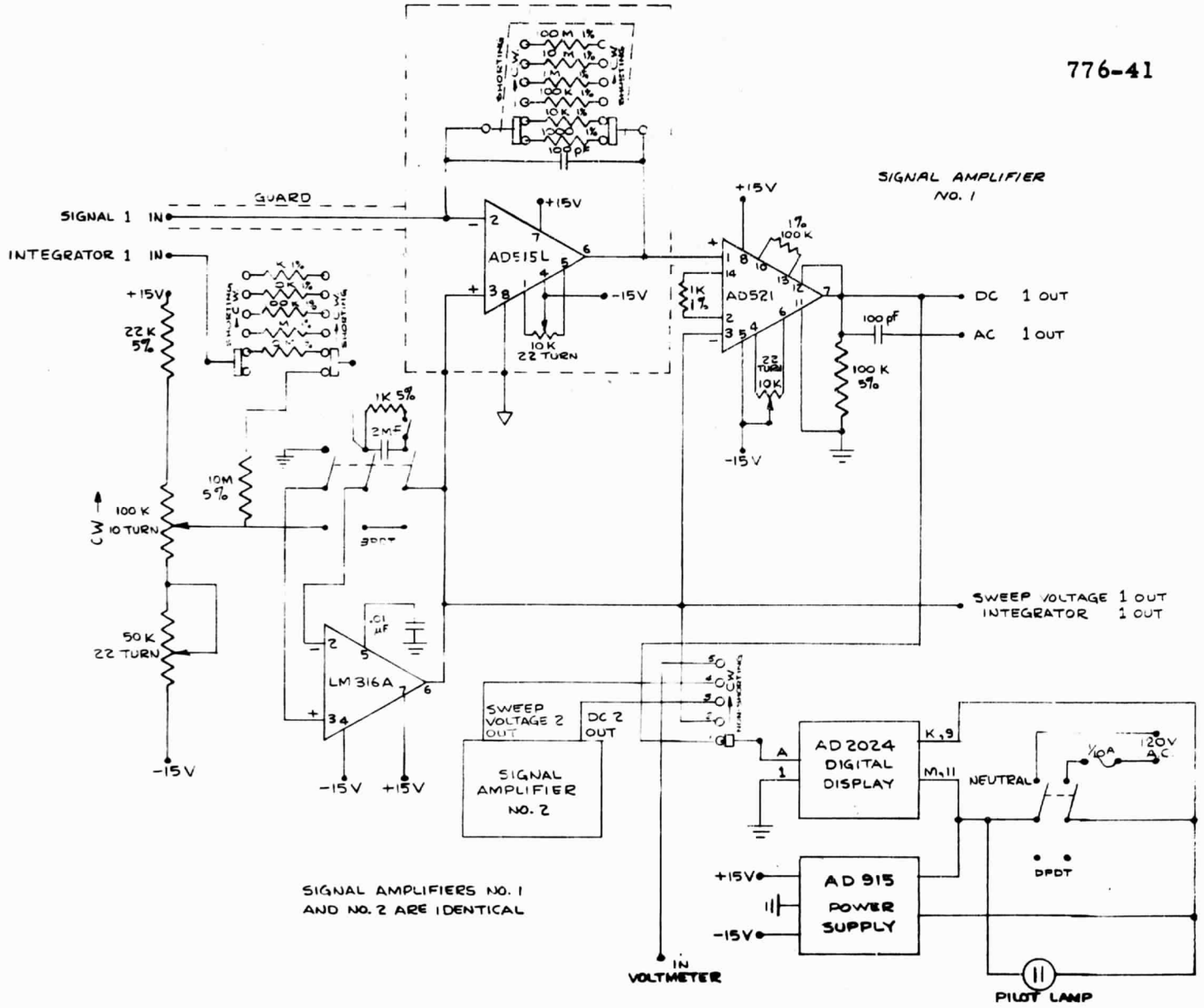

Figure 9. Surface Characterization Amplifier.

III. HIGH-EFFICIENCY DIODE EXPERIMENTS

A. INTRODUCTION

Experiments were continued to analyze the effects of oxygen additives on collector performance. Direct oxygen addition, as well as the use of oxides as a collector coating were investigated. The standard, variable-spacing converter used in these studies (Figure 10) has been described in an earlier report (ref. 16). A silver tube was used for direct oxygen admission. For the oxide experiments, the coating was evaporated directly onto the collector substrate and the tube was not used.

The surfaces examined were: lanthanum hexaboride with oxygen, tungsten oxide on columbium with 1% zirconium, and titanium oxide.

B. CONVERTER EXPERIMENTS

1. Tungsten Emitter, Lanthanum Hexaboride Collector (Converter No. 144)

This variable-spacing converter with a tungsten emitter uses a silver tube leak to supply oxygen to the interelectrode space (Figure 10). After the initial outgassing of the converter, the silver tube leak was operated for three hours at 925 K with the outside of the tube opened to atmosphere. Such a conditioning period is required to clean the silver leak of sulfur and organic contaminants (ref. 17). Oxygen diffusion into the interelectrode space can be regulated in two ways: either by opening the outside of the silver tube to the atmosphere, and then heating it to approximately 875 K; or by reversing this procedure (i.e., maintaining the leak at 875 K with vacuum on the outside), and then opening the tube to atmosphere when oxygen is desired. The latter method has the advantage of allowing the silver tube to be operated at collector temperatures at all times in order to avoid cold spots in the converter during testing.

After conditioning the silver tube and establishing control of the oxygen leak, the converter was outgassed again. Even with the silver tube, initial low-temperature power data indicated that oxygen was present in the converter and that the emitter appeared oxygenated (Figure 11). Heating the collector dispensed oxygen, thus increasing the emitter saturation current at a fixed cesium pressure (Figure 12).

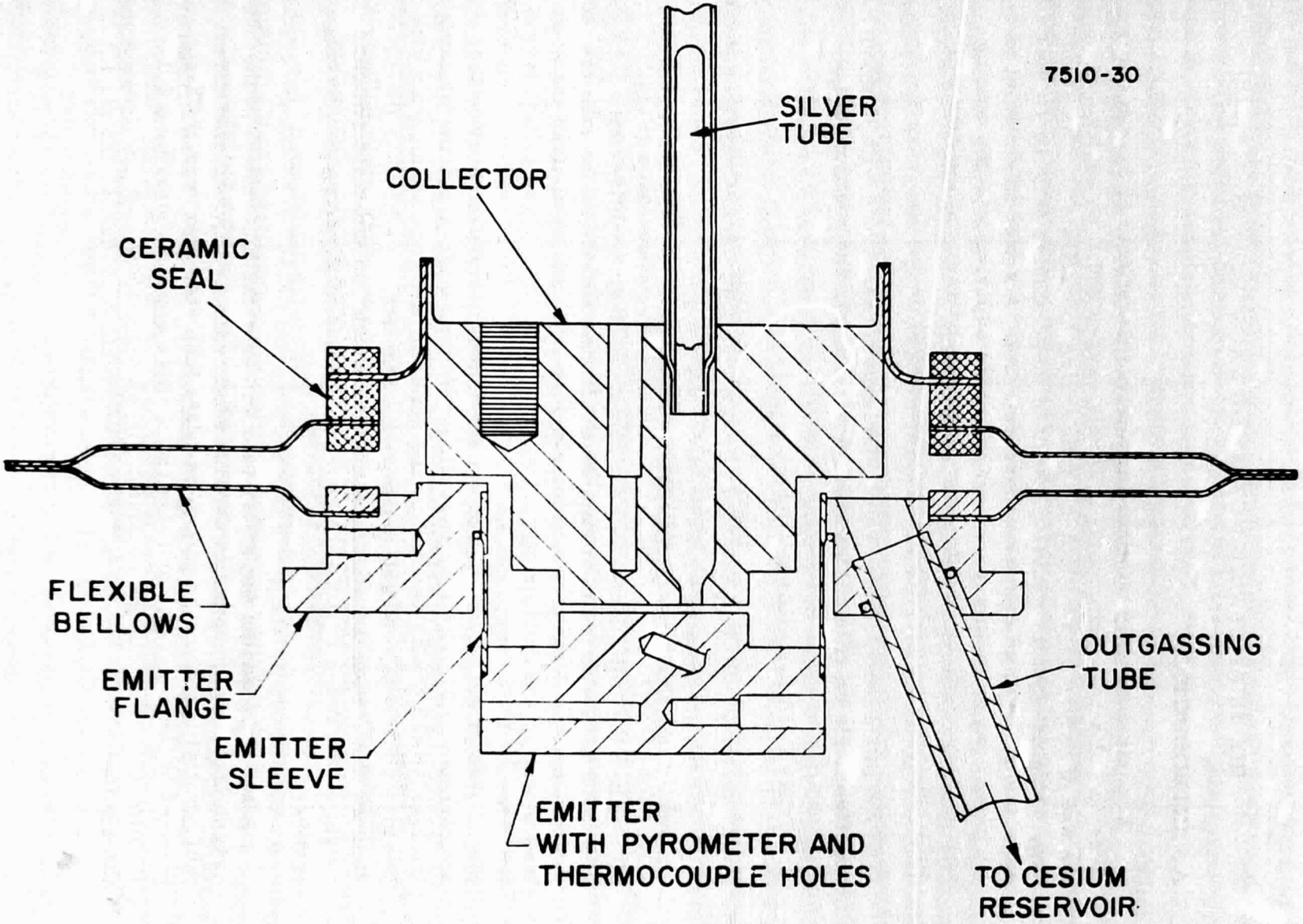

Figure 10. Cross Section of the Standard Variable-Spacing Converter with Silver Tube for Oxygen Addition.

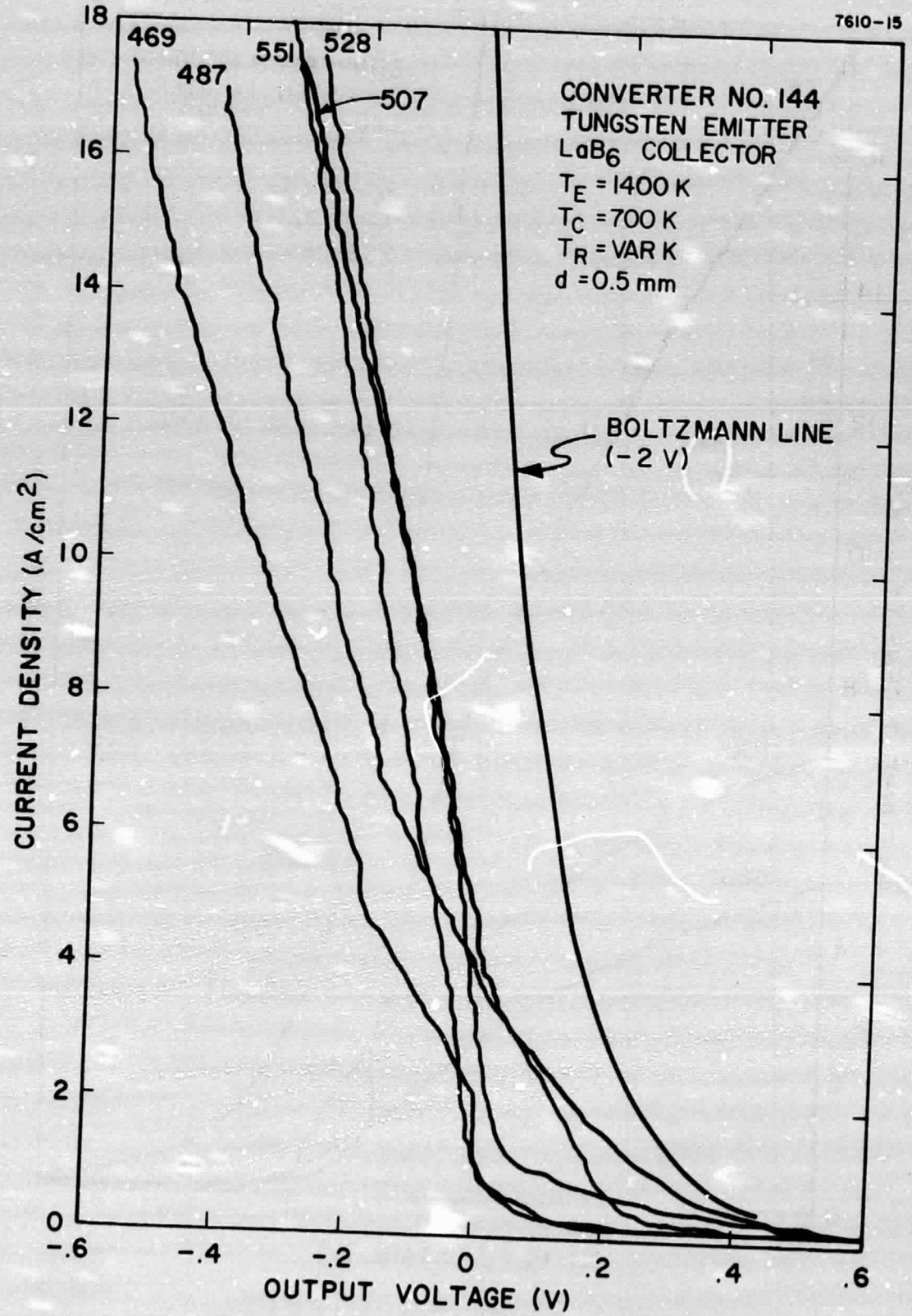

Figure 11. Cesium Family for Converter No. 144 at T_E = 1400 K, T_C = 700 K, and d = 0.5 mm.

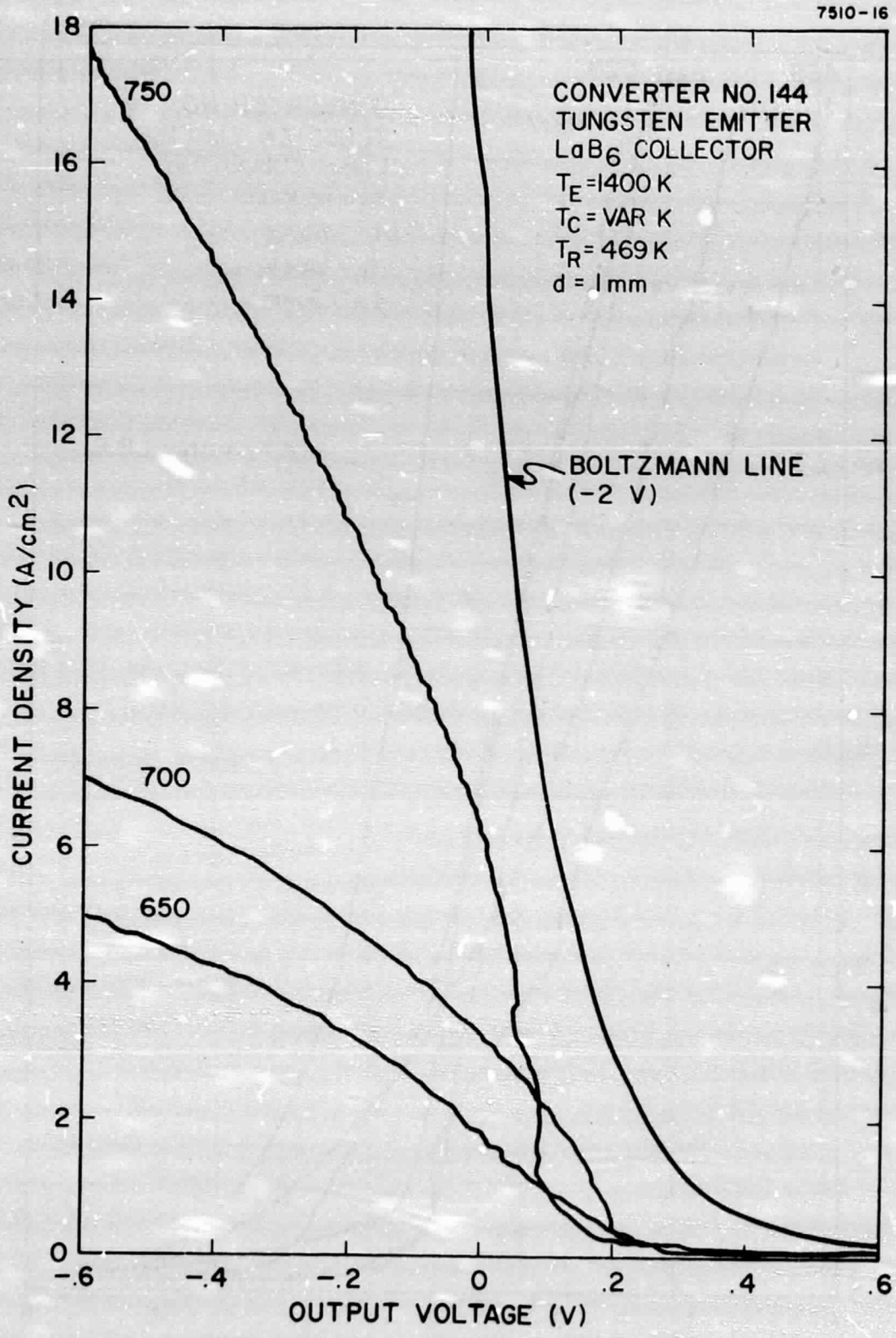

Figure 12. Collector Family for Converter No. 144 at T_E = 1400 K, T_R = 469, and d = 1 mm.

The performance of the converter was allowed to stabilize, and the collector work function was measured using both retarding potential and low-current dc back-emission methods. Retarding data gave a minimum work function of 1.42 eV, whereas back emission showed a lower minimum of 1.28 eV (Figure 13). Power data were taken at emitter temperatures of 1300 and 1400 K. The converter had a barrier index of 2.0 eV at both emitter temperatures, as shown in Figures 14 and 15.

In several experiments, various amounts of oxygen were admitted into the converter by maintaining the collector at 675 K, the emitter at 475 K, and the cesium reservoir at 300 K (cesium background pressure less than 5×10^{-6} torr). The temperature of the silver tube was raised to 925 K for 1/2 hour with the back of the tube exposed to the atmosphere, after which it was cooled to the collector temperature, and performance data were taken. The tungsten emitter appeared highly oxygenated; saturation current varied with collector temperature. Optimized performance was observed at a collector temperature of 750 K with a 1-mm diode spacing. A barrier index of 1.96 eV was measured. However, performance was not stable at these conditions and, after a few hours, the emitter saturation current dropped by a factor of 2, and the barrier index increased to 2.1 eV. Subsequent oxygen treatments lasting from 1 to 3 hours would "reactivate" the converter but never to the performance level seen after the first treatment.

In a second set of experiments, an attempt was made to admit oxygen into the converter in the presence of 10^{-2} to 10^{-1} torr of cesium. First, emitter saturation current was measured with a vacuum on the outside of the heated silver tube. Then oxygen was admitted by exposing the outside of the tube to the atmosphere. No change in emitter saturation current was observed even after three hours of silver tube operation, indicating that, if oxygen had penetrated to the collector, a negligible amount had reached the emitter.

2. Columbium-Tungsten Oxide Collectors

Several converters were constructed to examine the potential of using tungsten oxide coatings on substrates of columbium, a material particularly desirable for the construction of long-life hardware devices operating in vacuum. Columbium is easily electron-beam welded and is a good thermal expansion match for the usual ceramic

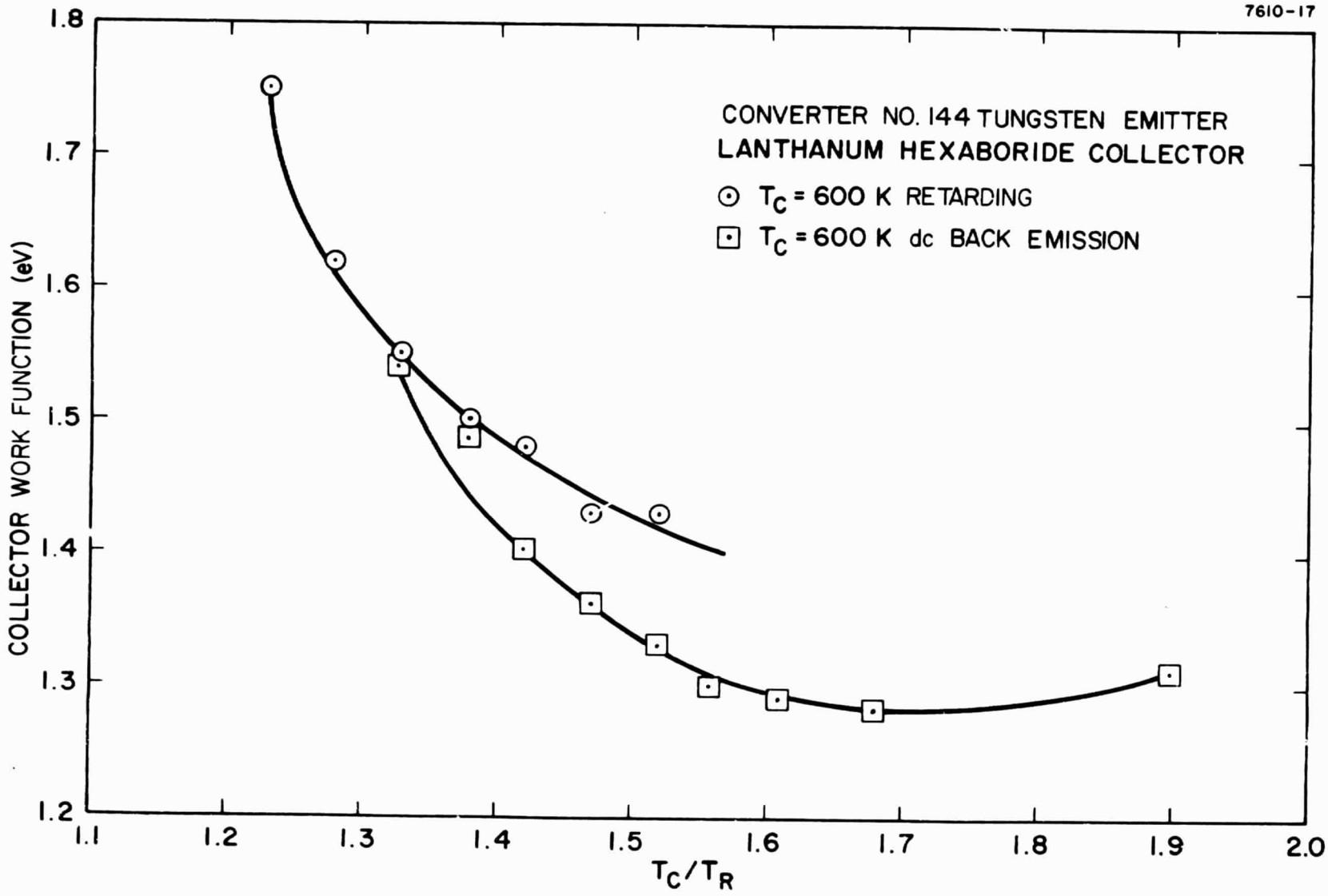

Figure 13. Collector Work Function Versus T_C/T_R.

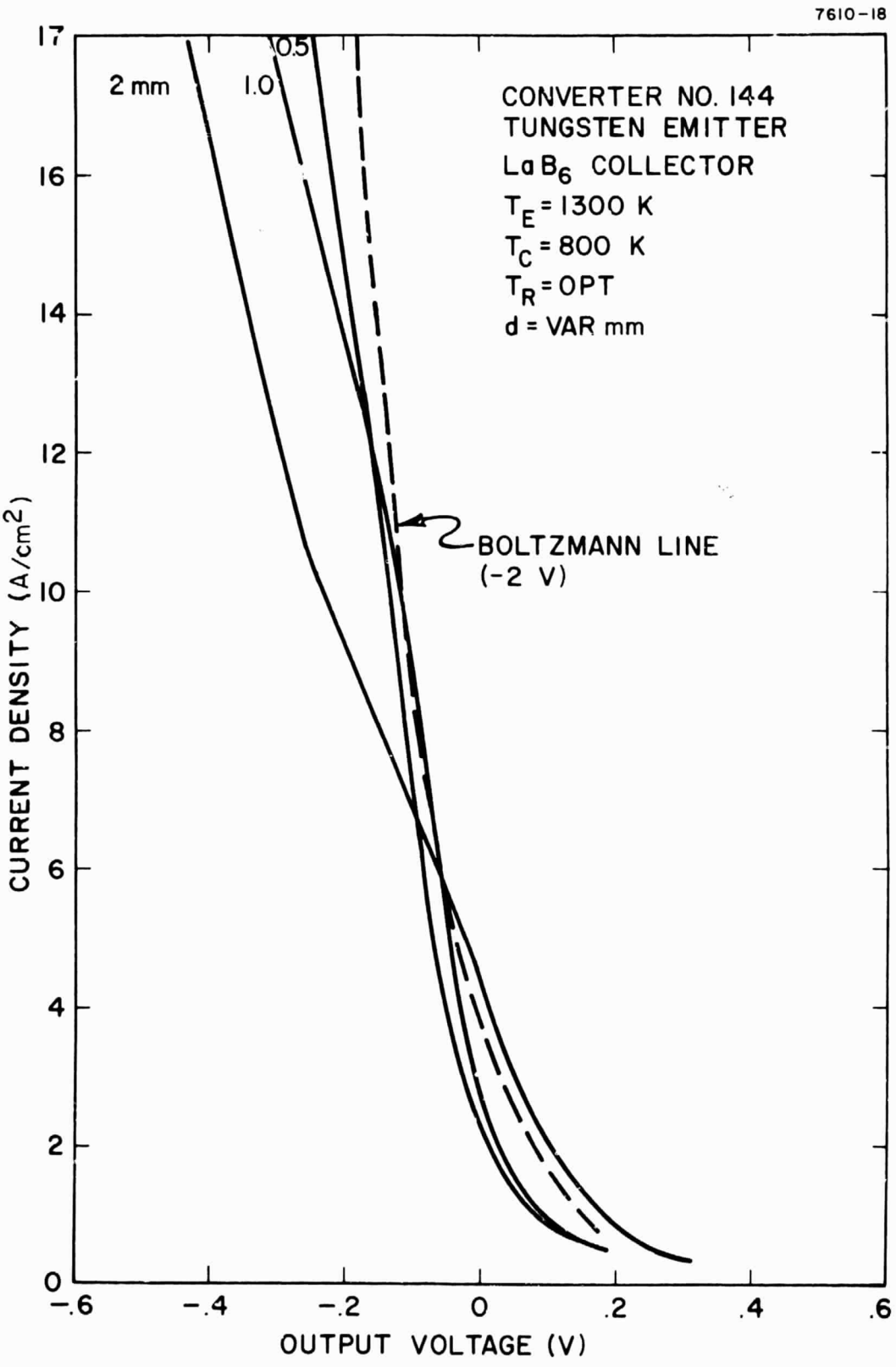

Figure 14. Cesium-Optimized Envelopes for Converter No. 144 at T_E = 1300 K at Several Interelectrode Spacings.

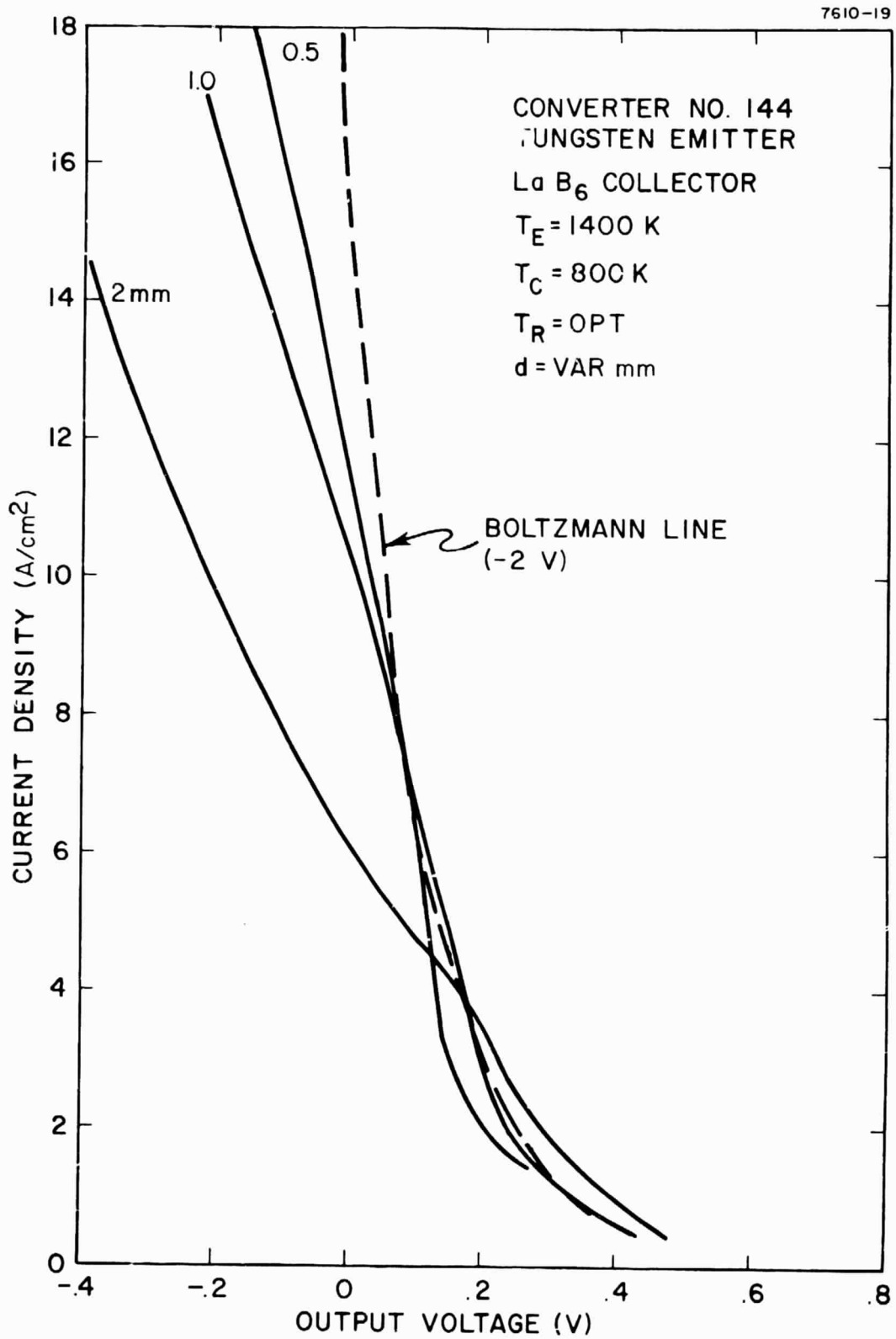

Figure 15. Cesium-Optimized Envelopes for Converter No. 144 at T_E = 1400 K at Several Interelectrode Spacings.

seal materials used in converters. However, this element is a getter for oxygen, making it difficult for converters using pure columbium to operate without oxygen and, therefore, optimizing performance at a relatively small electrode spacing. However, it should be noted that experiments conducted in 1973 showed that oxygen-saturated columbium would release this gas during converter operation (ref. 18). Consequently, if tungsten oxide, like tungsten, could be deposited on columbium, the oxide could serve as an oxygen source. Improved performance would be expected, and the wider optimized spacing would greatly simplify device construction.

Three converters were constructed and tested to evaluate tungsten oxide deposition techniques and resulting converter characteristics. These experiments are described below.

a. Tungsten Emitter, Columbium-1% Zirconium-Tungsten Oxide Collector (Converter No. 153)

This standard variable-spaced device had an electropolished tungsten emitter and a tungsten oxide collector on a substrate of columbium-1% zirconium. The tungsten oxide was evaporated directly onto the substrate from an oxidized tungsten slug following a previously developed procedure (ref. 18). Initial power data indicated that the collector was in the preactivated state of tungsten oxide (barrier index of 2.1 eV). Subsequent operation in cesium did not improve the performance, as would normally be expected. Emitter saturation currents continued to decrease during testing, indicating a reduced oxygen supply to the emitter. In an effort to regain the initial condition, the collector was heated to 800 K. Cesium families taken at 100-degree intervals of the collector temperature showed some degradation in the current-voltage characteristics above 600 K. Indication of electrical resistance was observed as the curves began to tilt away from the Boltzmann line. The output stabilized at a collector temperature of 800 K for several days, implying that no oxygen was reaching the emitter. Testing was terminated when an irreparable spacing problem developed, inhibiting proper alignment of the electrode surfaces.

Subsequent visual inspection showed the collector to be metallic gray with no evidence of damage to the surface. Auger analysis showed tungsten to be present, but there was no indication that columbium or zirconium had migrated to the surface.

b. Tungsten Emitter, Columbium-Tungsten Oxide Collector (Converter No. 159)

This converter is similar to Converter No. 153, previously discussed, without the 1% zirconium in the substrate. Its purpose was to determine whether the poor oxygen-dispensing properties observed in Converter No. 153 were due to the reaction with, or gettering of, the oxygen by the zirconium during "activation" treatments.

DC back-emission work function measurements gave a minimum collector work function of 1.37 eV at a T_C/T_R of 1.6 (Figure 16). Early power data indicated the converter was highly oxygenated, with unstable performance at a given cesium temperature. In order to stabilize the output, the converter was operated continuously at the following conditions: T_E = 1400 K, T_C = 650 K, T_R = 528 K. After one day, the emitter saturation current was observed to be down to the level typical for tungsten emitters. The collector was then heated to 700 K, causing the emitter saturation current, at a fixed cesium pressure, to increase, thereby indicating that oxygen was being dispensed by the collector. The converter was operated at this collector temperature for about 20 hours, at which time the emitter current had dropped to its previous level.

c. Tungsten Emitter, Columbium-1% Zirconium-Tungsten Oxide Collector (Converter No. 162)

Two vapor depositions of tungsten oxide on a columbium-1% zirconium substrate distinguish this diode from Converter No. 153. Following the first deposition, the substrate was heated in vacuum to 775 K for 6.5 hours in order to diffuse the oxide layer into the substrate. Then another layer of tungsten oxide was vapor-deposited on top of the first coating, and the collector received a predegas treatment to 475 K. This heating allowed the columbium to become saturated with oxygen so that the second deposition could then supply oxygen for converter operation.

Initial power data did not indicate the presence of oxygen typical of tungsten oxide converters. The performance was stable, but the emitter saturation currents were no greater than those for nonoxygenated tungsten emitters. However, operation of the converter for several days with the collector at 750 K and in 0.25 torr of cesium

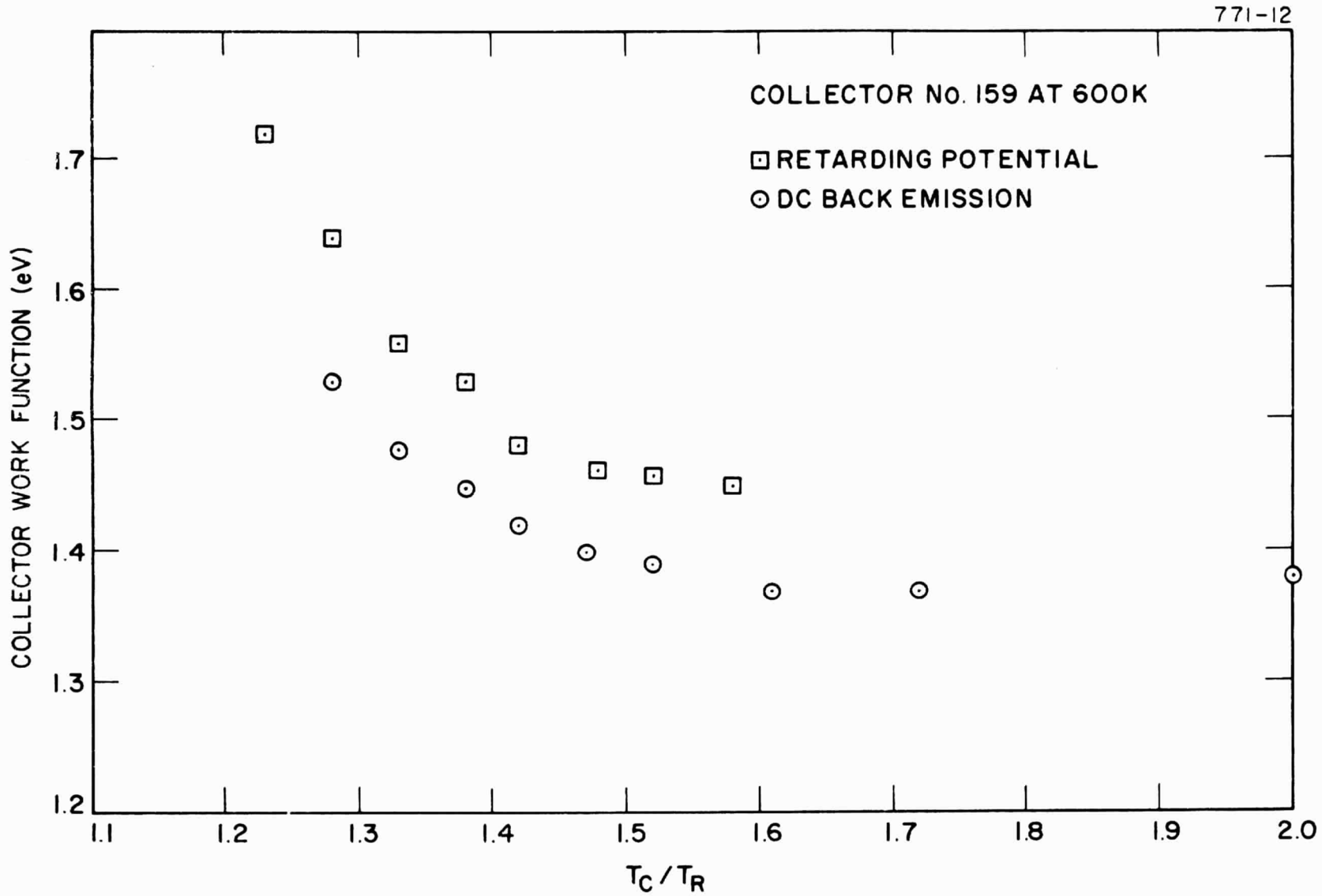

Figure 16. Collector Work Function of Converter No. 159.

increased the saturation currents by a factor of about three, thus indicating that oxygen was dispensing slowly from the collector. After the performance stabilized, the collector was heated to 800 K, and once again an increase in emitter current was observed over a period of a few days. At this point, the converter had sufficient oxygen to operate at a high emitter temperature and still maintain a 1-mm spacing. The converter ran several days at T_E = 1600 K, T_C = 800 K, T_R = 528 K, and d = 1 mm, with a barrier index of 2.05 eV. Power output was 2.7 W/cm^2 at a current density of 8 A/cm^2. After operating at these conditions for 200 hours, the barrier index increased to 2.1 eV, and the power output decreased to less than 1.6 W/cm^2 at 8 A/cm^2. The collector temperature was then raised to 850 K, which again dispensed oxygen to the emitter and increased the saturation current. The converter performance became stable after approximately one day at this higher collector temperature, with a barrier index of 2.05 eV and power output greater than 3 W/cm^2 at 10 A/cm^2 (Figure 17). After operating the converter for over 2200 hours, the power output was still greater than 2.7 W/cm^2 at 8 A/cm^2, with a barrier index of 2.06 eV. A chronological comparison of output characteristics is shown in Figure 18.

3. Titanium Oxide Collectors

a. Tungsten Emitter, Titanium Oxide Collector (Converter No. 158)

Titanium oxide has shown a potential to form a low work function collector electrode (ref. 19). A titanium collector (Converter No. 123) was constructed, but the best barrier index that could be obtained was 2.1 eV. Auger analysis showed nickel contamination on the surface of the collector, caused, in all probability, by diffusion of the nickel-brazed material through the thin titanium substrate. Consequently, the thickness of the titanium slug was increased from 0.25 mm to 1.25 mm. The oxide surface of the collector of Converter No. 158 was prepared by heating the titanium to 725 K in one atmosphere of oxygen for three hours. A 0.20-mm layer was then machined off, and the resultant surface was mechanically polished and chemically etched to eliminate surface contaminations. Back-emission measurements yielded a minimum collector work function of 1.43 eV at a T_C/T_R of 1.5 to 1.6, and retarding potential measurements gave a minimum of 1.57 eV at a T_C/T_R of 1.3 (Figure 19).

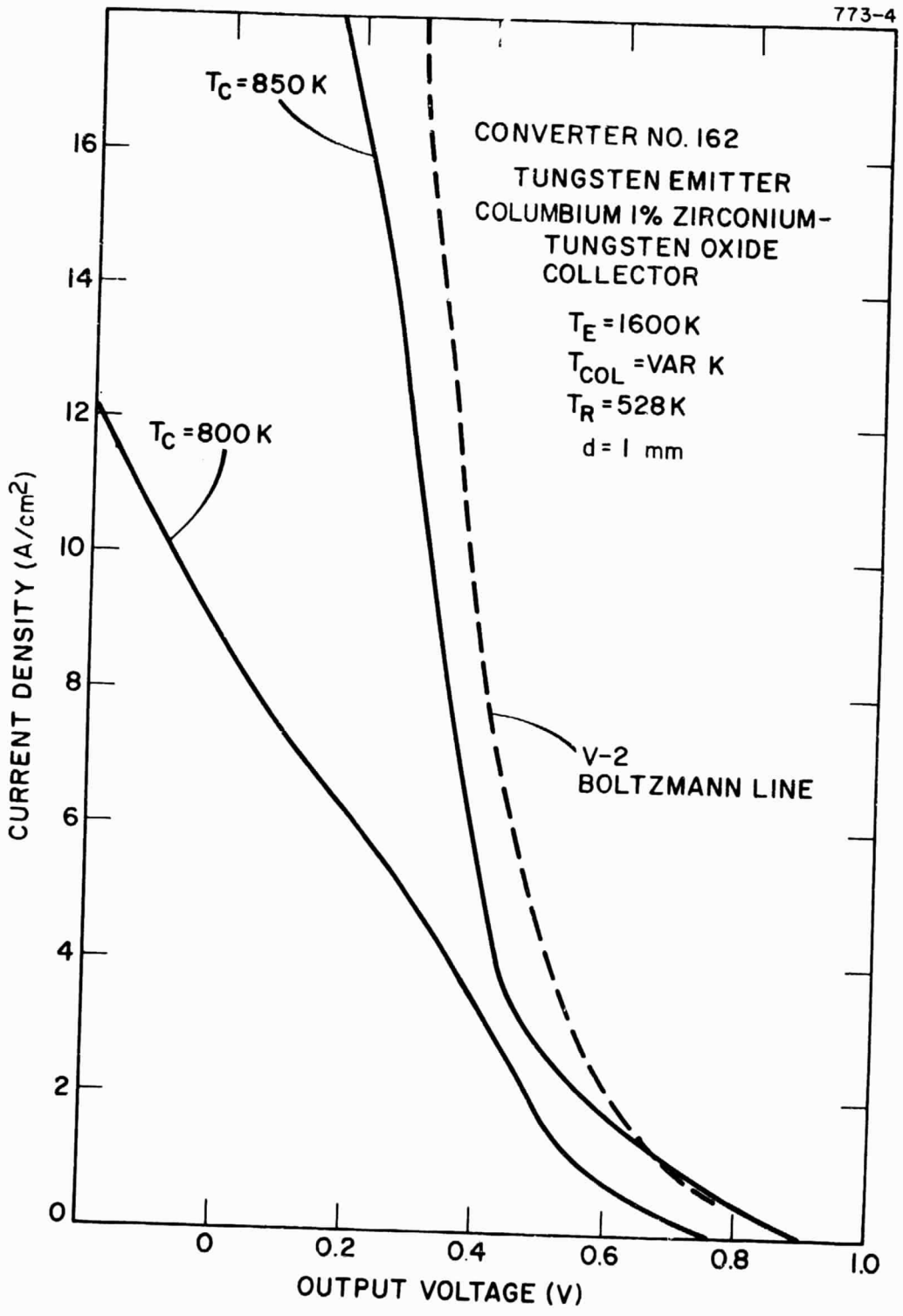

Figure 17. Effect of Increased Collector Temperature on Performance.

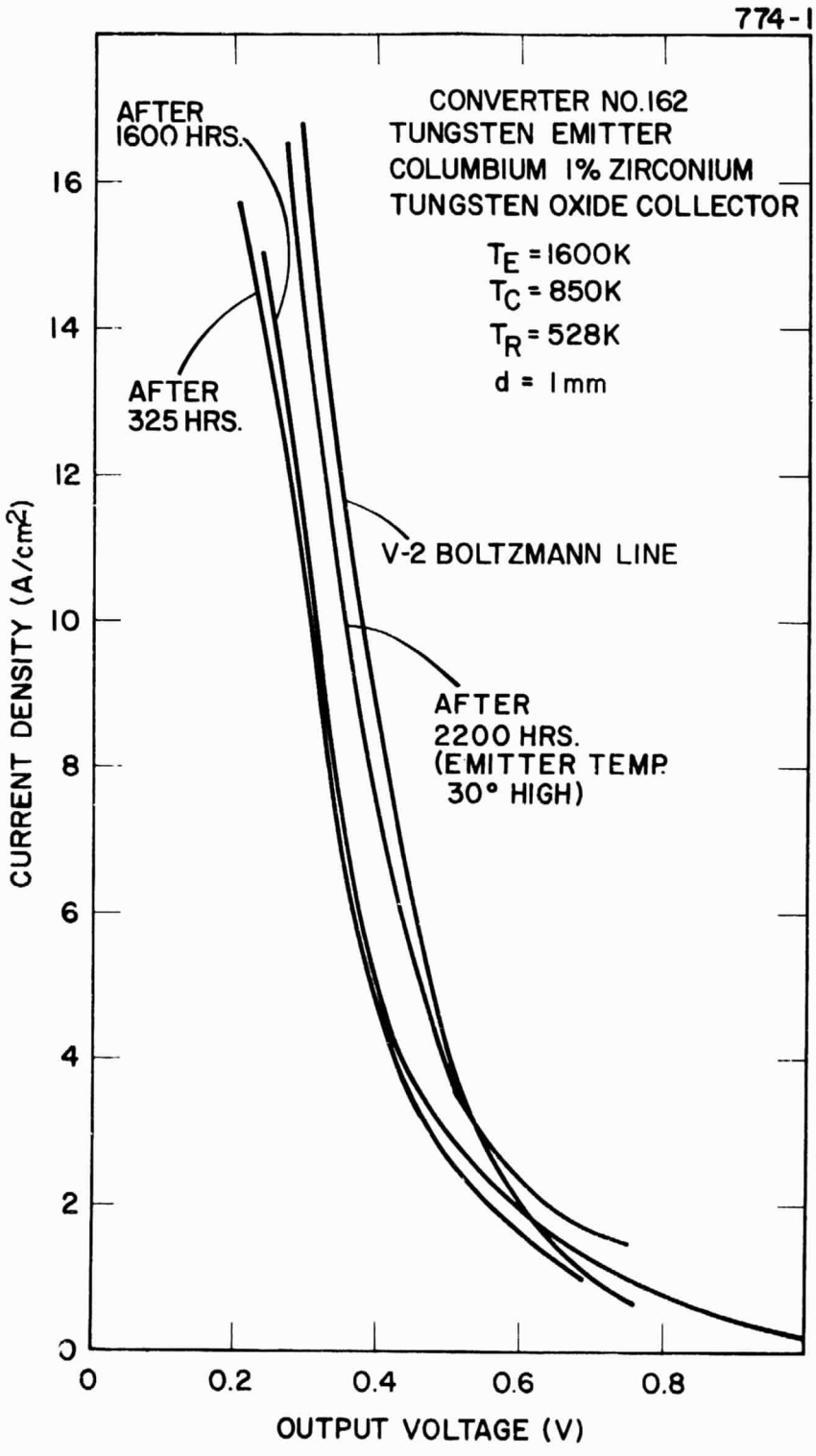

Figure 18. Life Test Converter Performance.

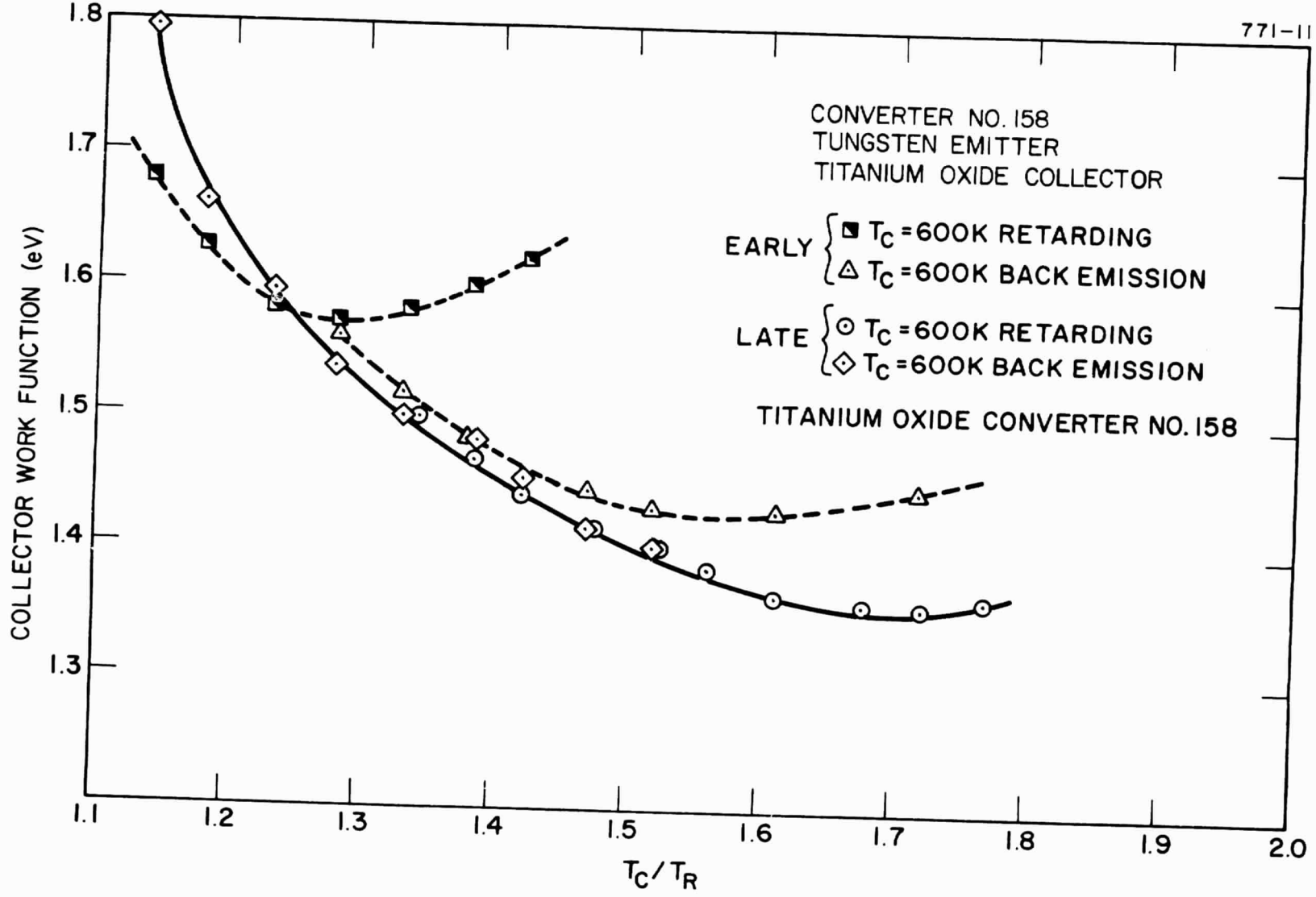

Figure 19. Collector Work Function of Titanium Oxide Converter No. 158.

Following a run-in period of one day, during which the converter was operated at T_E = 1400 K, T_C = 700 K, T_R = 507 K, the collector was heated to 900 K for 5 minutes in an effort to "activate" the surface, similar to the procedure used with tungsten oxide. This treatment produced a lower barrier index of 2.05 eV at optimum collector temperature. Subsequent measurements of collector work function by back emission and retarding potential now agreed well with each other and gave a lower minimum value of 1.35 eV at T_C/T_R = 1.6 (Figure 19).

Performance data for cesium families were then taken at emitter temperatures of 1400, 1500, 1600 and 1700 K, with optimized collector temperatures and electrode spacings of 0.25, 0.5, and 1 mm. Over this range of emitter temperatures, the converter had a barrier index of 2.05 to 2.15 eV. However, this performance gradually deteriorated and, after several days of operation, the minimum collector work function had risen to 1.6 eV. At this point testing was terminated.

b. Platinum Emitter, Titanium Oxide Collector (Converter No. 163)

This standard converter was essentially a repeat of Converter No. 158, but with a platinum emitter in place of the usual tungsten. Data from Converter No. 158 had indicated that titanium oxide has a minimum work function at T_C/T_R values of 1.6 to 1.7. At favorable collector temperatures of 700 to 800 K, 10^{-2} to 10^{-1} torr of cesium would be required for the correct coverage of the collector to obtain the minimum work function. Unfortunately, this pressure of cesium is too low to obtain adequate emission from a tungsten emitter. However, the lower cesiated work function of platinum will allow a suitable match of the material as an emitter with the titanium oxide collector.

The performance history summarized in Table IV shows an initial performance (V_B = 2.1 eV) typical of refractory metal converters. After a bake at low collector temperatures, followed by excursions to higher collector temperatures, the performance improved to a V_B = 1.96 eV (Figure 20) in a manner similar to that observed with tungsten oxide collector devices. However, there was no observable oxygen effect on the platinum emitter from the titanium oxide collector, and the minimum collector work function measured by retarding potential in a cesium pressure of 0.25 torr was 1.5 eV, compared to 1.4 eV for the tungsten emitter diode (Figure 21). Such variations are attributed to minor changes in collector construction. After about 50 hours, the performance decayed by 0.1 eV, with a corresponding increase in the minimum collector work function to 1.6 eV.

TABLE IV

TEST SUMMARY OF CONVERTER NO. 163

Performance					Collector Work Function		Remarks
T_E (K)	T_C (K)	T_R (K)	d (mm)	V_B (eV)	Min ϕ_C (eV)	T_C/T_R	
1300	800	528	0.5	2.1	1.68	1.4	Initial
1300	650	528	0.5	2.1			24-hour bake
1300	900	520	0.5				"Activation" 5 min.
1300	800	507	0.5	2.05			Test Curve
1300	750	507	0.5				24-hour bake
1300	900	507	0.5				"Activation" 5 min.
1300	800	507	0.5	1.96	1.5	1.6	Test curves
1400	800	507	1	1.96			
1400	800	507	1	1.96			48-hour operation
1400	800	507	1	2.05	1.6	1.6	Performance decay

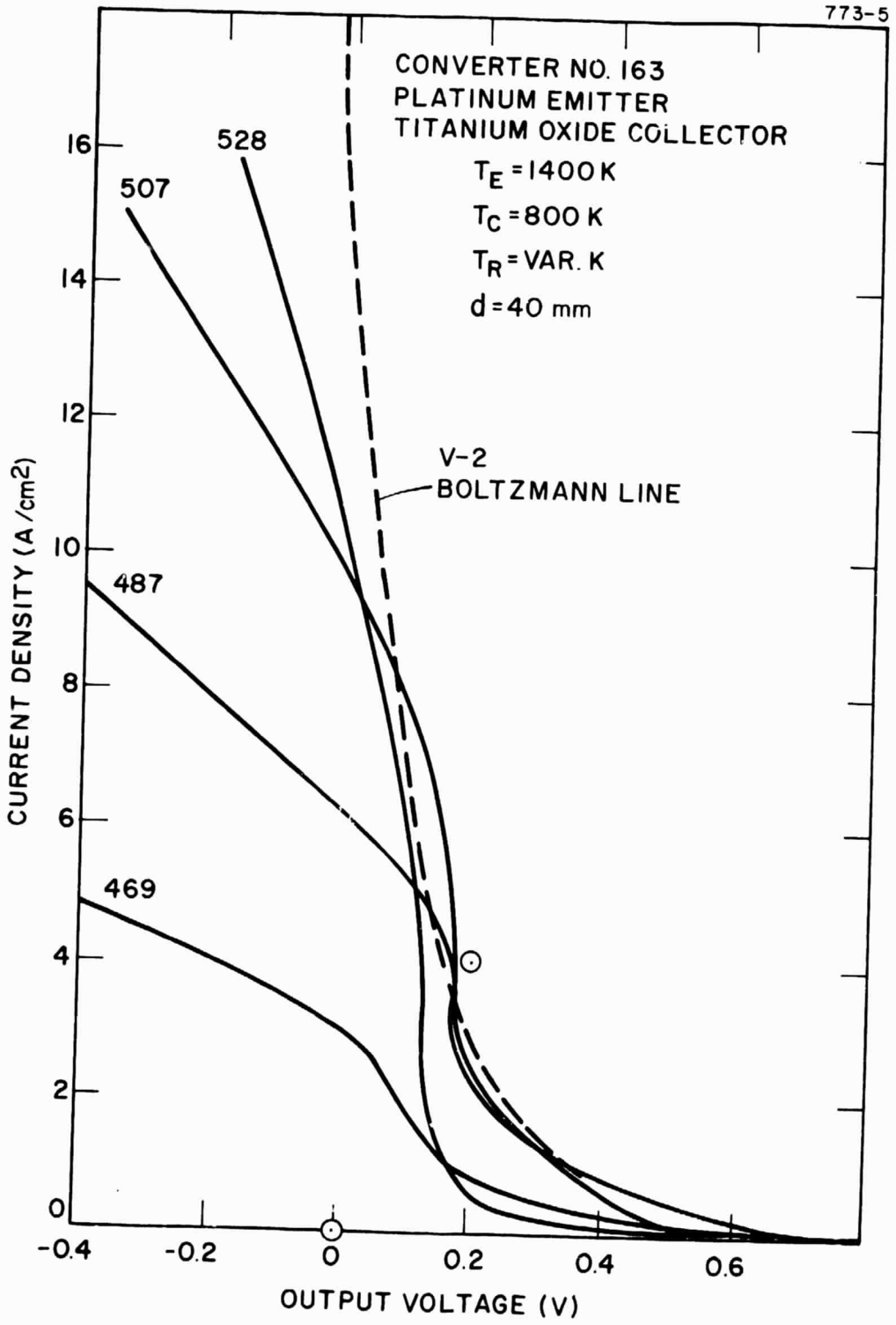

Figure 20. Cesium Family of Titanium Oxide.

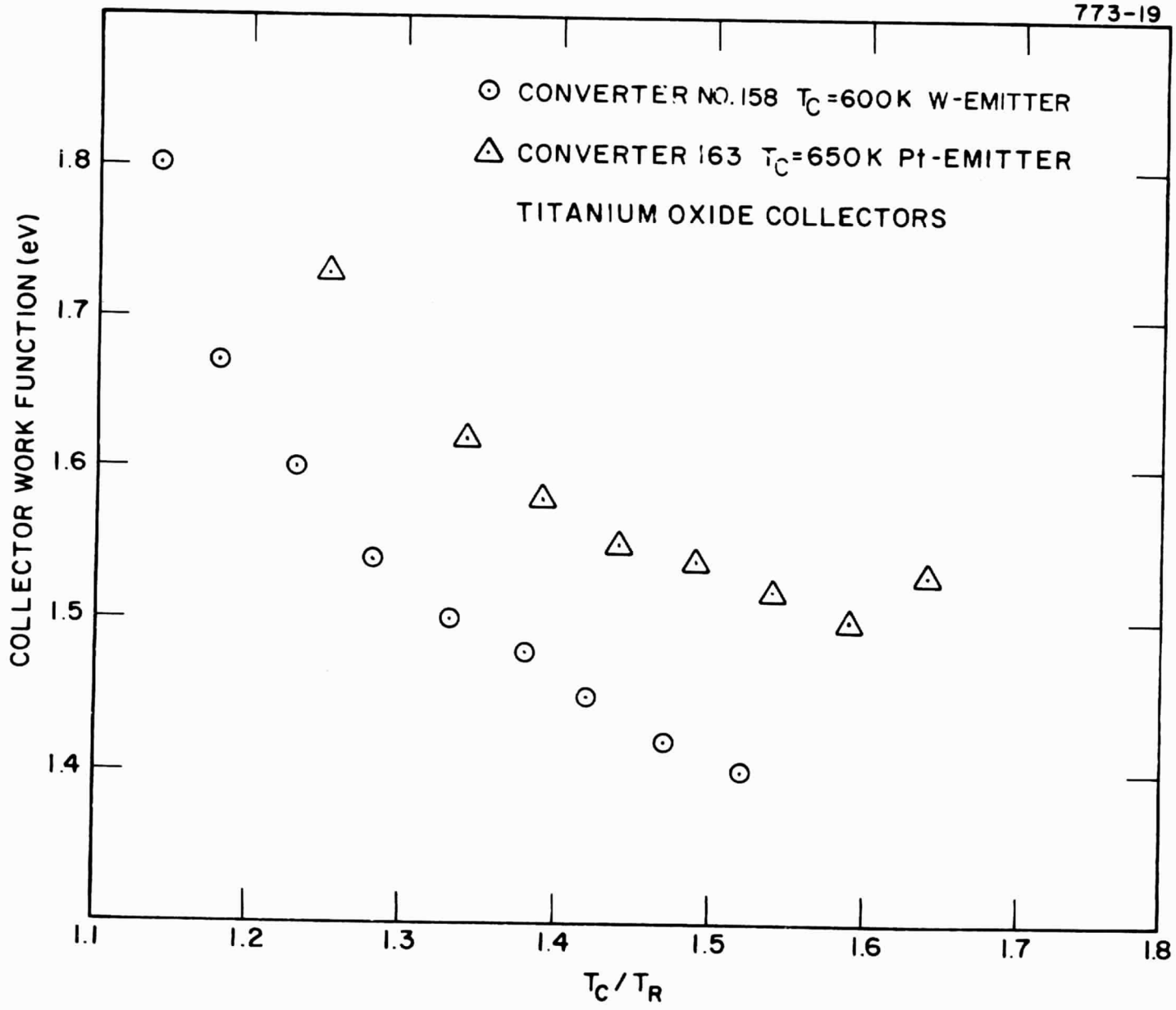

Figure 21. Data From Retarding Plots Made During Best Performance.

IV. TRIODE CONVERTER EXPERIMENTS

A. INTRODUCTION

The experimental program initiated last year and aimed at lowering interelectrode voltage losses was continued. These losses, associated with inefficient production of ions for space charge neutralization, must be reduced for converters operating in extraterrestial systems in which a minimization of system size and weight requires high-temperature, high-work-function collectors. A reduced voltage drop is possible by either of the following: incorporation of an auxiliary electrode to produce an efficient ion generating discharge (triode), or reduction of emitter-to-collector spacings to less than 0.005 cm (close-spaced diode). This section describes Thermo Electron Corporation's current research program in analyzing triodes; close-spaced diodes are treated in the next section.

In the previous annual report (ref. 16) a triode configuration was described in which an auxiliary four-wire grid electrode was interposed between the emitter and collector. Pulsed discharges in cesium-argon and cesium-xenon mixtures provided ions for space charge neutralization. Although current-voltage measurements indicated substantial thermionic output enhancement at cesium pressures up to 2×10^{-2} torr (Figure 22), power-producing currents were limited, for the Philips Type M dispenser emitter, to approximately 1 A/cm^2 at a reasonably high temperature (1550 K). Furthermore, the physical dimensions of the grid precluded emitter-to-collector separations less than approximately 0.2 cm. Recent calculations, however, indicate that coulombic resistance effects between the electrons and ions at practical current densities (~10 A/cm^2) may require smaller converter spacings of less than 0.05 cm (refs. 20 and 21). In order to reduce the interelectrode gap, a ring triode configuration was designed and tested. In this converter, the auxiliary electrode is a thin tantalum ring surrounding the main electrodes and positioned in a plane between them.

B. RING TRIODE EXPERIMENTS

A cutaway representation of the ring triode is shown in Figure 23. The emitter, similar to that in the grid triode, is a Philips Type M dispenser cathode with an area of 0.75 cm^2. The nickel collector is of equal area. The tantalum ring has an inside diameter of 1.4 cm,

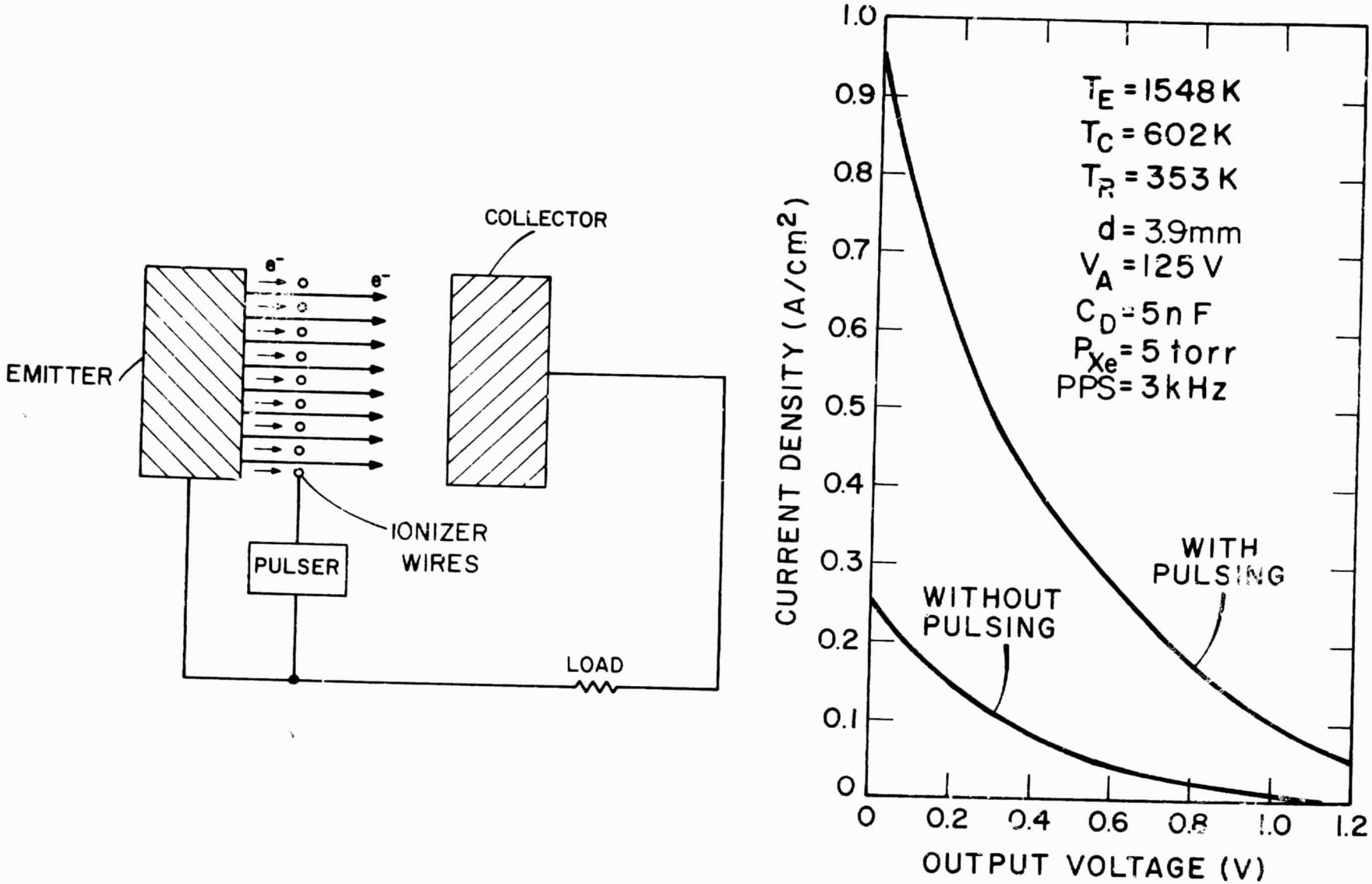

Figure 22. Pulsed Triode Converter.

774-7

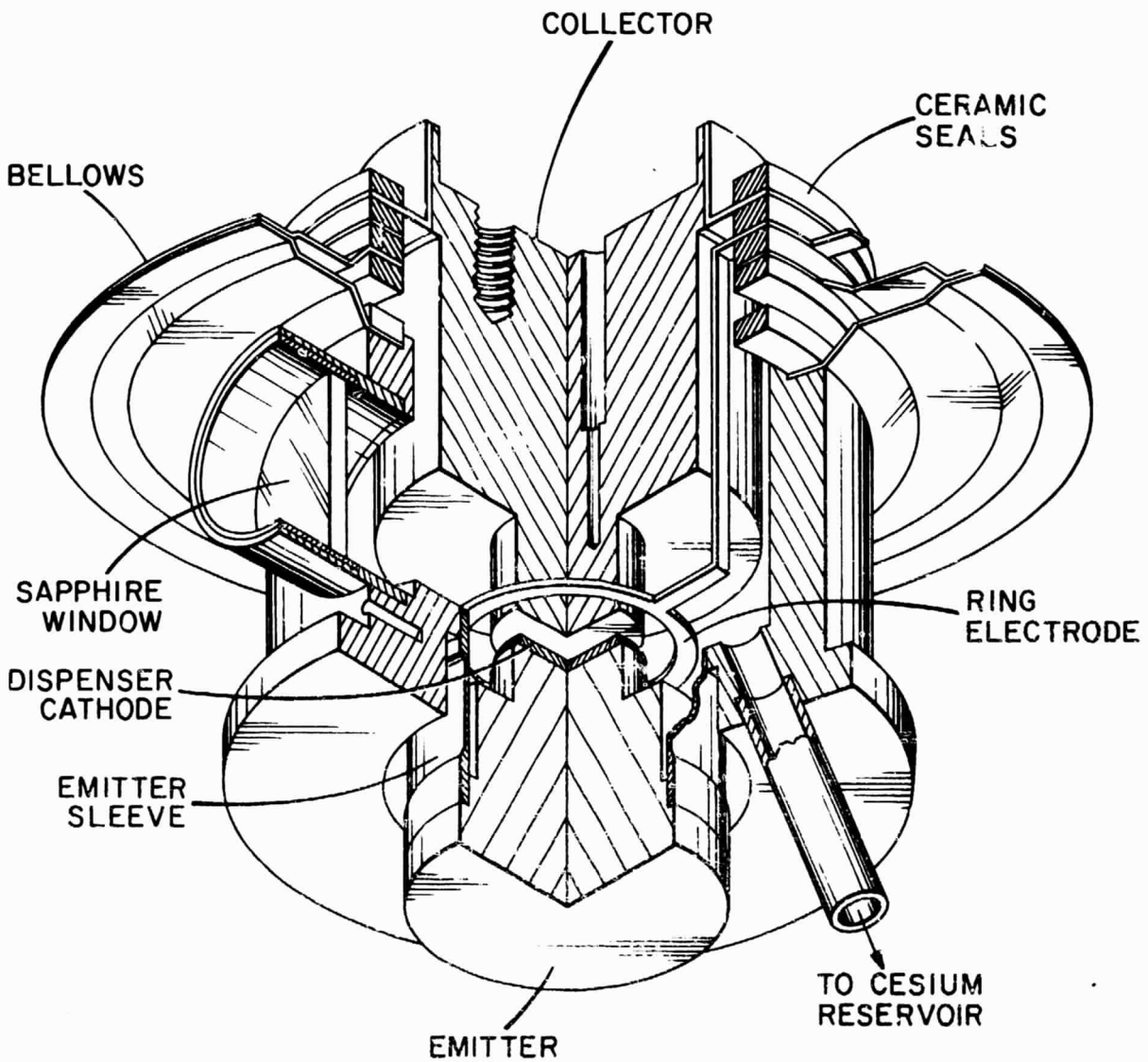

Figure 23. Cutaway View of Ring Triode Thermionic Converter.

width of 0.05 cm and thickness of 0.025 cm, and is structurally connected to the collector assembly. Bellows between the emitter and collector subassemblies permit continuous variation of the interelectrode spacing from 0.25 to 2.5 mm. Visual and spectral diagnoses of the discharge are possible through a sapphire window mounted in the side of the converter. A diagram of the converter and diagnostic apparatus is shown in Figure 24. The arrows (dashed shafts) to the ring electrode indicate the paths of the pulsed fast electrons, whereas the arrows (continuous shafts) from the emitter to the collector show the paths of the slower thermionic electrons. The pulsing circuit is shown in Figure 25, where V_A is the voltage from a regulated dc power supply, C is the pulsing capacitor, R_C the charging resistor, and R_L the variable load. The pulse generator (General Radio Company type 1217-B) triggers the transistor switch. A photograph is shown in Figure 26 of the operating converter pulsed in 2-torr xenon at 20 kHz with a C_D of 20 nF and a V_A of 100 V. Voltage and current probes determine the time-dependent auxiliary power delivered into the pulsed discharge. The spectral measurements were performed with a Jarrell Ash 0.25-m monochromator.

The ring triode was operated in a pulsed mode in xenon and cesium-xenon mixtures, similar to the procedure followed in testing the grid triode. As seen from the cross-sectional data of Figure 27, the rare gases combine high ionization cross sections, for energetic electrons with low elastic scattering near the Ramsauer minimum, for the thermionic electrons. Pulsed operation enables optimum ionization to occur by allowing maximum discharge voltages substantially above dc breakdown levels. Furthermore, in the pulsed mode a spatially uniform glow was observed around the ring, with significant penetration of the discharge into the interelectrode region. In comparison, dc discharges usually concentrated to a point on the ring.

The design of the experimental apparatus allowed a large number of parameters to be varied independently in order to investigate the effect of each on converter operation. For a constant emitter temperature of 1420 K and a pulse width of approximately one microsecond, the following parameters were sequentially varied: collector temperature (T_C), cesium reservoir temperature (T_R), power supply voltage (V_A), pulsing capacitance (C_D), and pulsing repetition rate (PPS). Because it is possible that sweeping enhances ion production, dc I-V curves were favored in the parametric studies.

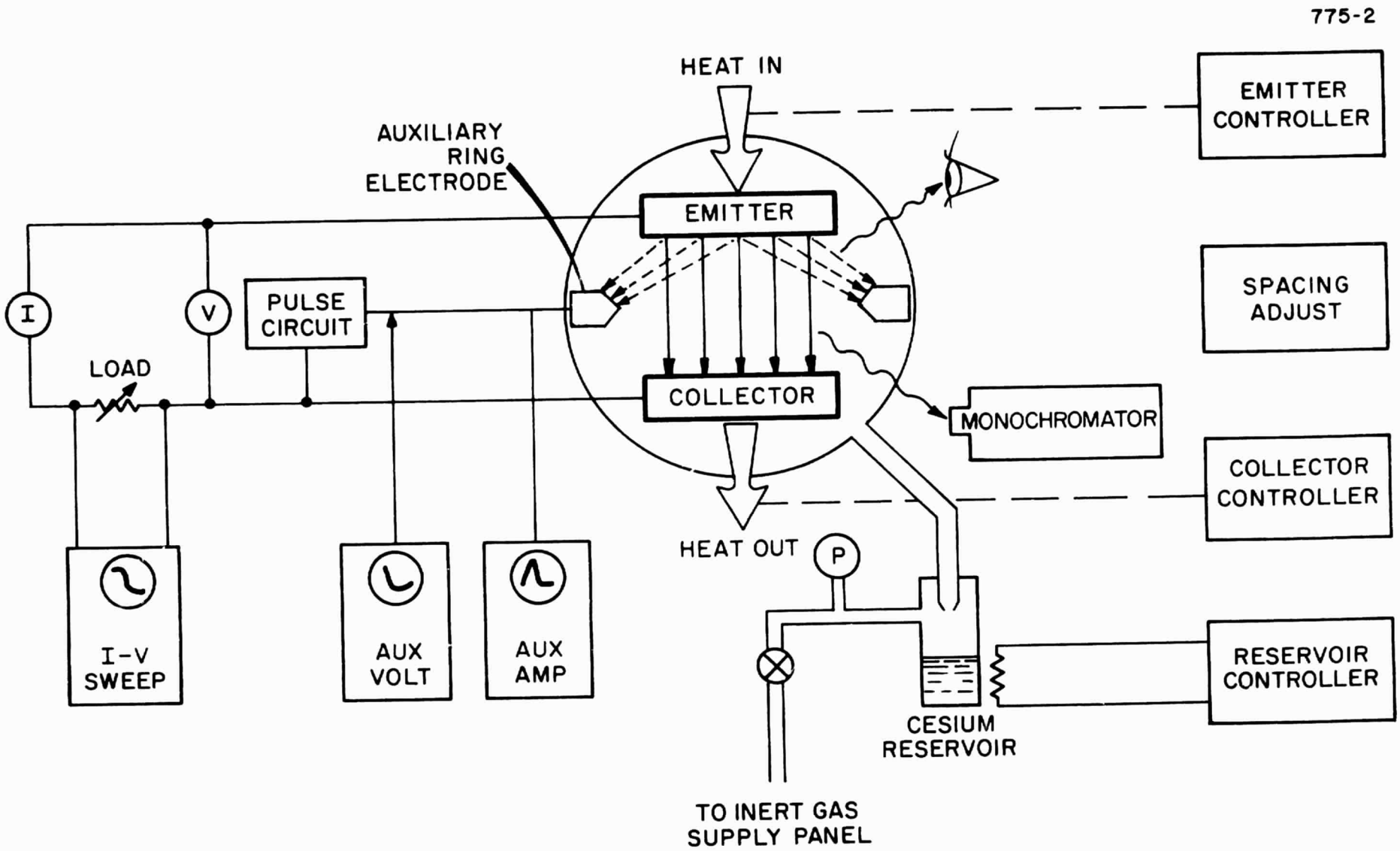

Figure 24. Diagram of Pulsed Triode Experimental Arrangement.

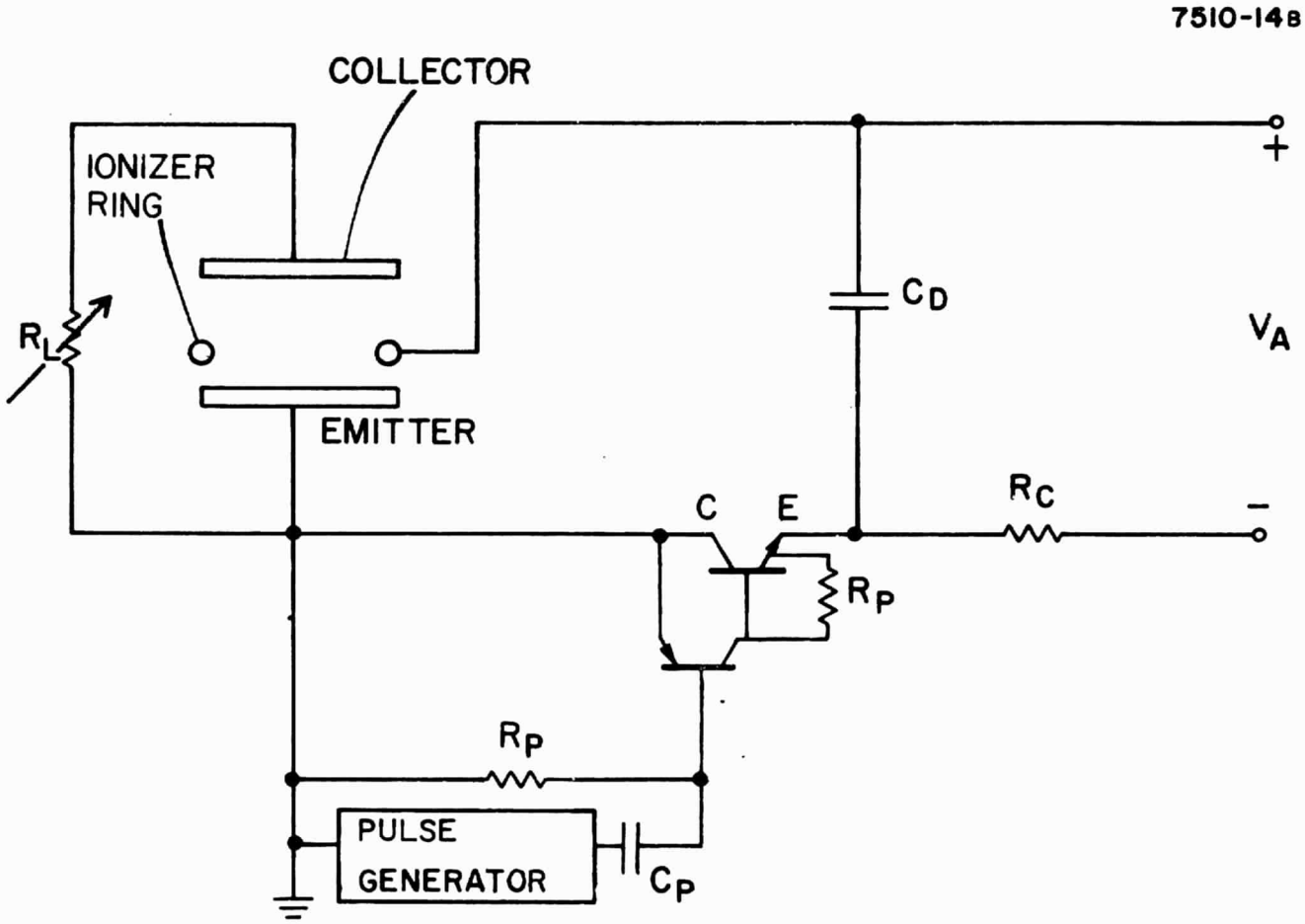

Figure 25. Pulsing Circuit for the Ring Triode Converter.

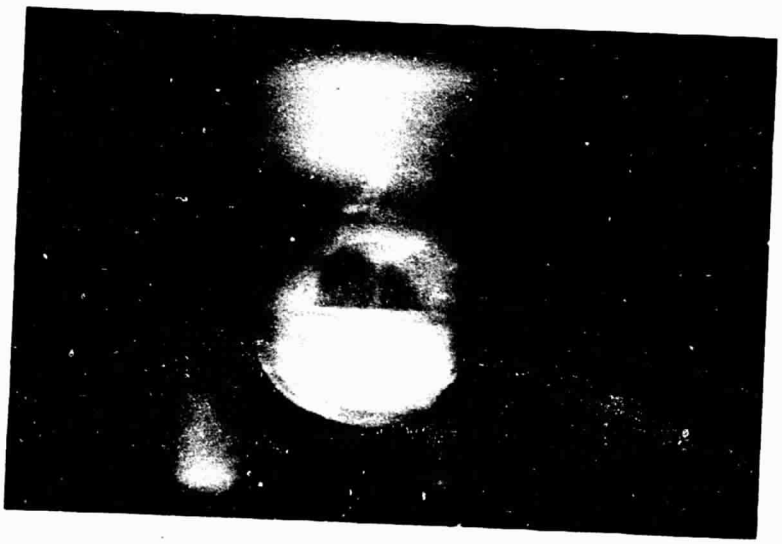

Figure 26. Pulsed Triode Converter.

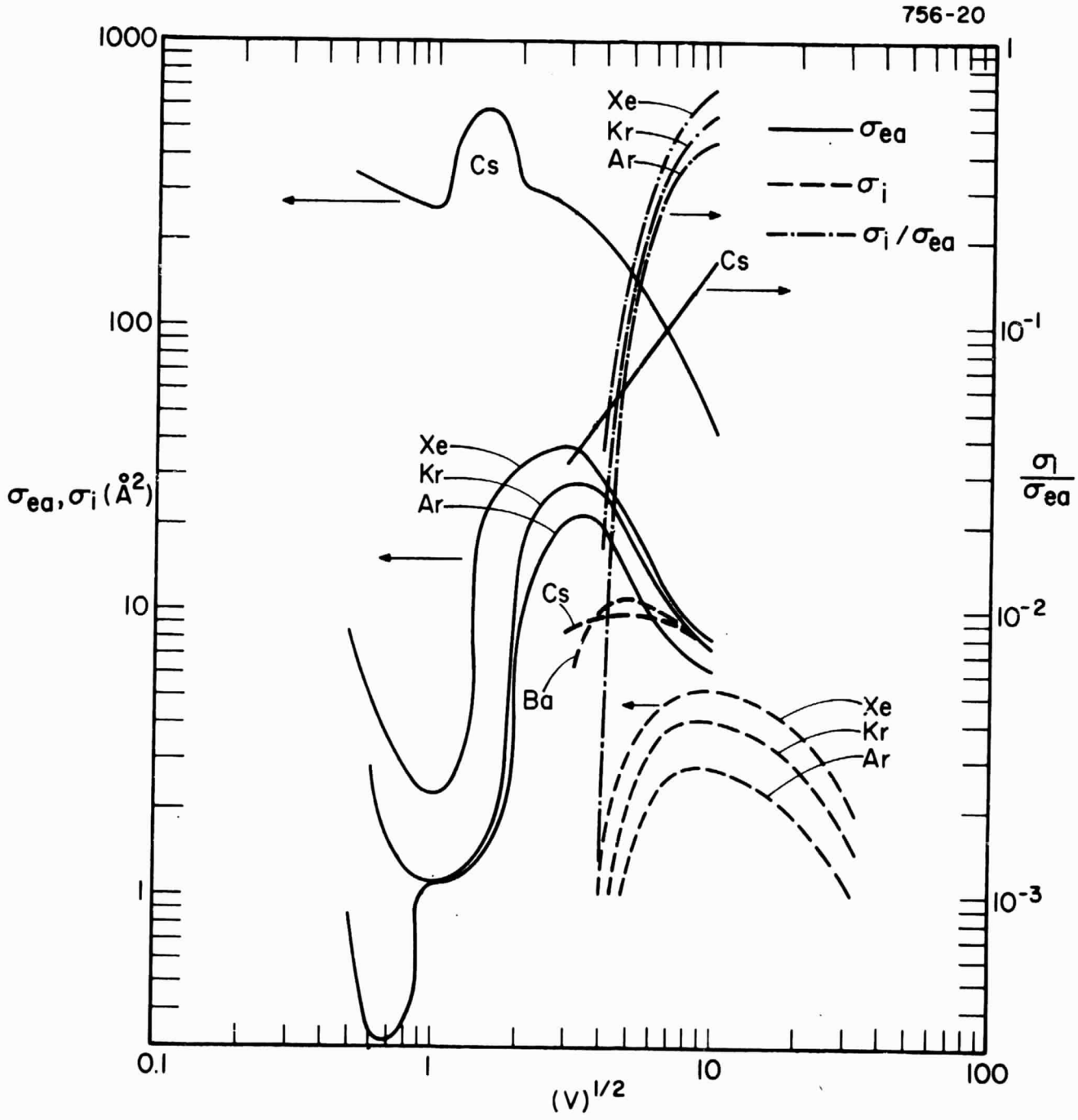

Figure 27. Electron Collisional and Ionization Cross-Sections for Cs, Ba, A, Xe and Kr.

In the initial series of experiments, only xenon filled the interelectrode region. The results for various electrode spacings are shown in Figure 28. The observed increase in power output with larger spacing is assumed to be due to improved electron penetration. The Boltzmann line, which represents the theoretical upper limit of operation, is shown displaced by two volts. The humps in the curves may be due to the interplay between ions created by the pulse, and to partial self-ignition by the thermionic electrons.

Because cesium is essential in reducing the work functions to the required levels of presently used converter electrode materials, various amounts of these atoms were mixed with the xenon. Penetration of both elements into the interelectrode region was confirmed spectroscopically by monitoring various atomic lines. A baseline set of parameters that produced substantial current was chosen. Each parameter was then varied from its baseline value while all other parameters were kept constant. These baseline values were: $T_C = 447$ K; $T_R = 422$ K ($p_{cs} = 8.1 \times 10^{-3}$ torr); d = 1 mm; $P_{Xe} = 12.5$ torr; $V_A = +100$ V; $C_D = 20$ nF; and PPS = 20 kHz.

The full results of these parametric variations were presented at the 1977 IEEE Plasma Science Conference, May 1977, Troy, New York. In contrast to the grid triode, enhanced output was observed in the ring triode. Relative to the baseline conditions, the effect of increasing cesium pressure is shown in Figures 29 and 30. Without pulsing, no output is observed in the power-producing region; with pulsing, the highest output is achieved at the lowest cesium pressure. However, even at the maximum reservoir temperature of 528 K (corresponding to a cesium pressure of 0.5 torr), the pulsed discharge is seen to have a significant effect.

Changes in thermionic emission with varying effects of electrode spacing are shown in Figures 31 and 32. Substantial enhancement is observed at the desired spacing of 0.5 mm. At spacings up to 1.5 mm, self-ignition is suppressed in the power-producing quadrant whereas, at 2- and 2.5-mm spacings, the pulsed discharge has essentially no effect.

In Figure 33, the output characteristics are given as a function of xenon pressure. Below 8 torr of xenon there is a rapid reduction in output at the 1-mm electrode spacing with decreasing gas pressure.

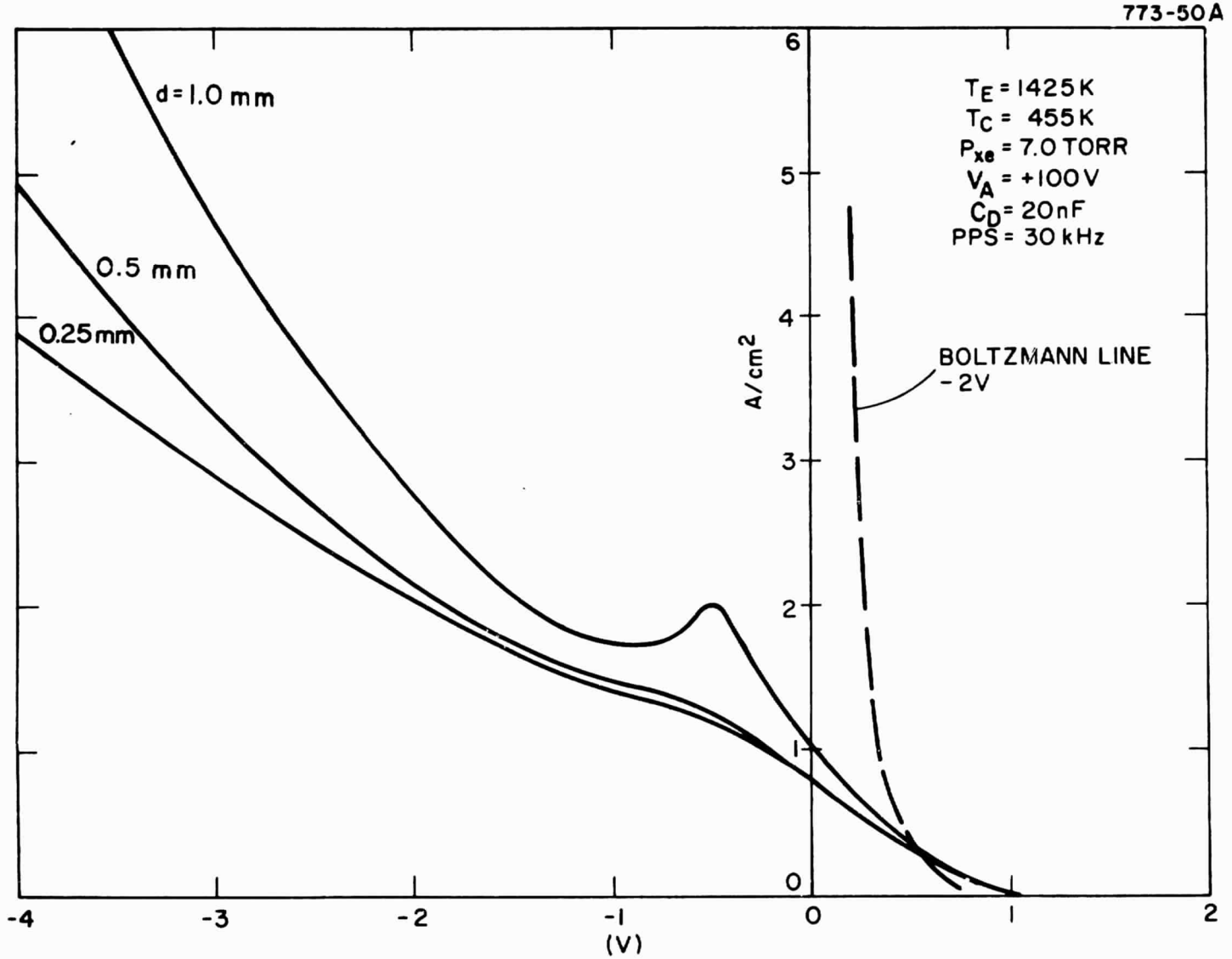

Figure 28. DC Output Characteristics in a Xenon Atmosphere as a Function of Emitter-Collector Spacing.

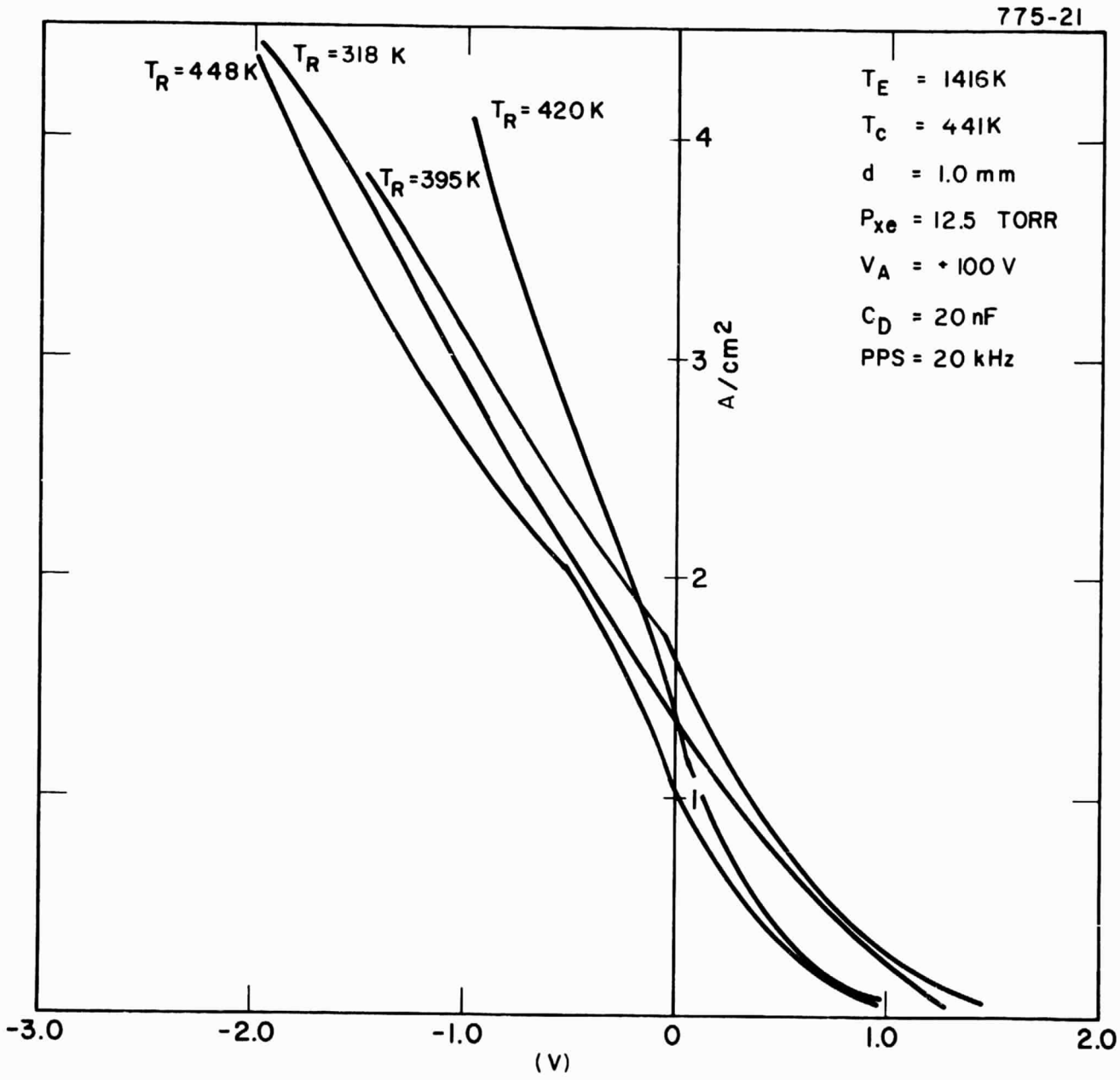

Figure 29. DC Output Characteristics in a Cesium-Xenon Atmosphere as a Function of Cesium Reservoir Temperature.

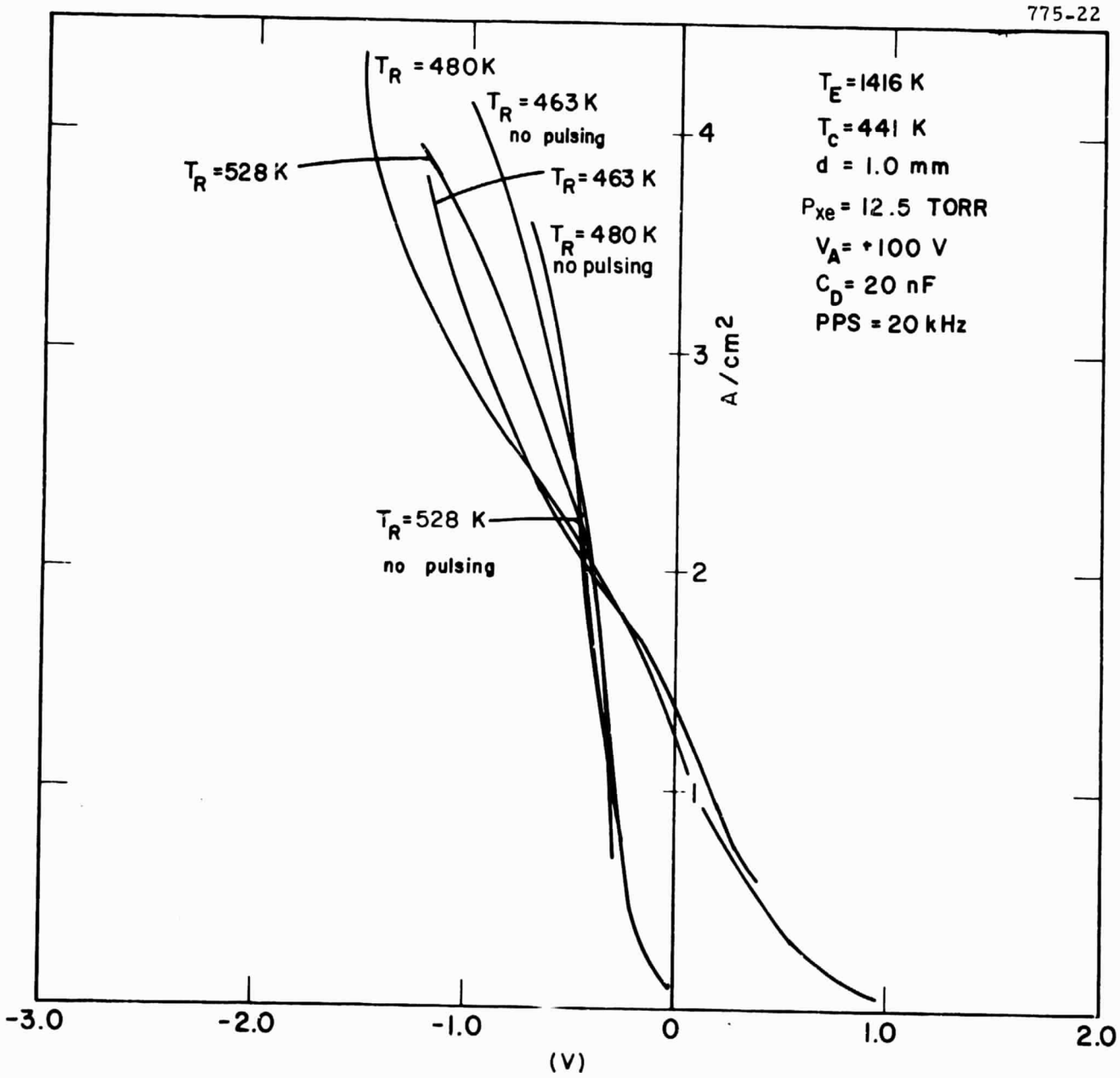

Figure 30. DC Output Characteristics in a Cesium-Xenon Atmosphere as a Function of Cesium Reservoir Temperature.

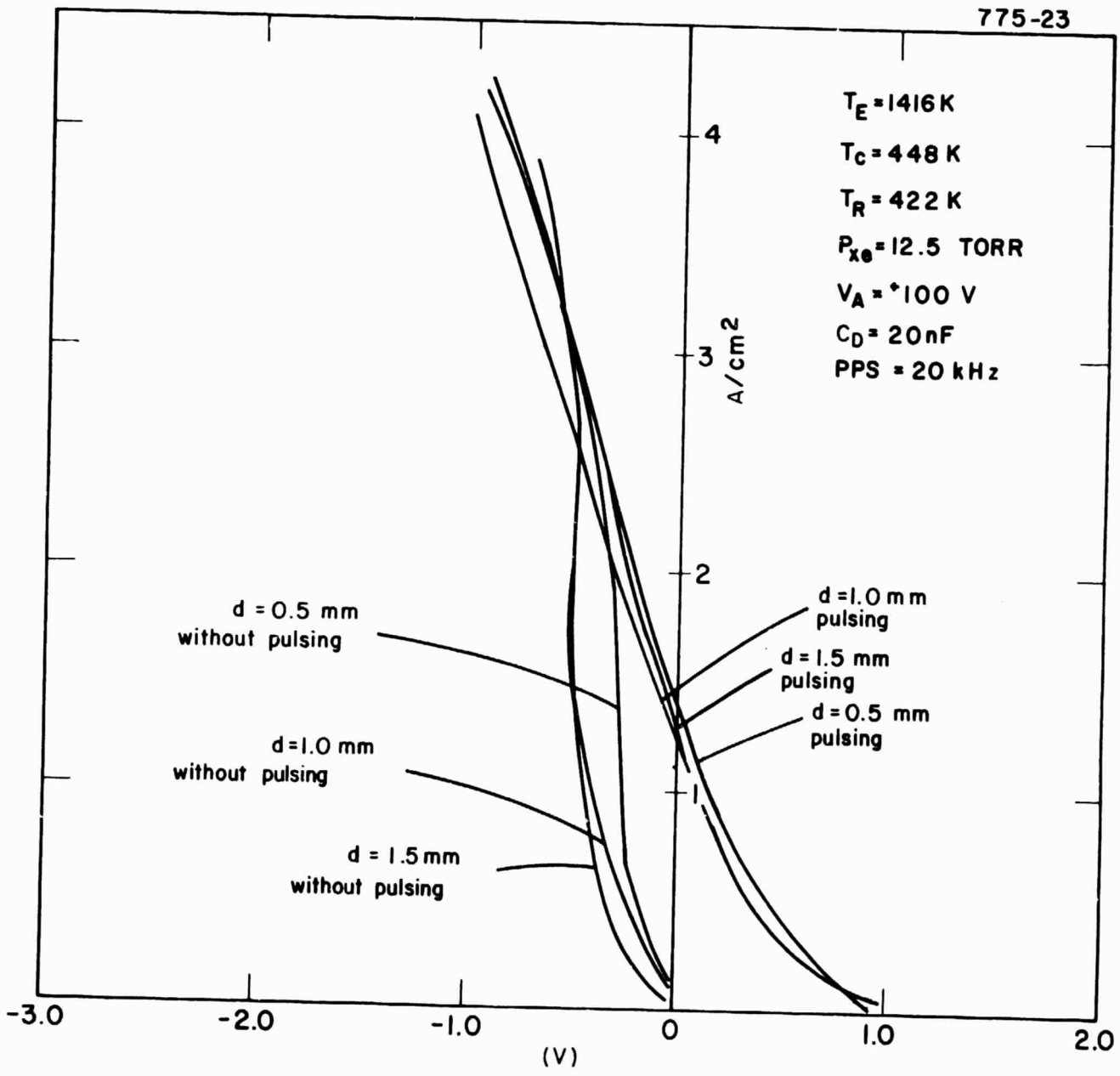

Figure 31. DC Output Characteristics in a Cesium-Xenon Atmosphere.

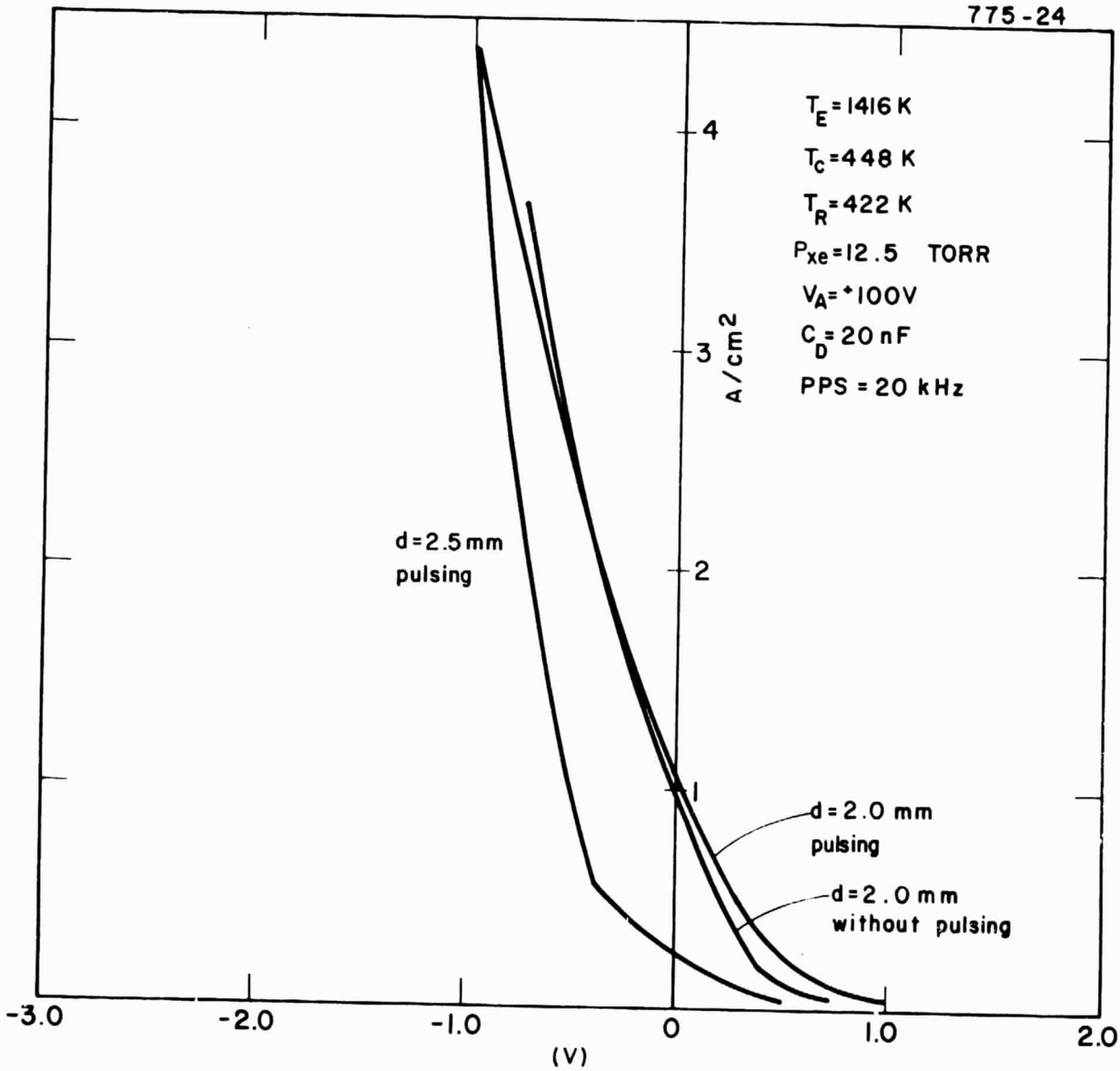

Figure 32. DC Output Characteristics in a Cesium-Xenon Atmosphere.

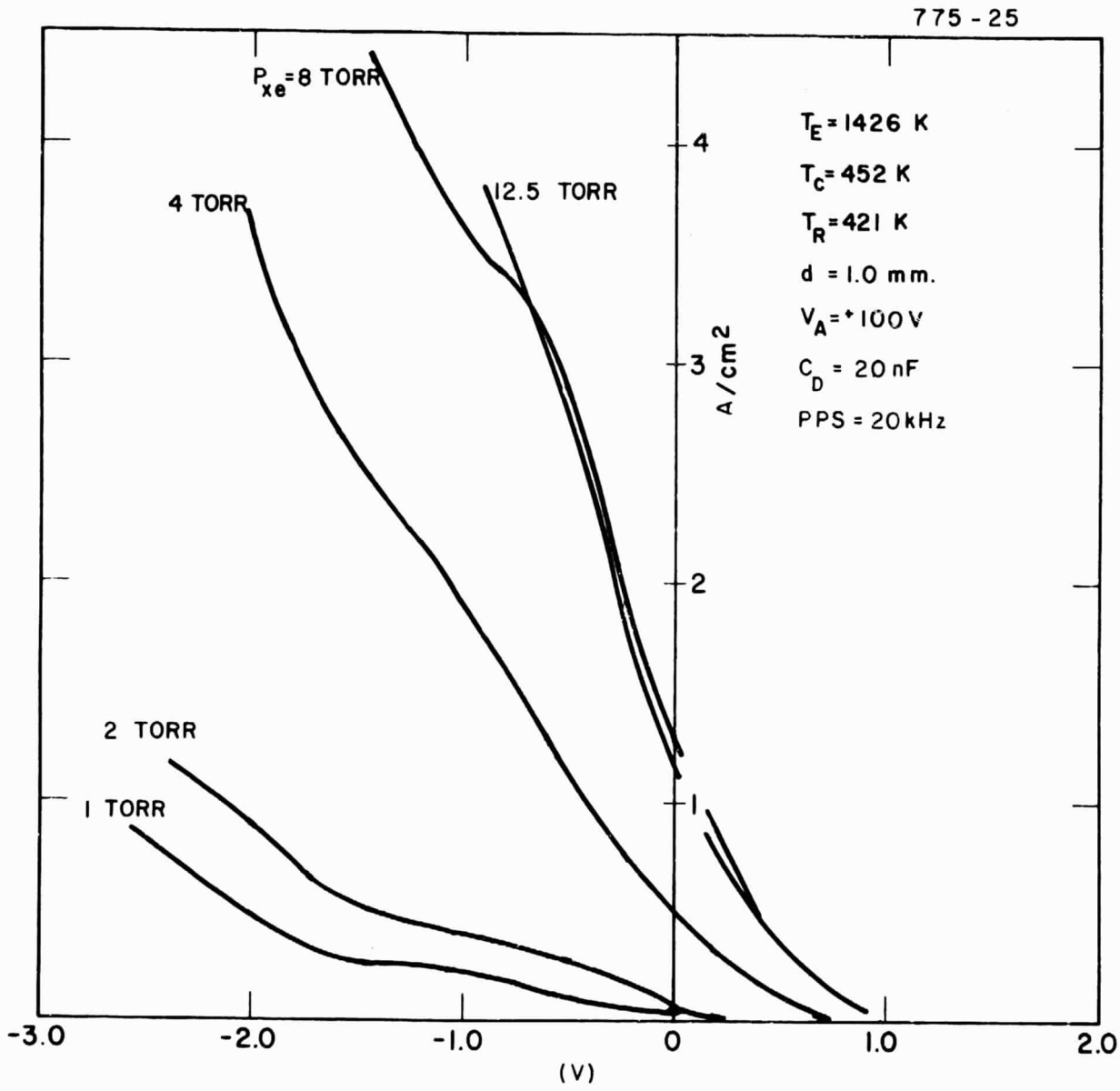

Figure 33. DC Output Characteristics in a Cesium-Xenon Atmosphere as a Function of Xenon Pressure.

Polaroid records of the temporal voltage and current profiles associated with each load characteristic allowed calculation of the power discharged into the plasma by the pulses. Comparison of these values with the current enhancement measured in the associated I-V curves at maximum thermionic power output enabled the equivalent voltage drop per thermionic electron to be determined. Equivalent loss varied between 0.6 and 1.2 V, which is higher than expected. Quite likely, the equivalent voltage drop values will decrease substantially when the pulsing parameters have been more fully optimized.

V. PARTICULATE-SPACED DIODE

A. INTRODUCTION

Development of a particulate-spaced diode (PSD) continued. The principal advantages of such a cesium-filled, close-spaced thermionic converter are zero arc drop, negligible electron scattering losses, and no auxiliary electrodes. Two potential major problems with PSD's are thermal distortion of the hot emitter and/or significant cesium coverage of the particulate spacers, both of which might be sufficient to electrically short the electrodes.

For output power levels of 5 W/cm^2 PSD's will require emitter-to-collector spacings 2.5 to 5 μm, with cesiated emitters at 1400 to 1600 K, and 1.4 eV work function collectors (Figures 34 and 35). The particulate spacers must be electrically and thermally insulating, and resistant to chemical decomposition or evaporation. Figure 36 shows three diode configurations used in analyzing and developing this type of converter. The upper two designs represent potential operating converters in which thermal deformation of the emitter is absorbed by a "floating" collector. In one case a thin foil collector is sufficiently flexible to comply with emitter distortion, whereas in the second case the collector is a rigid structure that can be displaced vertically for spatially uniform thermal expansion of the emitter. The lower configuration represents the diode designed for rapid analysis of thermally distorted electrode surfaces, particulate characteristics, and diode spacing problems under vacuum conditions.

B. PARTICULATE-SPACED EXPERIMENTS

The majority of experiments to determine electrode and particulate characteristics were performed in the bell jar apparatus shown in Figure 37. Diode capacitance is determined with an rf vector impedance meter. Accurate measurements are possible at diode resistances as low as 100 Ω more than sufficient for an operational converter. In previous experiments, the diode had been incorporated into a self-contained tank circuit whose resonant frequency was measured with a grid-dip meter. However, that meter limited capacitance measurements to diodes with resistances over 1 kΩ.

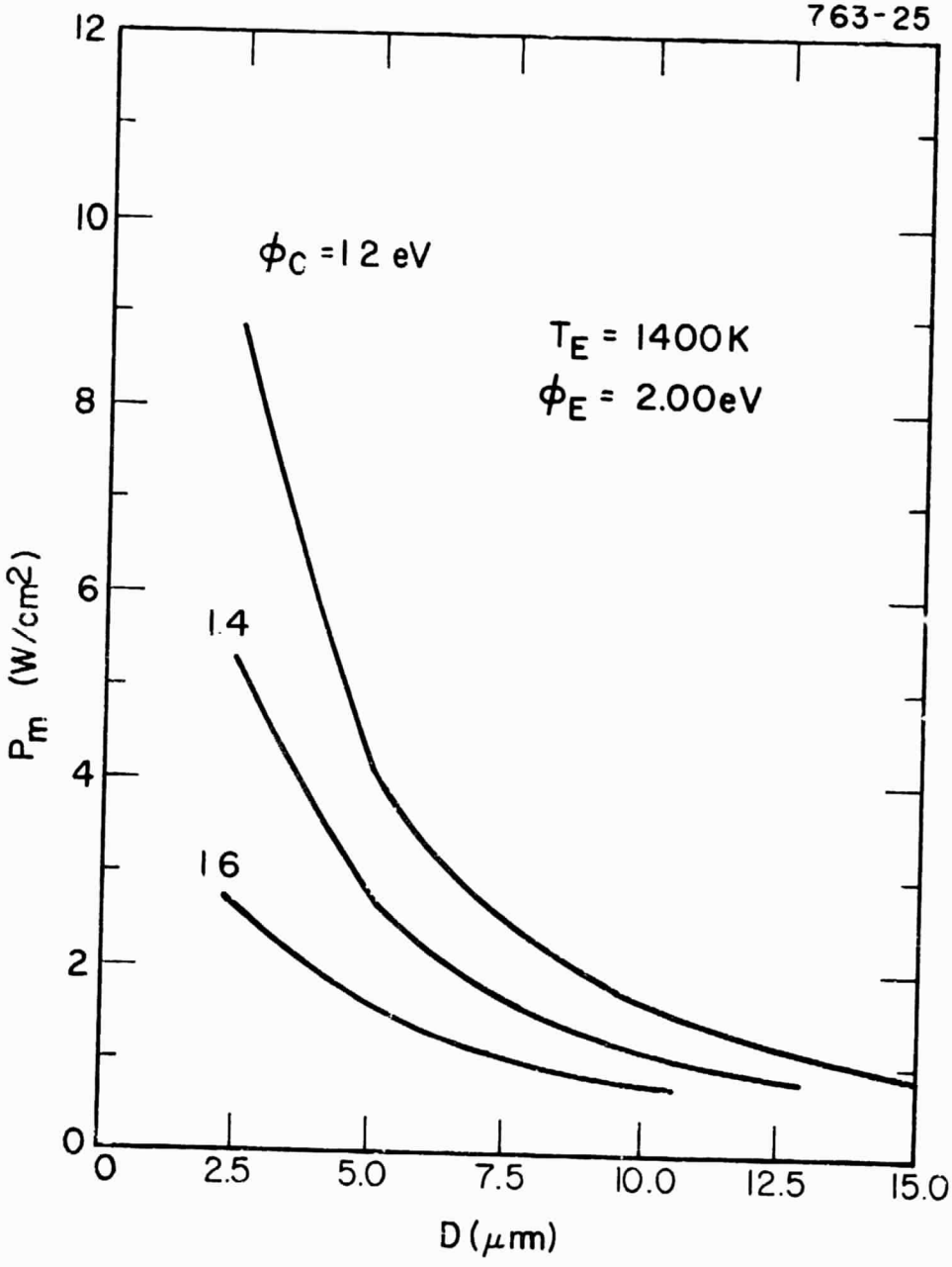

Figure 34. Close-Spaced Diode Power Density as a Function of Spacing for T_E = 1400 K and ϕ_E = 2.00 eV.

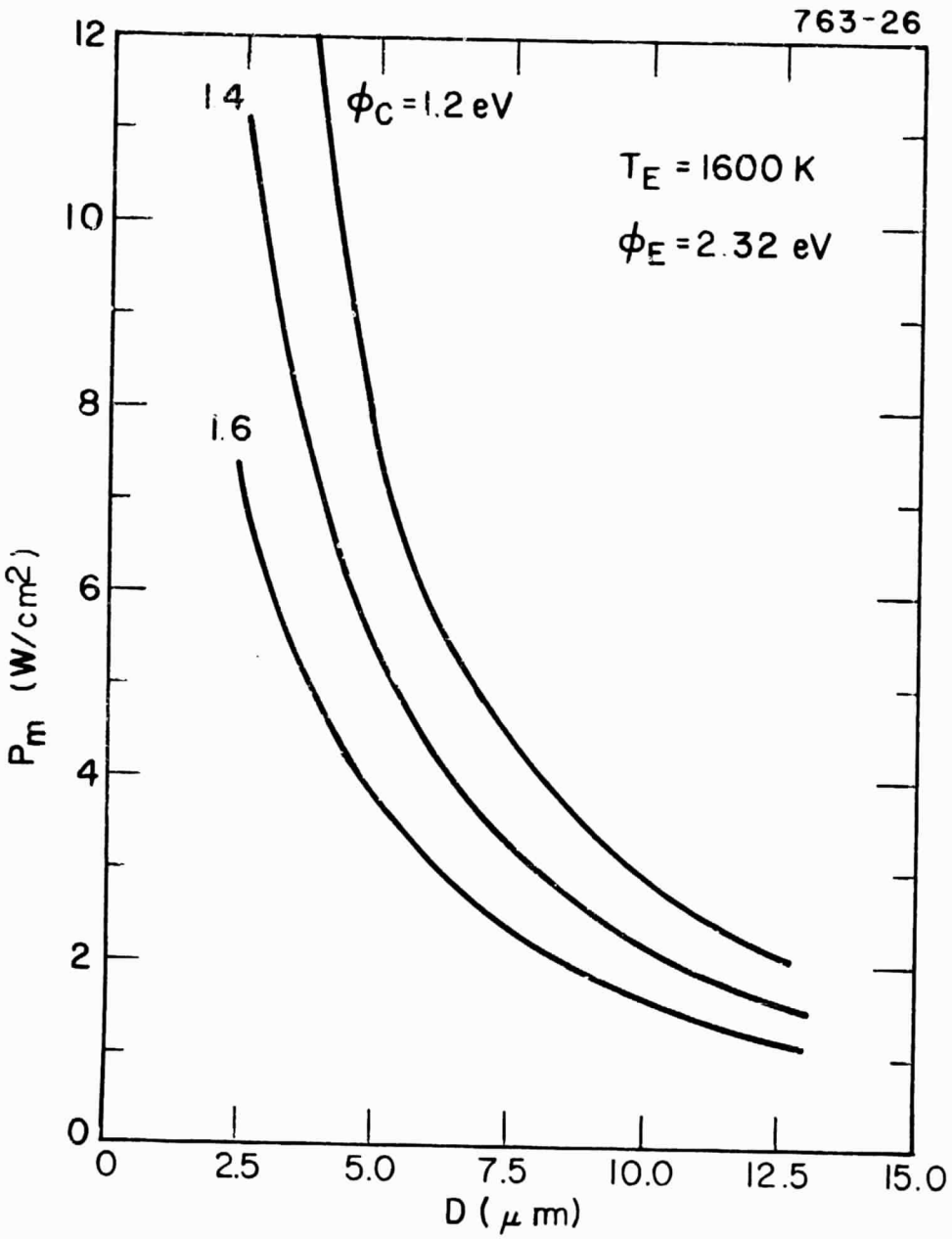

Figure 35. Close-Spaced Diode Power Density as a Function of Spacing for T_E = 1600 K and ϕ_E = 2.32 eV.

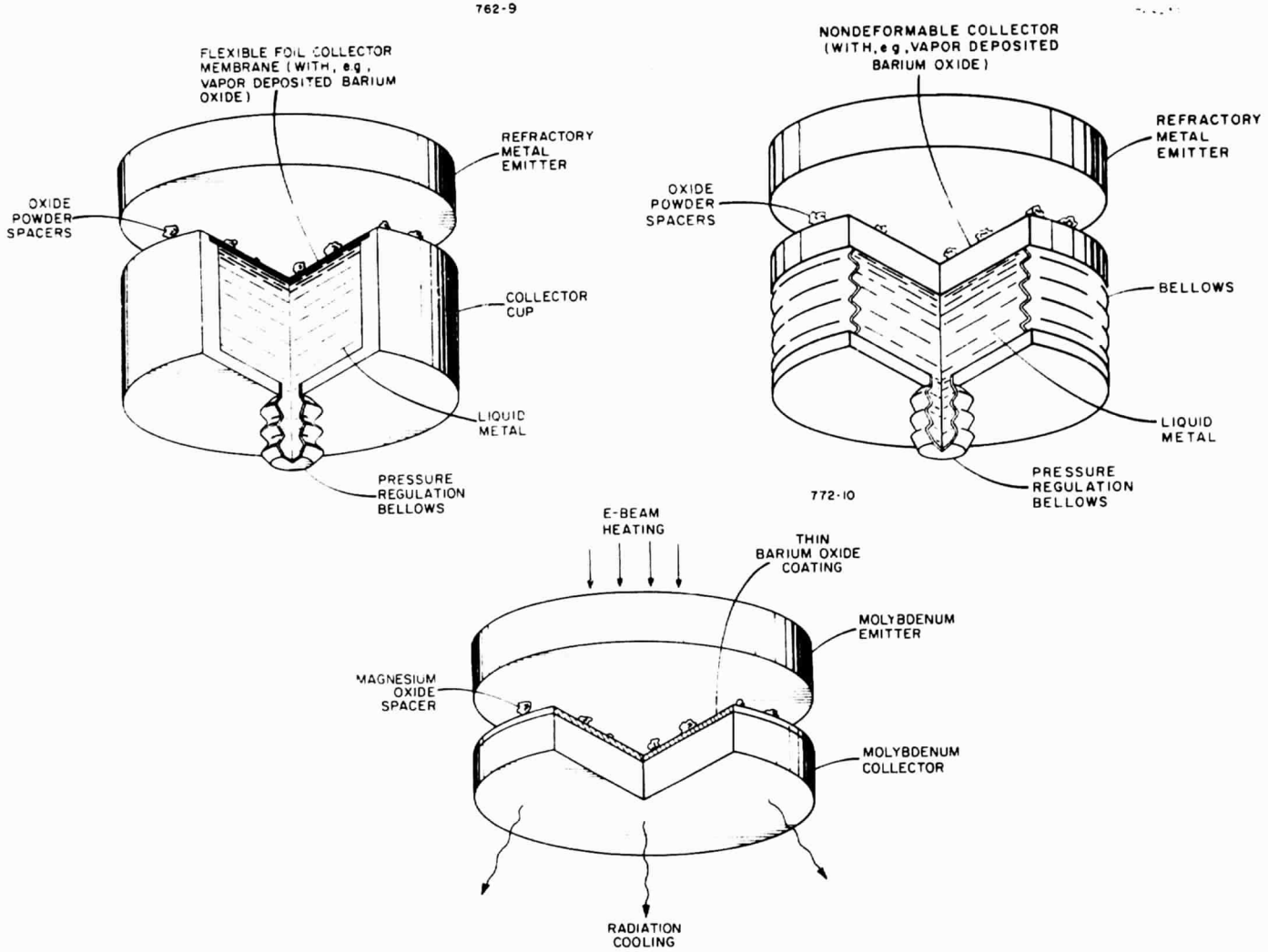

Figure 36. Particulate-Spaced Diode Configurations.

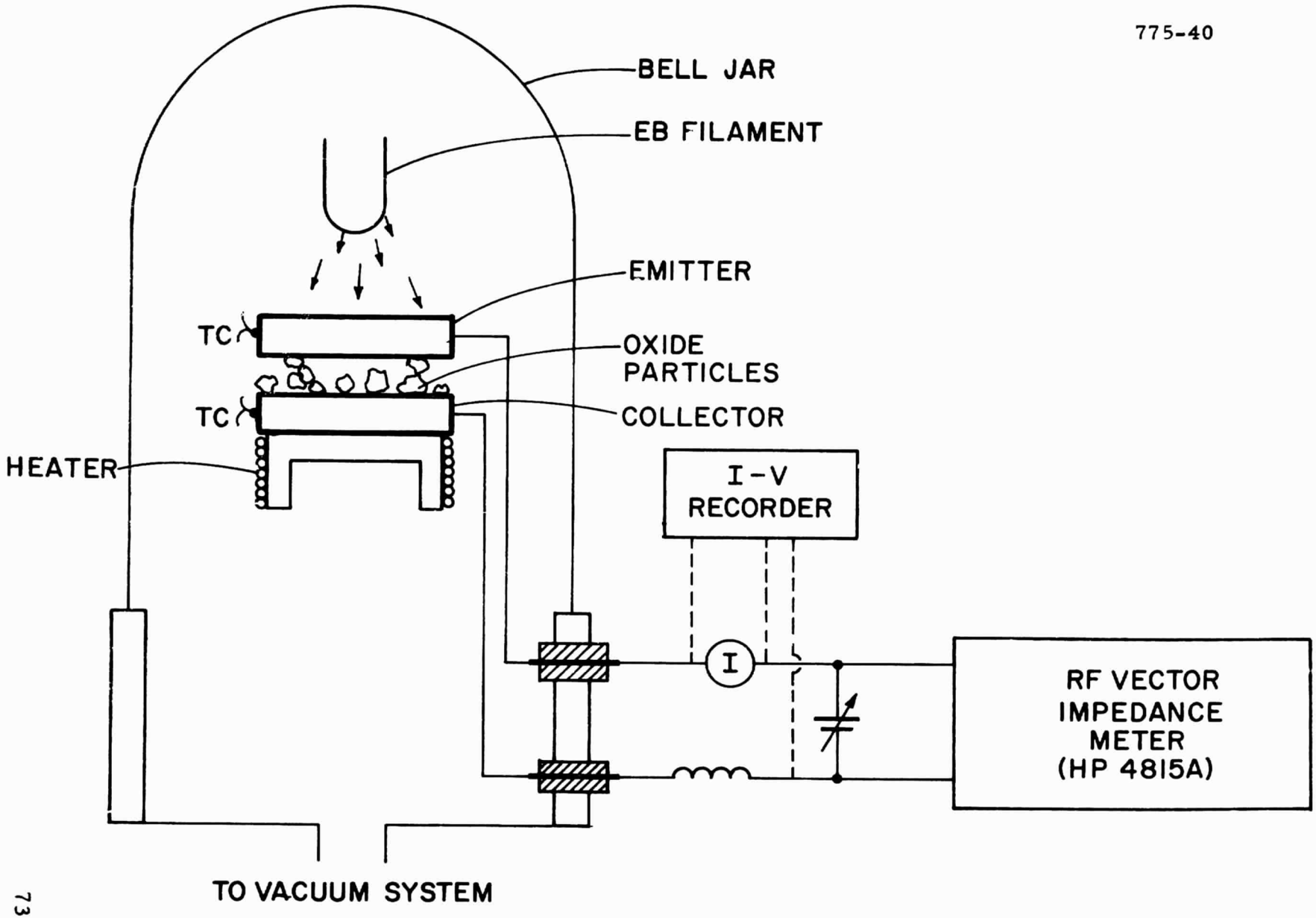

Figure 37. Experimental Bell-Jar Apparatus for Particulate-Spaced Diode Analyses.

Most tests were performed with 2.54-cm diameter, hand polished electrodes, usually made of molybdenum. A variety of sprayed semiconducting oxide coatings were examined for thermal stability and electrical resistivity. The results, tabulated in Table V, show that minimum electrode spacings of 12.5 μm were obtained at emitter temperatures slightly above 1400 K. Although thermally stable, aluminum oxide and zirconium oxide were observed in early tests to become electrically conductive at high temperature. However, in those experiments procedures for applying the coatings were relatively crude; future analyses may modify these results. Lightly coated combinations of barium, strontium and aluminum oxide (RCA mixture of barium oxide) on molybdenum were also noted to be unstable in those tests, whereas more recent experiments with heavier sprayed coatings resulted in much longer operation than had been expected from the earlier data. At high temperature, magnesium oxide was found to be the most stable compound, not only acting as a diode spacer, but also lowering the emitter work function. Inability to sufficiently heat the collector precluded measuring its work function. Excellent repeatability was noted in these tests. The addition of a second coating of RCA mixture of barium oxide on top of the magnesium oxide further reduced the emitter work function. Replacing the molybdenum emitter with nickel did not alter the results, whereas no thermionic emission was recorded for a tungsten emitter.

Figure 38 shows the temperature dependence of effective work function for an emitter coated with a RCA composition of barium oxide in combination with magnesium oxide particle spacers, and Figure 39 shows the I-V characteristics of this diode. In recent experiments with relatively heavy 25-μm thick coatings of an RCA mixture of barium oxide, reasonably large (over 1 A) currents were generated in the power-producing region of the I-V curve, at emitter temperatures of approximately 1450 K, and with "large" spacings of approximately 25 μm (Figure 40). Stable emission for over 100 hours was observed.

Highly magnified photographs of these oxide surfaces show a dense "spaghetti"-type covering (Figure 41) which has suggested that such coatings are, in fact, porous semiconductors. At high temperature, this interelectrode porous aggregate becomes filled with an electron gas (ref. 22) with a correspondingly large electrical

TABLE V

BELL JAR CLOSE-SPACED DIODE EXPERIMENTS

772-33

TEST	MATERIAL		SPACING (μm)	OXIDE COATINGS	$T_{E(Max)}$ (K)	$T_{C(Max)}$ (K)	ϕ_E (T_E Max) (eV)	COMMENTS
	EMITTER	COLLECTOR						
1	Mo	Mo	15	Al_2O_3	1000	—		LOW RESISTANCE AT HIGH TEMPERATURE
2	Mo	Mo	20	ZrO_2	1250	—		
3	Mo	Mo	25	BaO	1283	—		
4	Mo	Mo	25	MgO	1373	—	2.92	REPEAT TESTS
5	Mo	Mo	37.5	MgO	1372	747	2.92	
6	Mo	Mo	32.5	MgO(E) BaO(C)	1317	—	2.3	REPEAT TESTS
7	Mo	Mo	—	MgO(E) BaO(C)	1377	824	2.70	
8	Mo	Mo	27.5	MgO(E) BaO(C)	1302	801	2.67	
9	Mo	Mo	20	MgO(E) BaO(C)	1222	770	2.31	
10	Ni	W	—	BaO(E) MgO(C)	1158	965	2.05	REPEAT TESTS; $\phi_E = 1.5$ eV AT $T_E = 650$ K
11	Ni	W	17.5	BaO(E) MgO(C)	1141	1057	1.82	
12	W	Ni	—	MgO	1373	—	> 3	CURRENT LESS THAN 10 μA
13	Mo	Mo	12.5	MgO(E) BaO(C)	1313	1073	< 2.20	INCREASED EMISSION WITH COLLECTOR HEATING; ϕ_C SIMILAR TO Ni COLLECTOR; <1 VOLT REQUIRED TO PREVENT ARCING
14	Mo	Mo	12.5	BaO(C)	1423	1103	< 2.47	MgO NOT REQUIRED FOR SPRAYED BaO; SEM SHOWS POROUS BaO COATING
15	Mo	Ni	17.5	BaO(C)	1369	1130	< 2.64	"PURE" BaO COATING STABLE ON Ni

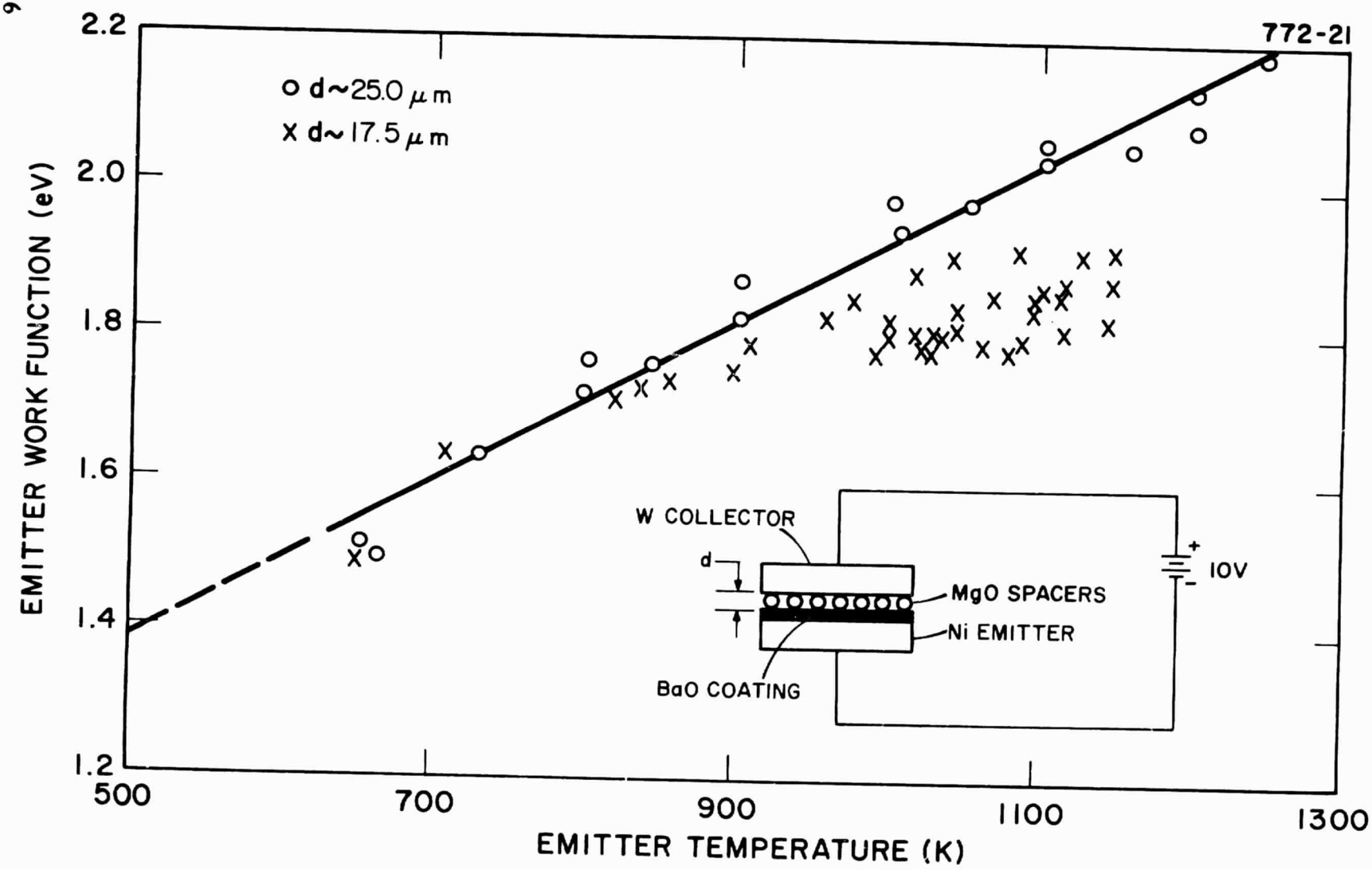

Figure 38. Variation of Emitter Work Function with Temperature for Particulate-Spaced Diode.

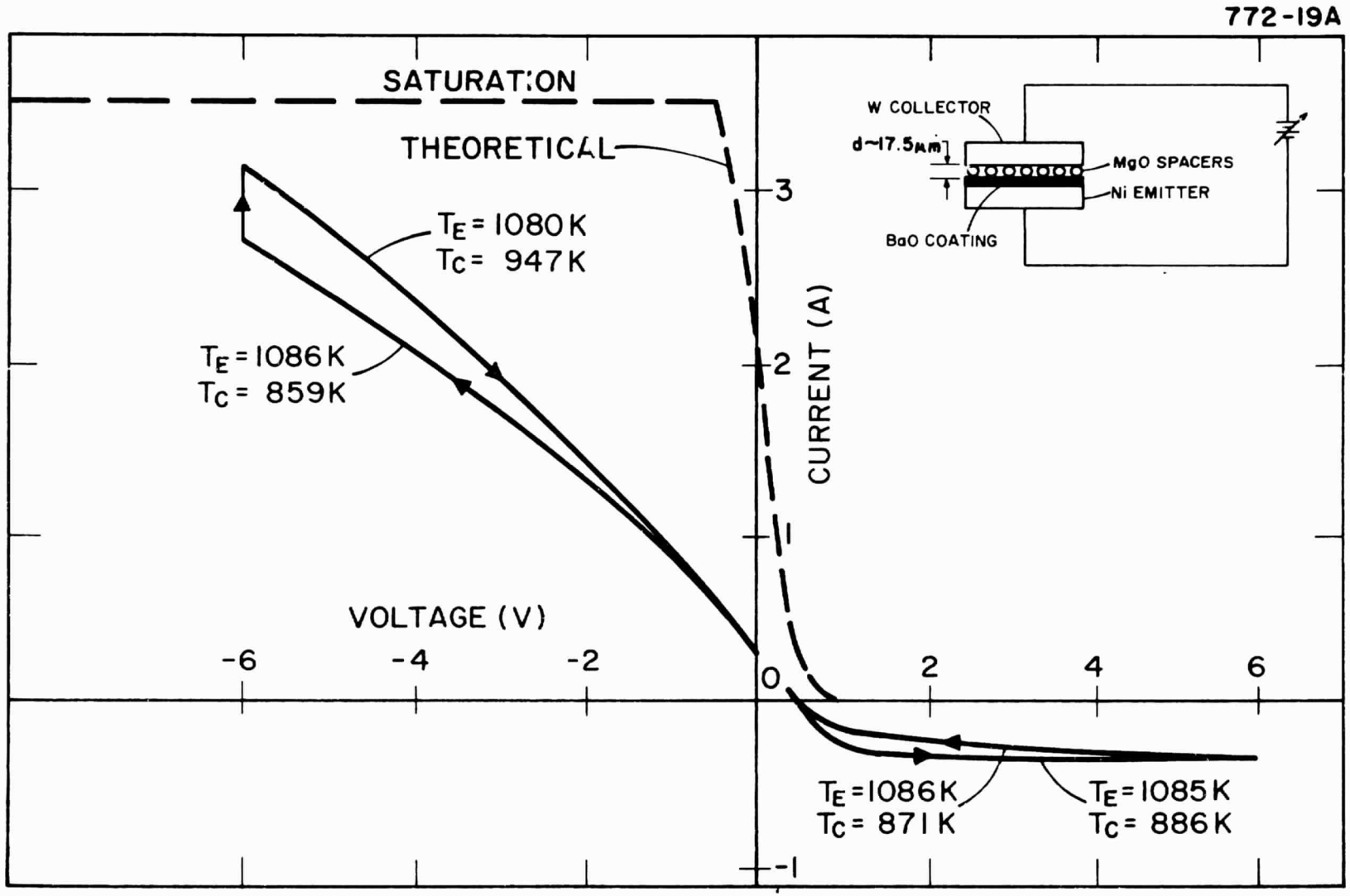

Figure 39. I-V Curve of Particulate-Spaced Diode.

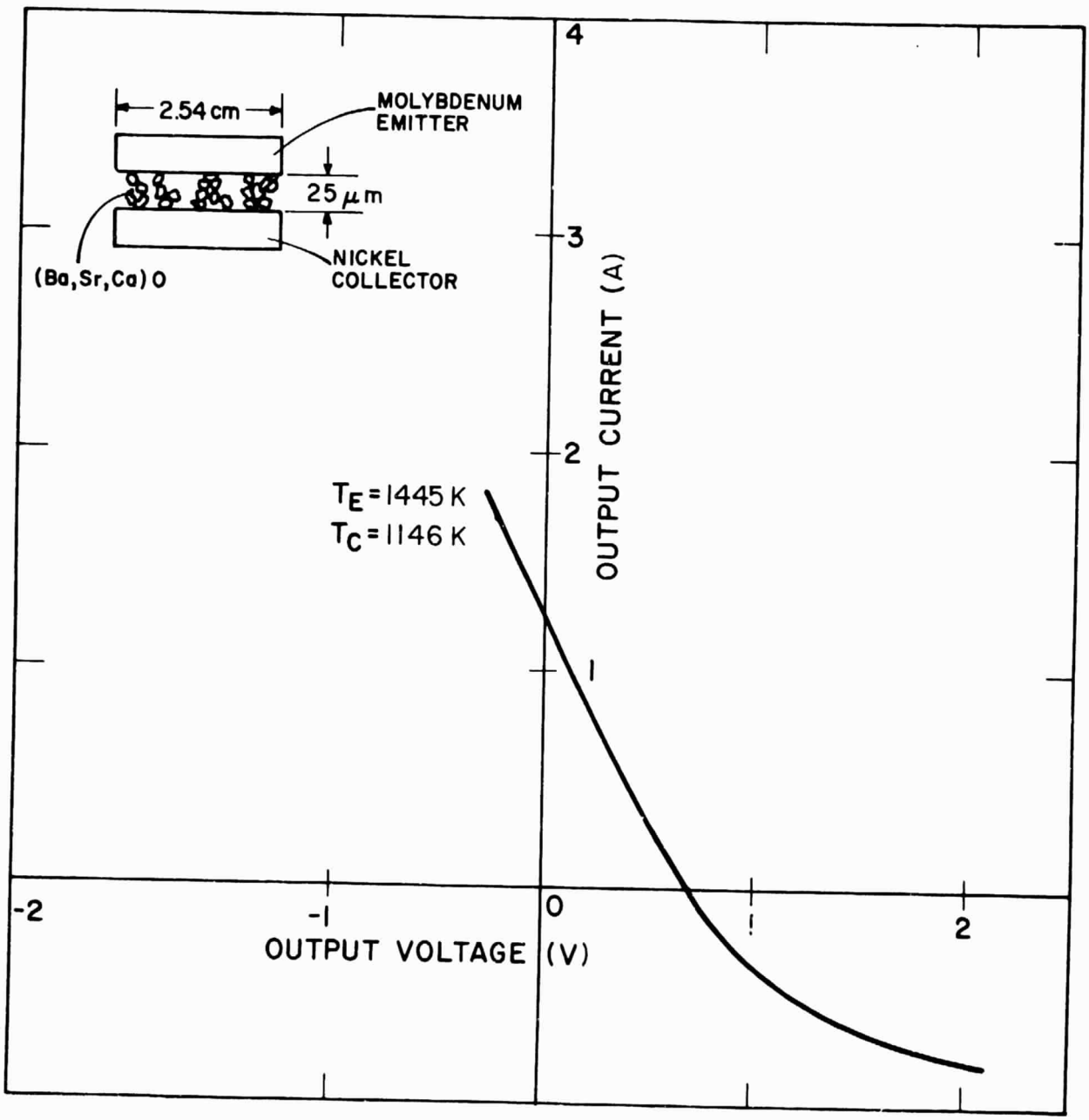

Figure 40. I-V Characteristics of Particulate-Spaced Diode with "Heavy" Coating of (Ba, Sr, Ca)O.

Figure 41. Scanning Electron Microscope Photograph of Heavy Coating of RCA BaO on Molybdenum (Magnification of 1000x).

conductivity. In essence, the space charge effects of small pores are substantially less than would exist across the same interelectrode gap in the absence of the semiconducting material. In fact, the pore conductor can be regarded as a whole series "minidiode" thermal converters. Measurement of the short circuit current from this device shows it to be directly dependent on collector temperature (Figure 42), a consequence of the higher pore conductivity produced with increasing average semiconductor temperature. However, Hensley's analysis of such a converter indicates that it will have limited efficiency. Consequently, the emphasis in close-spaced diode development should remain with lightly sprayed coatings and very small electrode spacings of 2.5 to 5 μm.

During the past few months, attention has been focused on reducing the interelectrode gap from the observed 12.5-μm spacing to the necessary lower values. Such minimal spacings require interelectrode particles with diameters below 3 μm, as well as extreme flatness and smoothness of the emitter and collector surfaces.

The surface topography of in-house polished test electrodes was investigated with a Sloan Dektak Surface Profile Measuring System with which resolution down to a few hundred Angstroms is possible. Electropolished surfaces yielded the smoothest finish, but showed the greatest degree of "crowning," or surface curvature. Similarly, substantial crowning was observed on in-house mechanically polished surfaces (Figure 43). Such a curvature has, most likely, had a significant effect on diode analyses to date. Measured spacings were actually mean values across an undefined fraction of the electrode surfaces, and observed thermionic currents, likewise, were restricted to a reduced surface area. In an effort to solve this problem, copper and molybdenum mirrors, polished out-of-house to laser specifications, were analyzed. These surfaces showed the highest degree of flatness and smoothness. Topographical deviations across the 2.5-cm diameter of these mirrors were within 1.25 μm (Figure 44). Using a Hewlett-Packard 4815A RF Vector Impedance Meter, room temperature electrode spacings as low as 3.25 μm were recently measured. The equivalent electronic circuit for these measurements is shown in Figure 45. In this sketch, C_p is the lumped parasitic capacitance of the test arrangement; L_s is the stray lead inductance, which is made negligibly small by using coaxial cables; R refers to the rf measuring coil, which provides ac isolation from the dc bias source; V_B is the

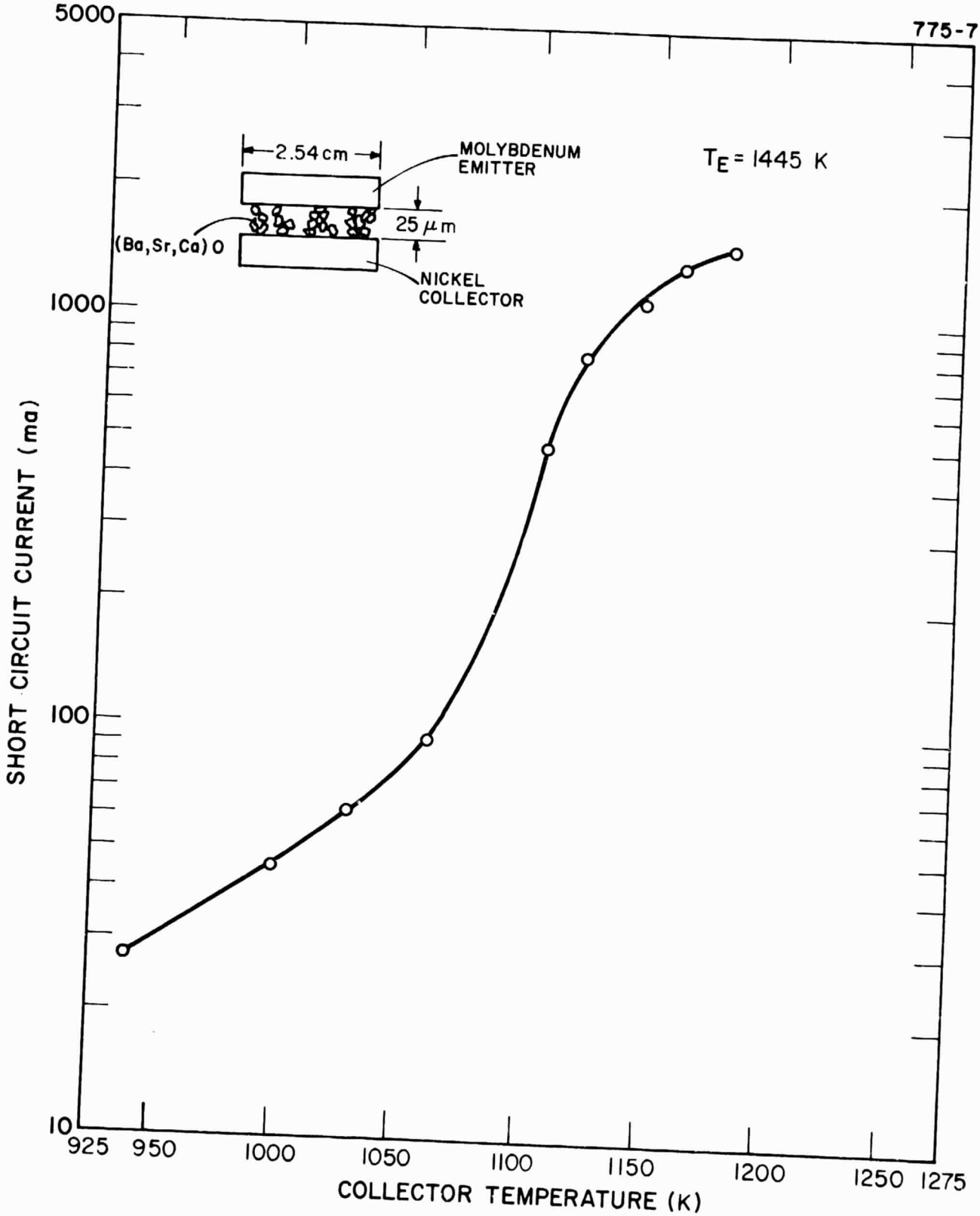

Figure 42. Short-Circuit Current Versus Collector Temperature for Porous Semiconductor Diode.

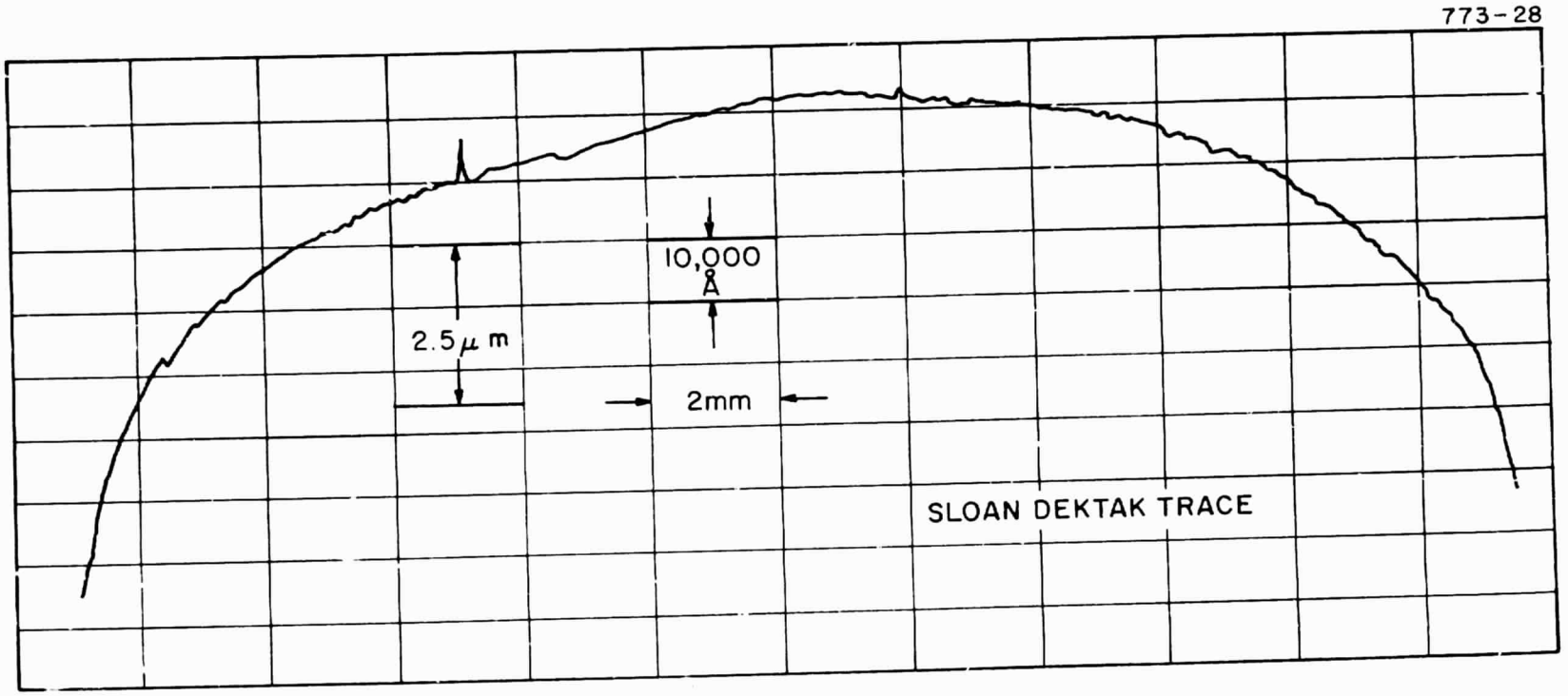

Figure 43. In-House Mechanically Polished Nickel Surface.

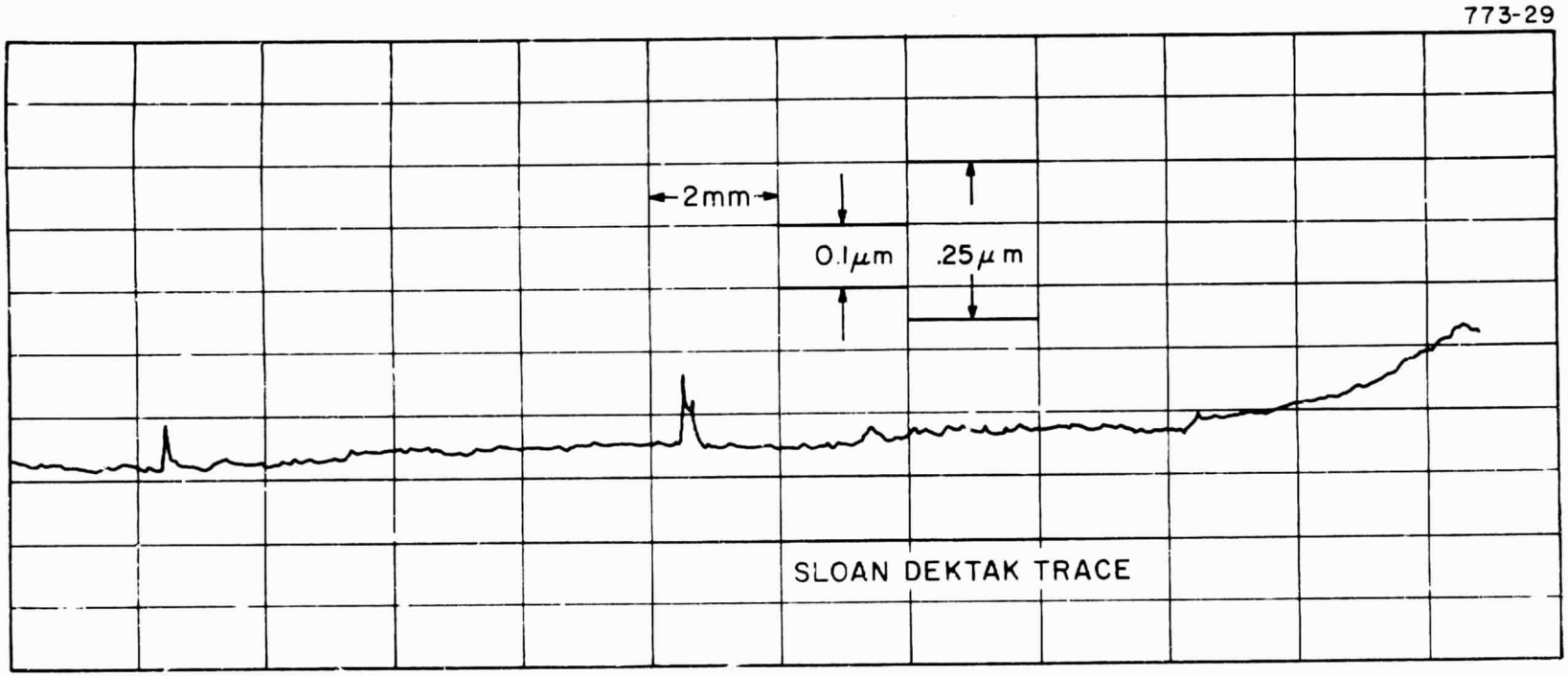

Figure 44. Copper Mirror Polished to Laser Specifications.

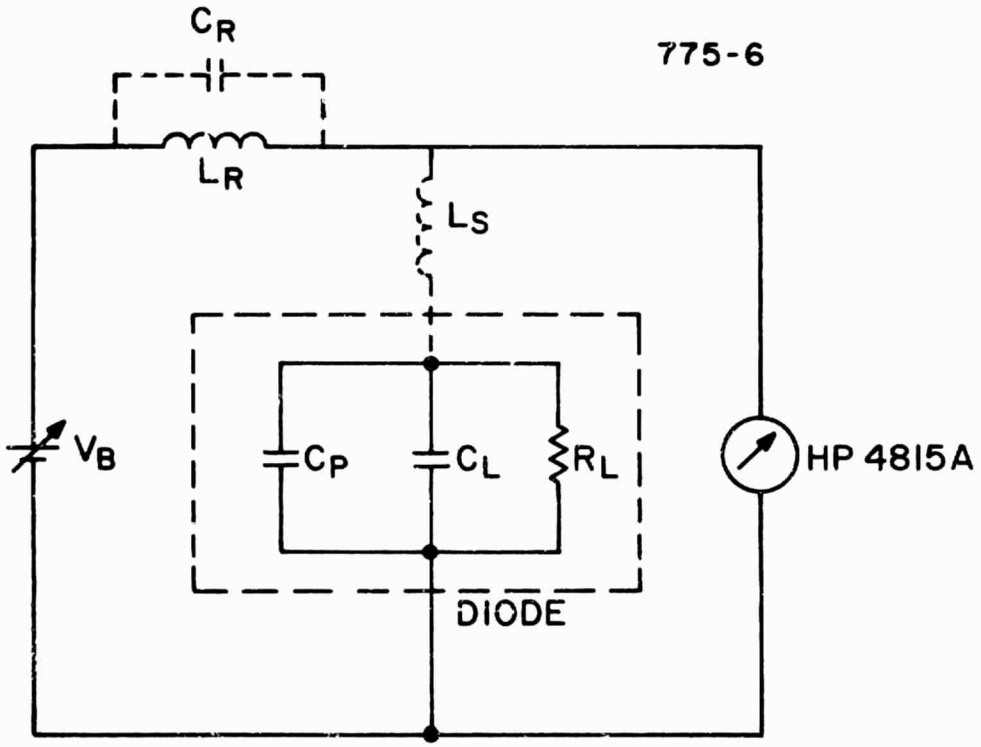

Figure 45. Lumped Parameter Model of Test Setup for Characterization of the Particle-Spaced Diode.

vector impedance meter test signal at the resonant frequency; C_L denotes the interelectrode capacitance, which allows the interelectrode spacing to be determined; R_L is the electrical resistance of the particulate spacers.

Substantial thermionic output will be observed if low spacings of 3.25 μm, measured at room temperature, can be retained at operating converter temperatures and cesium pressures. Tests are currently in progress to determine such thermal effects on diode spacing. At the same time, preliminary measurements on an actual flexible foil collector diode (upper left hand sketch of Figure 36, and in more detail in Figure 46) have shown that acceptable electrical resistance can be maintained at operating temperatures across at least 25 to 50 μm magnesium oxide particulate spacings in the presence of cesium at pressures near 0.1 torr.

763-8

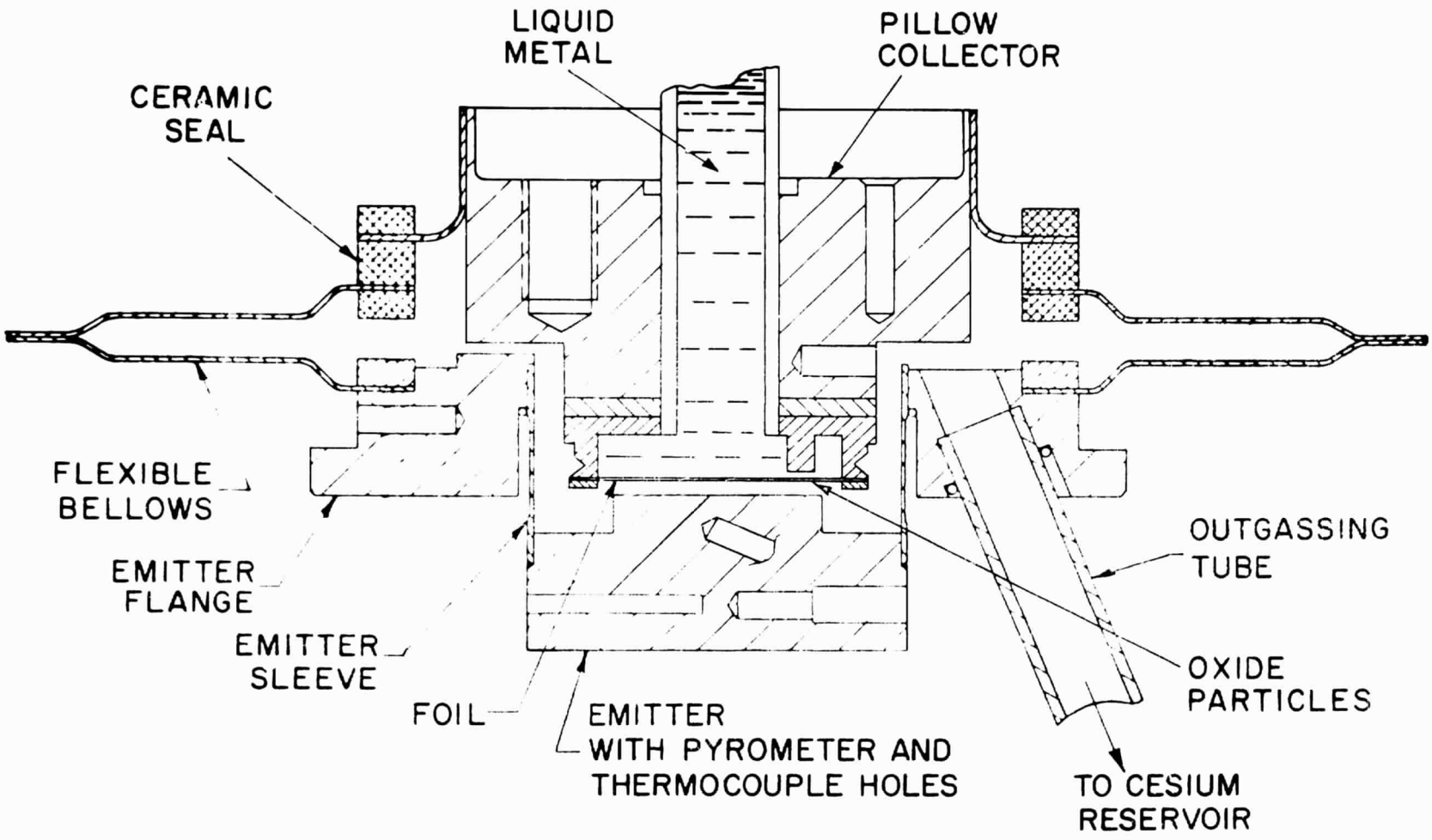

Figure 46. Powder Puff Diode with Flexible Foil Collector.

VI. DISCUSSION OF RESULTS

In the foregoing sections, the principal thermionic activities important to NASA missions were detailed. This section presents an analysis of the more significant results.

One of the most promising semiconducting collector materials, which has continued to receive substantial attention, is BaO. Unlike ZnO (which chemically reacts with cesium near 700 K, and thereby critically limits its usefulness in thermionic converters for space applications), BaO is quite stable up to 1000 K. Unfortunately, however, this material has a high electrical resistance, which necessitates ultrathin coatings in thermionic converters. Experiments conducted with evaporated films of BaO less than 100 Å in thickness have shown bare work functions approximating 1.4 eV, with only a slight temperature dependence in the test region from 400 to 750 K. Within this temperature interval, the work function of the evaporated film was consistently less than for the thicker sprayed material. For example, a decrease of 0.2 eV was measured at a temperature of 650 K. Interestingly enough, exposure to low-pressure cesium vapor did not improve the work function of the evaporated material, contrary to results observed with sprayed BaO coatings. However, exposure to air permanently damages the evaporated film, necessitating double evaporation techniques in converter construction (i.e., evaporation onto the emitter followed by reevaporation in the evacuated, sealed converter onto the collector). Unfortunately, tungsten detrimentally reacts with thin BaO films, precluding the use of tungsten emitters in such double evaporation procedures.

Enhancement of converter operation by the addition of small amounts of oxygen is well known. However, efficient methods of either directly injecting this electronegative species or dispensing it from an oxide surface in the presence of a high cesium pressure have not been developed. Apparently the cesium pressures typical of ignited mode diodes rapidly getter any oxygen provided by these means.

Direct addition of oxygen, by a silver leak tube, into a converter using a LaB_6 collector temporarily produced a collector work function of 1.28 eV (as measured in back emission) at low cesium pressures. Longer oxygenated operation (2200 hours) at 0.25 torr cesium pressure

was obtained from a double evaporation of tungsten oxide on a substrate of columbium with 1% zirconium. The first of these films is thought to diffuse into the substrate to saturate the columbium with oxygen. The second layer is then able to provide the oxygen supply for converter operation. ESCA spectral analyses of tungsten oxide collector surfaces taken from converters in various stages of activation suggest that oxygen is released from such a surface by cesium reduction of the oxide layer.

The possibility of introducing both oxygen and cesium with a single substance was strengthened in preliminary experiments conducted with the compound cesium carbonate. Work functions of 1.05 to 1.15 eV were measured on a nickel sample exposed to the products of a heated cesium carbonate-coated platinum strip. Thermal decomposition of this substance may liberate both cesium and oxygen in stoichiometrically optimum amounts to produce low work function surfaces. Variation in the Cs:O ratios is accomplished by changing the temperature of the evaporation sources. Corresponding changes in work function were measured using FERP. Observations suggest that the molecule responsible for generating the best coatings is Cs_2O. Experiments will shortly begin on a converter equipped with a reservoir filled with cesium carbonate in place of the usual cesium metal.

Replacing the auxiliary grid electrode in the previous triode configuration by a ring electrode surrounding the emitter and collector reduced interelectrode plasma losses. Visual and electronic observations of the positively-pulsed triode converter indicated that uniform discharges can be sustained in cesium-xenon mixtures across 0.75-cm^2-area electrode surfaces spaced as low as 0.5 mm. Such close spacings seem essential in reducing coulombic resistance effects to tolerable limits. Substantially enhanced output in the power-producing quadrant was observed in pulsed operation at even the highest experimental cesium pressures of 0.5 torr. Such pressures become meaningful in terms of creating emitter surfaces that will generate the desired high-saturation current levels at moderate temperatures. Although triode power levels are still significantly below those required for efficient converter operation, further optimization of the pulsing parameters is expected to improve the ring triode's performance.

An alternative approach to reducing electron space charge effects, thereby increasing interelectrode electrical conductivity, is to position the emitter and collector surfaces sufficiently close to one another.

Spacings of 2 to 3 μm are required to generate the desired 5 W/cm^2 of power with cesiated emitters at temperatures of 1400 to 1600 K, and collector work functions near 1.4 eV. At such small spacings, mechanical stability and thermal distortion become major problems. Electrode surfaces are separated by microscopic particles. Such particle spacers severely limit the flow of thermal energy across the gap and provide high electrical resistance. Noncesiated experiments conducted with numerous semiconductor materials during this reporting period showed that a 13-μm minimum separation of hand-polished molybdenum electrodes, one of which was heated to 1400 K, was feasible. Short-circuit currents of over 1 A were generated with 5-cm^2 molybdenum electrodes spaced with a porous BaO layer less than 25 μm thick; at these elevated temperatures, nonshorting operation was possible for over 100 hours. Although porous semiconductors such as BaO can reduce electron space charge effects, theoretical analyses have shown their effectiveness to be limited. Lightly coated ultralow spaced electrodes are, in fact, necessary for high-efficiency thermionic conversion without ion neutralization of space charge. Using extremely flat molybdenum laser mirrors at room temperature, electrode spacings of 3.3 μm have been obtained. Experiments are in progress to determine if these small spacings, sufficient for substantial thermionic output, can be maintained at operating temperatures.

The possibility of electrical breakdown in close-spaced devices due to cesiated coatings on the particulate spacers was preliminarily investigated in a flexible tantalum foil collector diode. High electrical resistance was maintained at operating temperatures for electrodes spaced 25 to 50 μm with MgO particles at cesium pressures of 0.1 torr. Configurational constraints precluded making accurate measurements at closer spacings.

VII. CONCLUSIONS

This section lists the major conclusions arrived at during this reporting period:

- Evaporated thin film BaO coatings produce nearly temperature-independent bare work functions, which are lower than those of the sprayed material. Minimum values approximating 1.4 eV were measured.

- Heated cesium carbonate dispenses cesium and oxygen in an optimum ratio to produce a coating on several substrates with a work function of between 1.05 and 1.15 eV.

- Back-emission work functions of 1.28 eV were measured from oxygenated lanthanum hexaboride used as a collector in an operating diode at low cesium pressure.

- A collector formed by a double tungsten oxide vapor deposition on columbium with 1% zirconium produced a converter operating for 2200 hours at a power density of nearly 3 W/cm^2 and a barrier index of 2.06 eV.

- Improved performance was obtained by replacing an auxiliary grid electrode with a ring in a pulsed triode. This configuration allowed emitter-to-collector spacings to be reduced to 0.5 mm, and cesium pressures in cesium-xenon mixtures to be raised to 0.5 torr with ring potentials up to 100 volts.

- Short-circuit currents of over one ampere were observed from noncesiated particulate-spaced diodes with molybdenum electrodes spaced less than 25 μm by porous BaO coatings. No electrical shorting occurred for over 100 hours at emitter temperatures up to 1450 K. Room-temperature electrode spacings as low as 3.3 μm were measured with highly polished molybdenum laser mirrors. Preliminary experiments in a cesiated flexible foil collector diode have indicated that no electrical shorting occurs at electrode spacings of 25 to 50 μm and cesium pressures up to 0.1 torr.

REFERENCES

1. Aldrich, L. T., J. Applied Phys., 22, 1168 (1951).

2. Hensley, E. B., J. Applied Phys., 32, 301 (1961).

3. Desplat, J. L., Surf. Sci., 34, 588 (1973).

4. Davey, J. E., J. Applied Phys., 28, 1031 (1957).

5. Martinelli, R. U., J. Applied Phys., 45, 1183 (1974).

6. Forman, R., J. Applied Phys., 47, 5272 (1976).

7. Simon, A., Z. Anorg. Allgem. Chem., 395, 301 (1975).

8. Lebeau, P., C. R., 137, 1255 (1903).

9. Klemm, W. and Scharf, H. J., Z. Anorg. Allgem. Chem., 303, 263 (1960).

10. Sommer, A. H., Photoemissive Materials, Wiley, New York, 1968, p. 141.

11. Borzyak, P. G., Bibik, V. F., and Kramerenko, G. S., Bull. Acad. Sci. USSR, Phys. Ser., 20, 939 (1956).

12. Sommer, A. H., RCA Rev., 28, 543 (1967).

13. Neil, K. S. and Mee, C. H. B., Phys. Stat. Sol., (a)2, 43 (1970).

14. Pakhomov, M. T., Melanid, A. Ye., and Gerchikov, Ya. B., Radio Eng. and Electron. Phys., 20, 147 (1975).

15. Hansen, M. and Anderko, K., Constitution of Binary Alloys, McGraw-Hill, New York, 1958.

16. Huffman, F. N., Sommer, A. H., Balestra, C. L., Briere, T. R., Lieb, D. P., and Oettinger, P. E., "High Efficiency Thermionic Converter Studies," Report No. NASA CR-135 125, TE4202-12-77 (1976).

17. Beavis, L. C., Rev. Sci. Instrum., 43, 1 (1972).

18. Gunther, B., Lieb, D., Richmond, C., and Rufeh, F., "Summary Report on Oxygen Additives," Report No. AEC TEE 3056-2, TE4166-6-74 (1974).

19. David, J.P., Floret, F., and Guerin, J., "Investigations on Oxidized Titanium Collector Converters," Proc. 1975 Thermionic Conversion Specialists Meeting, Eindhoven, Netherlands, Sept. 1975, p. 227.

20. Oettinger, P.E., "Plasma Resistance Effects in Thermionic Converters," Thermo Electron Corp. Report No. 4220-77-77, January 1977.

21. Lam, S.H., "Plasma Arc Drop in Thermionic Energy Converters," COO-2533-3, Princeton Univ., 1976.

22. Hensley, E.B., "Thermoelectric Properties of Porous Semiconductors," Chapter 12 in Thermoelectricity, Paul H. Egli, ed., Wiley, New York, 1960, pp. 193-206.